laser technology

MICROWAVES

JULY
1977

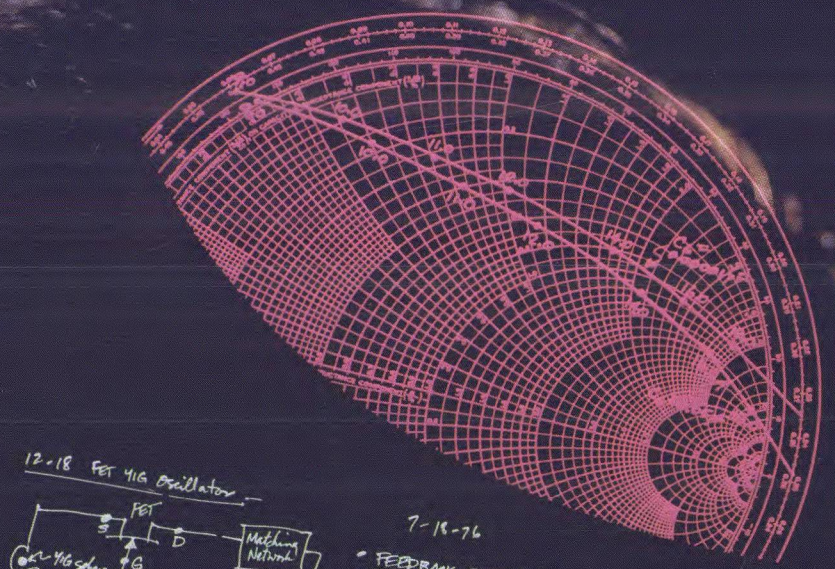

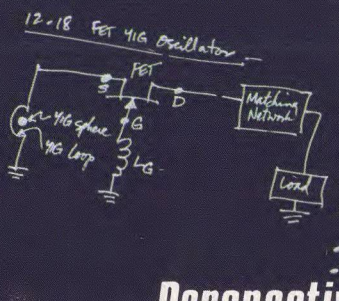

Perspectives on:

OSCILLATOR DESIGN

- GaAs FETs rival Gunns
- Try CAD for cavity VCOs
- Testing VCO subsystems

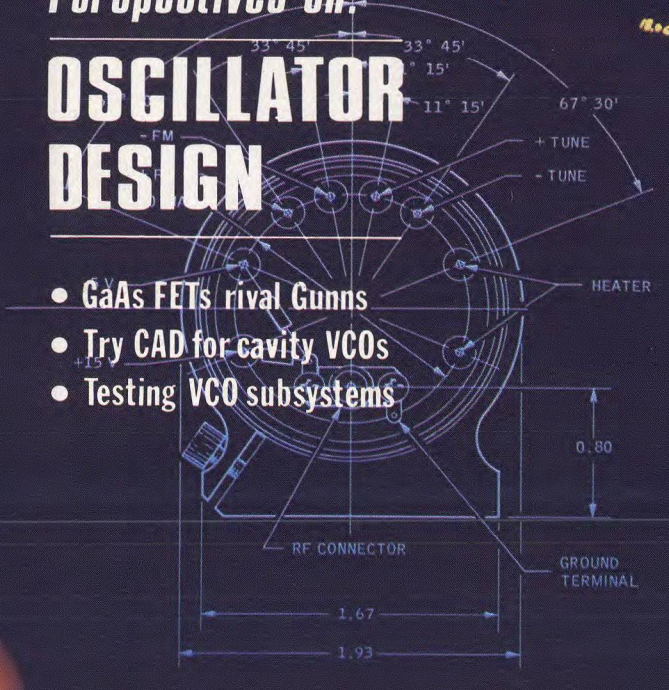

PRODUCT FEATURE:
GaAs FET oscillators break into K-band

MICROWAVES

July 1977
Vol. 16, No. 7

news

editorial

technical

Sources

departments

About the cover: The mind's eye is confronted with thousands of images when a designer sets out to build a solid-state oscillator. Articles in this month's issue will help separate constructive concepts from idle thoughts. Photograph courtesy of Avantek, Santa Clara, CA. Photography by Gary Traviss, Photographic Alliance, Santa Clara, CA.

coming next month : Communications

A series of special reports will examine trends in a variety of communications fields ranging from land mobile and terrestrial systems to domestic and international satellite communications. Included will be the latest news from the International Communications Conference and the International Microwave Symposium.

Publisher
Howard Bierman

Editor
Stacy V. Bearse

Western Editor
Steven Peliotis
1870-E Ednamary Way
Mountain View, CA 94040
(415) 969-9452

Washington Editor
Paul Harris
Snyder Associates
1050 Potomac St. NW
Washington, DC 20007
(202) 965-3700

Editorial Assistant
Gail Murphy

Production Editor
Sherry Lynne Karpen

Art Director
Robert Meehan

Art Illustrator
Janice Tapp

Production
Dollie S. Viebig, Mgr.
Anne Molfetas

Circulation
Barbara Freundlich, Dir.
Sherry Karpen,
Reader Service

Directory Coordinator
Janice Tapp

Editorial Office
50 Essex St.,
Rochelle Park, NJ 07662
Phone (201) 843-0550
TWX 710-990-5071

A Hayden Publication
James S. Mulholland, Jr.,
President

MICROWAVES is sent free to individuals actively engaged in microwave work. Prices for non-qualified subscribers:

	1 Yr.	2 Yr.	3 Yr.	Single Copy
U.S.	$25	$40	$ 60	$3.00
Foreign	$40	$70	$100	$4.00

Additional Product Data Directory reference issue, $15.00 each (U.S), $27.00, (Foreign), POSTMASTER, please send Form 3579 to Fulfillment Manager, MicroWaves, P.O. Box 13801, Philadelphia, PA. 19101.

Back Issues of MicroWaves are available on microfilm, microfiche, 16mm or 35mm roll film. They can be ordered from Xerox University Microfilms, 300 North Zeeb Road, Ann Arbor, MI 48106. For immediate information, call (313) 761-4700.

GaAs FETs Rival Gunns In YIG-Tuned Oscillators

FET oscillators are an evolutionary option for designers of RF instruments. This introduction focuses on the component's design, and reveals why it is an attractive replacement for Gunn sources.

TEN years ago, the standard X or Ku-band signal source in instruments such as sweep generators and spectrum analyzers was the backward-wave oscillator (BWO), a form of traveling-wave tube. The BWO required a high-voltage power supply, generated excess heat that had to be removed by forced-air cooling, and had a lifetime in the order of 2,000 hours.

Five years ago, BWOs in many instruments were largely supplanted by solid-state oscillators, constructed around a Gunn-effect device and tuned with a YIG sphere and electromagnet. Although far more compact, more linear and considerably longer-lived than the BWO, the Gunn-effect YIG-tuned oscillator (YTO) brought along its own special complexities. For example, it requires a low-voltage, high-current power supply, with additional current capacity to overcome the diode's threshold current characteristics. Cooling is also a problem with Gunn YTOs, due to the large amount of heat dissipated in the semiconductor. Finally, the transferred-electron device is often difficult to start when cold under pulsed or CW operating conditions.

Today, after about five years of Gunn-effect signal sources, the time has arrived to begin thinking seriously about the characteristics of a new type of oscillator for instrument applications: the YIG-tuned GaAs FET source. Gallium arsenide field-effect transistor technology has advanced to the point that for practically all instrument applications, the Gunn diode YTO can now be replaced with a GaAs FET component to gain several advantages (see, "GaAs FET or Gunn? Efficiency makes the difference").

This article will introduce the GaAs FET YTO, show briefly how it works and describe why it is useful. It seems clear that that GaAs FET oscillator is emerging on the horizon as the most significant new microwave oscillator in recent years and a likely candidate to supplant many other types of microwave oscillators in the years to come.

Tom Ruttan, Microwave Design Engineer, Avantek, Inc., 3175 Bowers Avenue, Santa Clara, CA 95051.

Consider the topologies

All oscillators can be analyzed by considering an active device operating in a negative resistance region, an approach that is most appropriate for oscillators operating at microwave frequencies. This negative resistance can be an inherent characteristic of the device, as in the case of a Gunn or tunnel diode, or it can be synthesized in a three-terminal amplifier, such as with the bipolar or GaAs field-effect transistor.

Consider the behavior of the three-terminal active device represented by the general model shown in Fig. 1. In the case of the FET, terminal 1 usually represents the source, terminal 2 the drain and terminal 3 the gate, although other connections are possible.

As an amplifier, typically in common-source configuration, the GaAs FET is quite stable in the X and Ku-band frequency regions; stability factor, K, is generally 1.4 or

GaAs FET or Gunn? Efficiency makes the difference

Probably the most dramatic difference between the GaAs FET YTO and other oscillator choices concerns efficiency and input power consumption. This means that the power supply design is simpler and less expensive than that required for existing Gunn designs. In addition, due to the fact that the FET dissipates less power, the FET YTO operates cooler and does not require extensive heat sinking to remove the heat generated by the active device. MTBF should be improved over existing designs due to the lower input power into the device and less power density.

Consider X-band YTOs with output power in the 30 to 50 mW range. A Gunn-diode YTO will typically have a threshold current of 700 mA and operating current of 500 mA at an operating voltage of 11 or 12 V (excluding regulators or dropping resistors). An FET YTO does not have to overcome a threshold current, and its operating current for a single-die oscillator is typically 50 mA, or 150 mA for the buffer amplifier/oscillator with an operating voltage of 7 to 8 V (excluding regulators or dropping resistors).

A serious problem concerns heat sinking when incorporating a Gunn-effect device into a YTO. One must mount the Gunn diode near the magnet gap somewhere in the middle of the oscillator structure. Since too much copper in the magnet gap causes eddy current losses, one must compromise the thermal design for the magnet design somewhat. This also makes it very difficult to hermetically seal the entire magnet structure, since one usually must bring some sort of heat sinking out to the mounting surface from the Gunn diode (copper, aluminum, etc.). Thus, the Gunn YTOs suffer from active device heat dissipation problems that the FET YTO simply doesn't have. This, along with the higher input power density of the Gunn YTOs, degrades the MTBF of the Gunn.

The Gunn YTO can also have problems with sidebands. The Gunn diode has potential instability even at DC, which can result in bias oscillation that cause sidebands on the output signal. The FET YTO has a simple resistor bias network which cannot cause these instabilities. In some applications, the YTO is switched on during part of the system operation. The Gunn YTO, at times, has a problem of cold starting during this pulsing. They tend to lock up at some resonance other than the desired one for part of the band. This has not been observed with FET YTOs.

The FM noise of an FET YTO is capable of being as low or lower than the Gunn YTOs (see Table 1). In some applications this is not important, but in others, such as LOs for spectrum analyzers or receivers, it is very important, and FET YTOs promise to compete quite effectively.••

more. There are, however, many possible combinations of series or shunt reactances that can be connected to the device to lower this stability factor and create a negative resistance at the input port, so the frequency can be easily controlled with an external resonant circuit. Some of the more common topologies are common source with capacitive feedback between source and ground, common-gate with capacitive feedback between the source and drain, and common-gate with inductive feedback between gate and ground.

The choice of circuit topology is dependent on the type of circuit used (MIC, waveguide, stripline, coaxial, etc.), the type of tuning scheme (YIG, varactor, fixed frequency), bandwidth, operating frequency and construction convenience. Common-gate with capacitive feedback, for example, offers negative resistance over a larger bandwidth than other approaches. Common-gate with inductive feedback presents a larger value of negative resistance, thus making the tank circuit coupling easier to achieve. Parasitics and reactance associated with the negative resistance must also be considered when choosing a topology. In short, one must define the type of oscillator needed, the circuit medium, analyze the parasitics involved, and choose a configuration best suited to these constraints.

Avantek's choice for octave-band, YIG-tuned circuits in X and Ku-bands is a common-gate circuit with inductive feedback. Figure 2 plots the complex impedance plane of the feedback inductor (jK_L). The shaded area shows that the inductor has a negative phase shift through the FET gate-source junction of slightly less than 90 degrees. Thus, this inductive reactance in the gate circuit, transformed by the phase shift through the FET, synthesizes a negative resistance in series with some inductive reactance in the source terminal. This can be proved somewhat more rigorously by circuit analysis of the equivalent circuit of the FET and the inductor.

The common-gate topology is very compatible with MIC circuit technology. The feedback inductor can be simply a gold bonding wire, which also forms the DC ground return for the FET. Its length, and thus the value of the feedback inductance, is easily adjustable to compensate for normal production variation of FET dies and circuit elements. The common-gate configuration is also compatible with YIG tuning, since the reactive part of the input impedance looking into the source of the FET is inductive and, therefore, cannot resonate the self-inductance of the YIG loop. Output power of the common-gate circuit is adequate for many applications. An attractive feature of the GaAs FET YTO built with MIC technology is that an FET buffer amplifier can be easily integrated within the same package. Figure 3 illustrates that well over 50 mW can be achieved in X-band with an oscillator/amplifier combination. The buffer amplifier also provides good load immunity, improved output power match and fewer interface problems for the system designer.

In general, the common-gate approach with inductive feedback provides a reproducible, and thus cost-effective design that performs very well in a wide variety of oscillator applications.

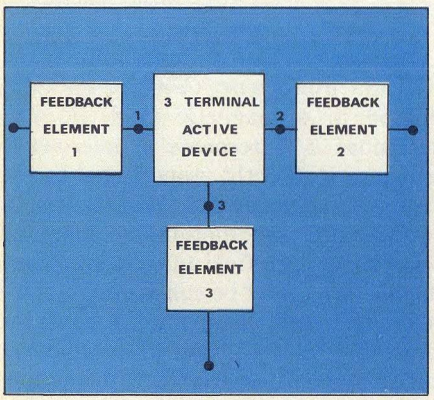

1. Feedback elements *can be added in a number of ways to synthesize negative resistance in a three-port device. Here, terminal 1 is the source terminal 2 the gate and terminal 3 the drain.*

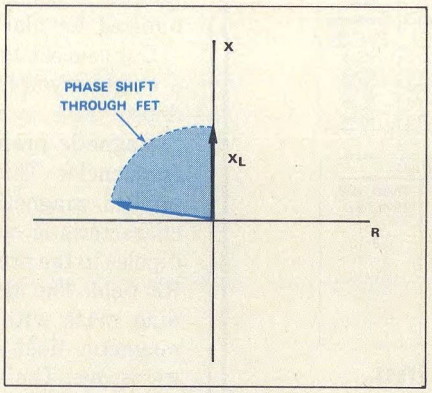

2. The reactance of an inductor *between gate and ground is transformed nearly 90-degrees to appear at the source terminal as a large negative resistance with a small, positive reactive component.*

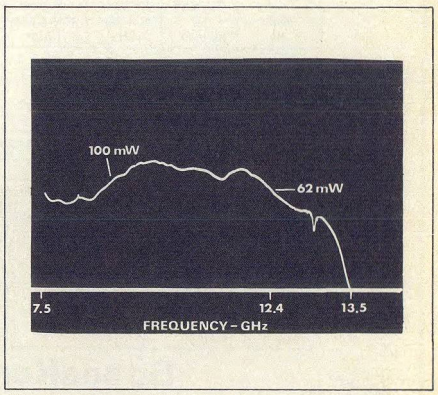

3. Fundamental output power *is sufficient for many applications, and can be raised even further by incorporating a buffer amplifier. Here, a maximum X-band output of 100 mW is achieved by an oscillator/amplifier.*

Evaluate s-parameters

With this background, let's consider the actual FET oscillator design. The GaAs FET, being a well-behaved three-terminal device, lends itself quite well to s-parameter analysis and characterization. Thus, the design procedure for GaAs FET oscillators is very similar to that of bipolar transistor components at lower frequencies.[1] The performance and negative resistance behavior of the GaAs FET is quite close to that of a silicon bipolar at 4 or 5 GHz lower in frequency.

But first, how does one choose an FET device for an oscillator application? Some very important factors to consider center on the FET device geometry. One wants to minimize parasitic bonding lead inductance for wideband oscillator design. Thus, the position of the source, drain and gate bonding pads should be such that the connections to the circuit require minimum bonding lead length. The area of the bonding pads should be minimized also, to reduce parasitic capacitance.

In order to achieve useful output power as an oscillator, the FET should have a high 1-dB compression point (the output power where the gain is compressed by 1 dB). High saturated drain current, I_{dss}, and substantial drain-to-source operating voltage are also required to achieve good output power and bandwidth (I_{dss} of 50 to 100 mA is

(continued on p. 44)

YIG-TUNED OSCILLATORS

suggested for a 500 μm device). High gain or low-noise figure are not necessarily required for a FET in an oscillator application.

It should be noted that the design outlined here uses unpackaged devices. In X and Ku-bands, the parasitic elements associated with packaged devices are prohibitive for all but a narrowband or fine-tuned oscillator design. When tunability is desired, parasitics reduce bandwidth significantly, increase output power variation and introduce spurious and resonant frequencies that make it difficult to achieve smooth, continuous tuning. In fact, one must use great care and imagination in circuit and device design in order to be able to operate over X and Ku-band, even with unpackaged chips. For example, one must resort to design techniques such as die attaching the FET chip to a Be 0 heatsink carrier for good thermal characteristics and low parasitics.

Once a device has been chosen, the first step in the design procedure is to measure the s-parameters of the FET in the configuration decided upon for the oscillator circuit (common-gate or common source). This data, along with circuit information, is best fed into a computer-aided design program to choose the load and feedback elements that will, on a small signal basis, provide negative resistance over the desired frequency range.

Normally, the FET is biased in its linear operating region and as oscillations begin, triggered by some noise pulse in the circuit, the performance of the oscillator can initially be analyzed using small-signal scattering parameters. As the oscillations increase in amplitude to some final limit, however, the device operates under large-signal conditions.

Consider the common-gate topology. Actually, since one port, the gate, and its associated inductive feedback element is common to both the input and output circuit, the three-port device can be treated as a two-port circuit element. Considering the port at which the negative resistance is present as port 1, we can say $|s_{11}|>1$. A convenient way to display this condition is to use the Smith Chart and refer to $1/s^*$. This transforms the s_{11} area inside the $|\rho| = 1$ circle to the negative resistance area. The conjugate of $1/S_{11}$ generates a plot to the same phase as the original S_{11} (see Fig. 4).

Some notes on YIG tuning

Now one must evaluate the scattering parameters of the tuning circuit that resonates the negative resistance of the active device. This tuning, or tank circuit can take many forms, but will usually be equivalent to the conventional parallel resonant circuit of Fig. 5 (parasitic reactances omitted for clarity).

Our concern here centers on the YIG tuning circuit. When a single crystal of yttrium iron garnet (YIG) or gallium-doped YIG is immersed in a magnetic field, its ferromagnetic properites cause it to resonate at microwave frequencies. This resonance is directly proportional to the applied magnetic field, changing it 2.8 MHz/Gauss, a characteristic associated with the motion of magnetic dipoles in the presence of a magnetic field and superimposed RF field. The spinning electron may be considered a spinning mass with precessional motion about the constant magnetic field—comparable to the classical mechanical gyroscope. The magnetic moment associated with the motion is comparable to the angular momentum of a spinning mass. If an RF magnetic field having the same frequency as the precessional frequency of the YIG sphere is applied perpendicularly to the constant magnetic field, RF energy is coupled to the spinning electron.

A complete YIG resonant circuit consists of a properly oriented YIG sphere, a coupling loop for the RF field and an electromagnet to provide the necessary high constant magnetic field. These elements are positioned so that the orientation of the magnetic field and RF field through the YIG sphere, when the RF current flows in the coupling loop, will cause an energy exchange and thus energy storage in the resonant circuit at the desired frequency.

The YIG tuning circuit suggested for FET oscillators is basically the same as that used with lower frequency bipolar oscillator designs. Naturally, the saturization magnetization (4πMs) is dictated by the frequency range, and the sphere diameter by the power handled by the YIG sphere. A pure YIG sphere with 4πMs = 1780 is typically used for oscillators operating in X-band and above. The s-parameter plot for a YIG tuning circuit as a function of frequency (S_T) looping into the terminals of the one-port tank circuit can be plotted on a Smith Chart, as shown in Fig. 4. The point where this plot crosses the real axis near the open circuit side of the chart is simply R_T (normalized to 50 ohms), which serves as a measure of the degree of coupling, and, therefore, of the external Q of the circuit. This crossover point moves closer to the open circuit point as the coupling to the YIG sphere becomes tighter. *(continued on p. 46)*

YIG-TUNED OSCILLATORS

Apply stability criteria

Stability criteria can be used to predict the conditions under which the circuit will oscillate. The stability of the two-port active device (the FET) with the tank circuit connected as in Fig. 6 can be evaluated by writing the characteristic equation of the system: $1 - S_T S_{11} = 0$. Nyquist's stability criteria states that the number of clockwise encirclements of the polar plot of $S_T S_{11}$ as ω varies from $-\infty$ $+\infty$ about the point -1 indicates the net number of zeroes (number of zeroes minus the number of poles) of the characteristic equation in the right half plane (RHP). If there are zeroes of the characteristic equation in the RHP, the system is unstable. This is a necessary condition for oscillations to occur. Since the YIG tuning circuit is relatively high-Q, near resonance it is rapidly changing function of frequency compared to S_{11}. We can then make the approximation that S_{11} is not changing with frequency, and, therefore, constant.

Manipulating the characteristic equation, we obtain $S_T = \frac{1}{S_{11}}$. Applying Nyquist's stability criteria to this, with S_{11} constant, for instability S_T must encircle $\frac{1}{S_{11}}$ in a clockwise manner as ω changes from $-\infty$ to $+\infty$ or must encircle $\frac{1}{S_{11}^*}$ in a counterclockwise manner. Since the Smith Chart is a bilinear transformation of the polar plot, the same graphic criteria holds for the Smith Chart. Thus, we can see from Fig. 2 that if $\frac{1}{S_{11}}$ falls inside the dashed-line circle, the necessary condition of oscillation is satisfied.

The final step to complete the oscillator design is to choose a load impedance for the active two port. The term $\frac{1}{S_{11}^*}$ is dependent on the load impedance and, in fact, it is possible to map the locus of all load impedances into the $\frac{1}{S_{11}^*}$ [2]. Choose a load using this plot, or emperically, to obtain satisfactory output power and bandwidth from the oscillator. One can estimate the oscillating frequency range by observing where the plot of $\frac{1}{S_{11}^*}$ vs. frequency enters and leaves the tank-circuit impedance plot circle on the Smith Chart.

All of our discussions so far have only used small signal analysis. But what happens under large signal conditions as the oscillations build up?

Once the oscillations start, they build up in amplitude and, if the zeroes of the characteristic equation were to remain in the RHP, the oscillations would grow without limit until the active device destroyed itself. We know this is not the case and, in fact, we know that stable oscillations occur rather quickly. As the amplitude of oscillation grows, the input impedance of the active device changes such that an equilibrium is reached, where the negative resistance equals in magnitude the positive resistance of the tank circuit. The reactive components of the tank and active circuit also exactly offset each other. Thus, the YIG tank circuit does not operate exactly on its resonance under stable oscillating conditions.

(continued on p. 48)

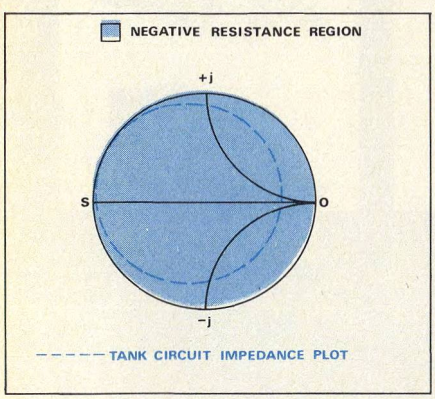

***4. Negative resistance** looking into the source terminal encompasses the area within the $|\rho| = 1$ circle.*

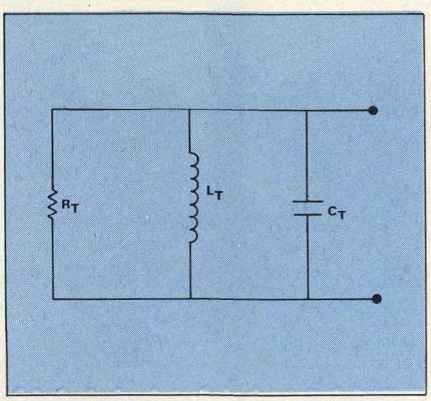

***5. Tuning circuit** can be represented as a parallel RLC combination, which must be compared with the FET S_{11}.*

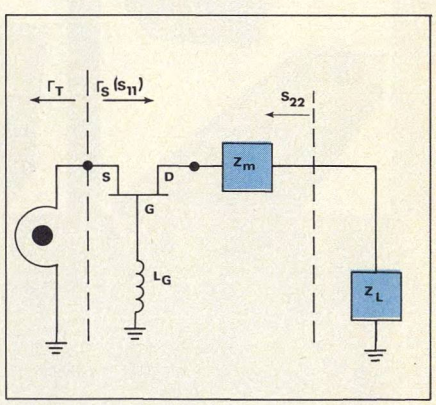

***6. Common-gate topology** transforms inductance to provide a negative resistance at the source.*

Noise performance encouraging

There has been much discussion and some amount of confusion since the arrival of FET oscillators concerning FM noise. It may be informative to share some of the observations and thoughts from Avantek's FET oscillator efforts on this subject. It is probably obvious, as with any YTO, that the FM noise is dependent on the YIG tuning circuit parameters. If the YIG sphere is dissipating too much power, it will approach a YIG limiting condition, and FM noise will increase dramatically. In general, the tighter the YIG sphere is coupled to the FET circuit, the higher the FM noise will be.

Table 1: Typical FM noise data at 10.25 GHz

Device #	Output Power (mW)	FM Noise (dBc) @20 kHz; 1 kHz BW
Bipolar 1	19	−77
Bipolar 2	10	−81
Fet-1	28	−57
Fet-2	7.0	−55
Fet-3	13	−63
Fet-4	16	−64
Fet-5	12	−75
Fet-6	17	−60
Fet-7	18	−58
Fet-8	21	−71
Fet-9	14	−69

At Avantek, we have found that the FM noise of an FET oscillator is very device dependent. Table 1 is a chart of FM noise data for many different FET devices, as well as some Si bipolar devices. The Si bipolar devices are included as a reference point of comparison. All of these results were recorded using the same YIG sphere. The sphere size was big enough to prevent YIG limiting even for the higher output power circuits. It can be seen that there is a wide variation of FM noise for the various FETs listed. The variations correlate with variations in the device fabrication, design, parameters, etc. One may conclude from this that, although the FET oscillator FM noise can be greater than desired for some applications, if the FET parameters were optimized for low-noise performance, it is possible to obtain very good FM noise characteristics and actually approaches that of a Si bipolar oscillator.••

Acknowledgement

The author wishes to thank Ira Rogers, Vince Grande and Northe Osbrink for their review and useful comments concerning this article.

References

1. P. M. Olivier, "Microwave YIG Tuned Transistor Oscillator Amplifier Design: Application To C-Band," *IEEE Journal of Solid State Circuits*, SC-7, pp. 54-60, (1972).
2. John J. Dupre, "A 1.8 to 4.2 GHz YIG Tuned Transistor Oscillator With A Wideband Buffer Amplifier," *G-MTT Symposium Digest*, pp. 436-438, (1969).
3. B. P. Lathi, *Signals, Systems and Communications*, John Wiley & Sons, Inc., New York, pp. 307, (1967).

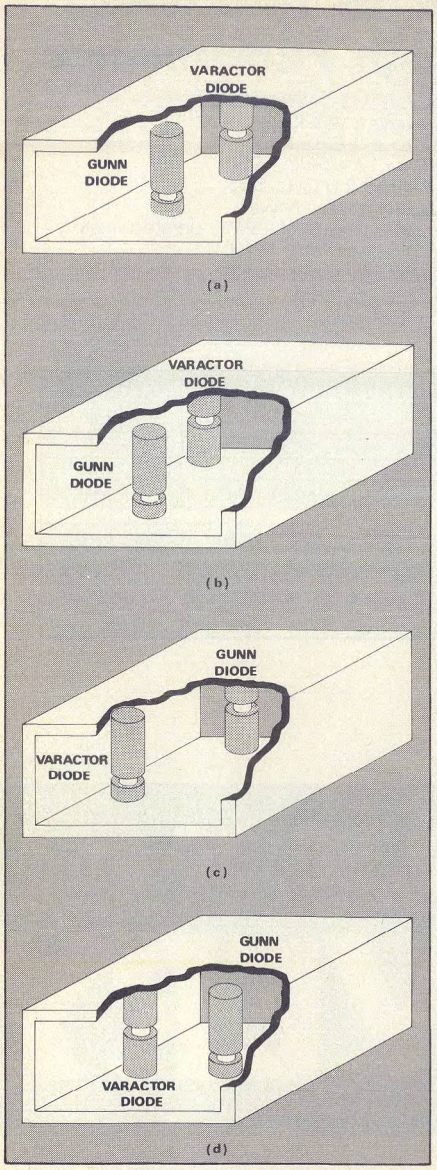

2. Waveguide VCOs can be built in many configurations *as these four examples illustrate. Symmetrical, "in-line" structures may place the Gunn device close to the output (a). A staggered version may include a thicker varactor mounting post (b). Some applications call for the varactor to be located between the Gunn device and the output (c). Yet another case is a coplanar arrangement in reduced-height waveguide (d). A unified theoretical approach is general enough to analyze all these geometries.*

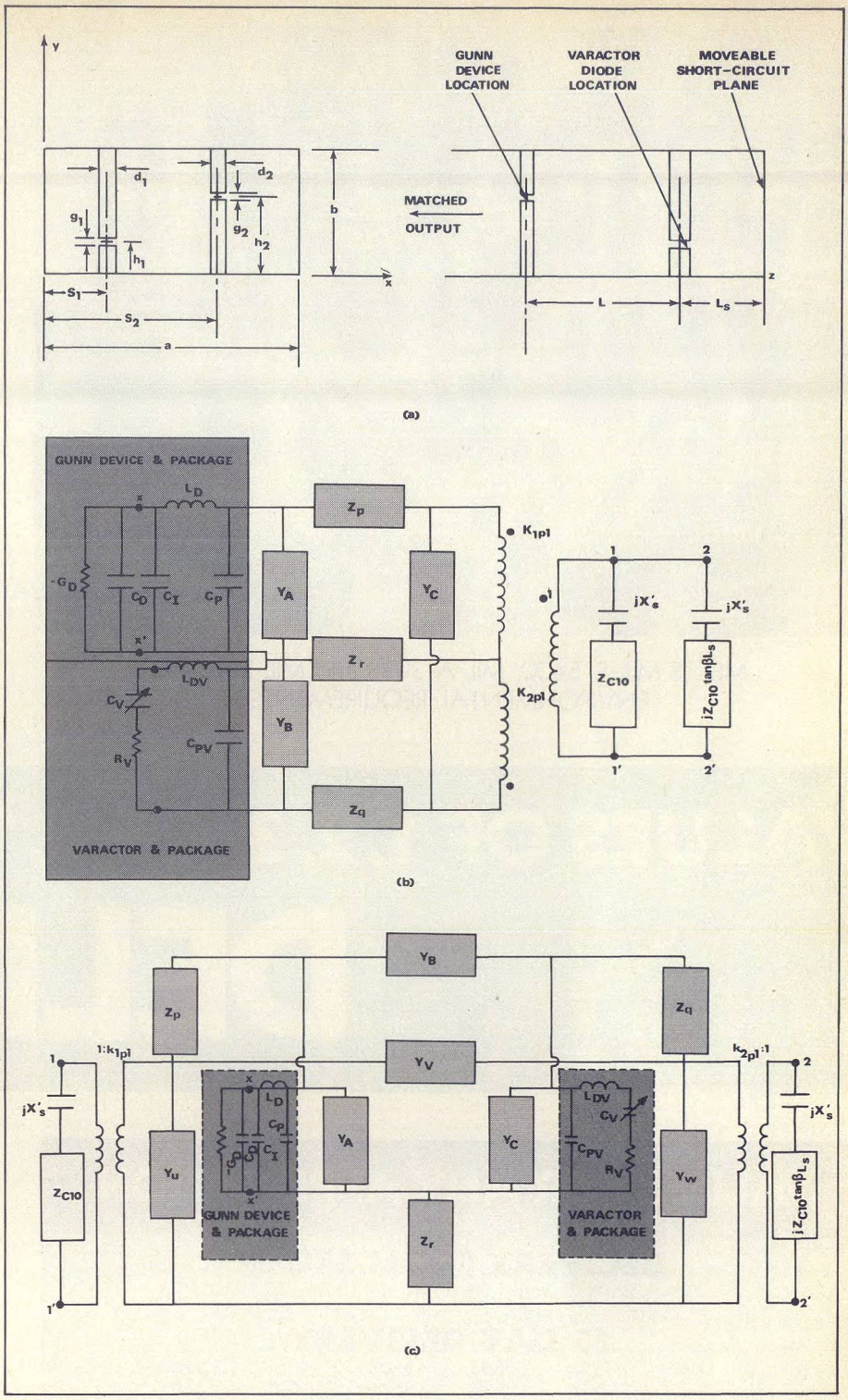

3. Equivalent networks *are based on a unified theoretical approach. Dimensions of the common two-post case (a) can be used to compute admittance and impedance values for the two important networks. Coplanar circuits can be handled with network (b) while the staggered post case can be described by network (c). See text for important distinction between circuit types 1 and 2.*

change in the package network, say from L-type to π-type, can be easily made by slight modification to the computer program. The generality of the computer-aided unified approach is demonstrated by Fig. 2, which illustrates four classes of circuits typically encountered in waveguide oscillator design.

The theory behind the unified network representation for the general post-waveguide circuit will not be elaborated on here, although rigorous references are available. What we will focus on, however, are two equivalent networks derived from the theory for the special case of two waveguide posts.

Figure 3 illustrates these two important equivalent networks, along with a reference drawing that defines physical parameters. Waveguide arms are assumed to be appropriately terminated, and the post thickness capaci-

(continued on p. 74)

Design VCOs Accurately With Computer Analysis

Two equivalent networks can be used to describe any type of two-post waveguide oscillator. Analyzed by computer, these networks consider the influence of 23 basic circuit parameters on VCO performance.

TRADITIONAL approaches to the design of varactor-tuned Gunn oscillators in waveguide cavities present several obstacles as the conventional, two-post circuit is changed to different topologies.

For example, most designers now use the network representations of Marcuvitz[1] or Eisenhart and Khan.[2] Marcuvitiz' results, explained in the classic MIT Radiation Laboratory Series, provide only limited data on centered, cylindrical posts with a gap at one end. The analysis of Eisenhart and Khan, offered more recently, considers a most general single-post location in the waveguide, and has been used to study the performance of mechanically-tuned sources.[3] To apply this to the electrically-tuned, two-post circuit shown in Fig. 1, however, one must assume that the posts are isolated and coupled by the usual line transformation formula; this procedure thus ignores higher-order mode interaction between the two posts. Clearly, it cannot be applied to the case where the posts are located in the same cross-sectional plane of the guide, and also in the case where the two posts are close together and proximity effects between the posts are significant.

To summarize, neither analysis can be used to accurately describe a general case of N posts with a high degree of confidence. Perhaps the most serious difficulty with waveguide post circuits is that they are not easily understood, and are rarely analyzed in detail. For example, the effect of varying Gunn and varactor diode post diameters, the heights at which the diodes are mounted in the posts, post offsets from the sidewalls, distance between the posts and the short circuit, and their multiple interaction may not be immediately obvious, especially when the interactions between various components must be considered over an extended frequency range.

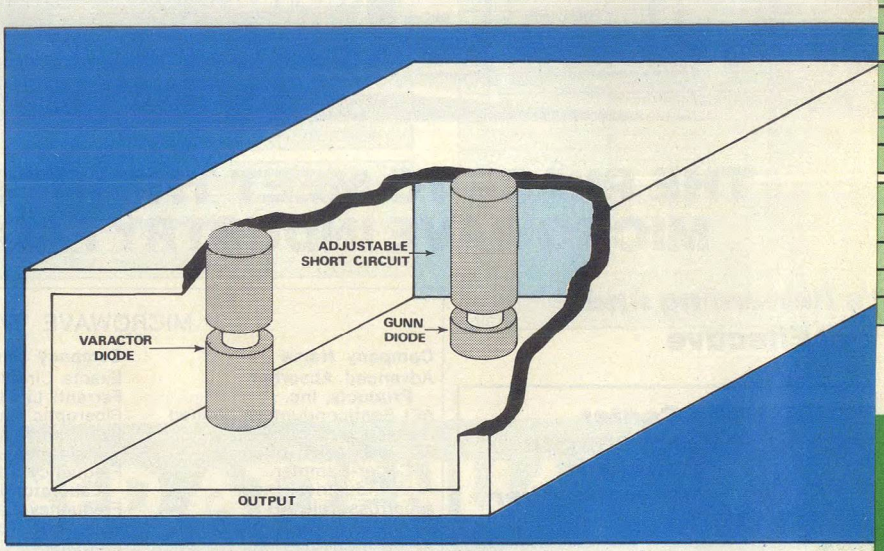

***1. A typical, electronically tuned waveguide oscillator** places semiconduc devices in cylindrical posts parallel to the electric field vector. One wavegu arm is terminated in a short circuit, while the other is coupled to a matc output.*

Ralph M. Eaton, Dr. Jai S. Joshi, Mullard, Ltd., Bramhall Moor Lane, Hazel Grove, Stockport, SK7 5 B. J. Cheshire, England.

Needed: A unified theory

It is with a view to overcoming these difficulties in the design and analysis of varactor-tuned Gunn oscillators that the general theory of N posts in a rectangular waveguide was developed. The computer-aided design approach outlined here is based on the special two-post case (N = 2) of a recently published unified network representation for waveguide post configurations.[4,5] The obstacle network for the dominant H_{10} waveguide mode for a general configuration is used in the work.

The attractive feature about the computer approach to analysis is its inherent generality.

- A single program can be writ for all circuits from L to Q band
- Frequency variation with varac bias and/or short-circuit position be predicted.
- "Allowed" varactor post positi and bias levels can be determine
- General post locations for both Gunn and the varactor diode can considered.
- The computer program caters all common types of active (Gu Impatt or tunnel diodes) and pass (varactor, PIN) devices.
- The routine can be modified use with doubly excited sources, s as those with two Gunn diodes i single cavity.

There is virtually no restriction any of the geometrical parame used in the analysis. Different type active and passive devices and t packages can be accommodated ea by entering appropriate device package parameters. Any sim

Table 1: The 15 key equations

1. $$Z_{mn} = j \frac{\eta b}{ak\,(2 - \delta_n)} \frac{k^2 - k_y^2}{(k_x^2 + k_y^2 - k^2)^{1/2}}$$

where:

$$k_x = \frac{m\pi}{a}, \quad k_y = \frac{n\pi}{b}, \quad k = \frac{2\pi}{\lambda} = \frac{2\pi c}{f}$$

$$\Gamma_{mn} = (k_x^2 + k_y^2 - k^2)^{1/2}$$

$\eta = 120\pi$ ohms: free space impedance

m, n: mode indices for field variation in x and y directions, respectively

c = free space velocity of propagation

and δ_n is an indicator with the definition

$\delta_n = 1$, for $n = 0$

$= 0$, for $n \neq 0$

$\beta = -j\,\Gamma_{10}$ = propagation constant for H_{10} mode

$$= \sqrt{(\frac{2\pi}{\lambda})^2 - (\frac{\pi}{a})^2}$$

2. Z_{C10} = characteristic impedance of H_{10} mode

$$= \eta \frac{2b}{a} \frac{k}{\beta}$$

3. $$k_{ipm} = \sin k_x s_i \frac{\sin \theta_{im}}{\theta_{im}}$$

4. $$k_{ign} = \cos k_y h_i \frac{\sin \theta_{in}}{\theta_{in}}$$

for i = 1, 2 for posts 1 and 2, respectively.

where $\theta_{im} = \frac{m\pi\omega_i}{2a}$

$\theta_{in} = \frac{n\pi g_i}{2b}$

$\omega_i = 1.8\,d_i$

and k_{ipm} and k_{ign} are post and gap coupling factors for posts 1 and 2, respectively.

5. $$Y_u = \frac{j}{2Z_{10}} \left[\frac{1}{k_{1p1} k_{2p1} \sin \beta L} - \frac{1}{k_{1p1}^2 \tan \beta L} \right]$$

6. $$Y_v = -j \frac{1}{2Z_{10} k_{1p1} k_{2p1} \sin \beta L}$$

7. $$Y_w = \frac{j}{2Z_{10}} \left[\frac{1}{k_{1p1} k_{2p1} \sin \beta L} - \frac{1}{k_{2p1}^2 \tan \beta L} \right]$$

8. $$Z_p = j\eta \frac{bk}{a} \sum_{m=2}^{\infty} \frac{k_{1pm}^2 - k_{1pm} k_{2pm}\, e^{(-\Gamma_{m0} L)}}{\Gamma_{mo}}$$

9. $$Z_q = j\eta \frac{bk}{a} \sum_{m=2}^{\infty} \frac{k_{2pm}^2 - k_{1pm} k_{2pm}\, e^{(-\Gamma_{m0} L)}}{\Gamma_{m0}}$$

10. $$Z_r = j\eta \frac{bk}{a} \sum_{m=2}^{\infty} \frac{k_{1pm} k_{2pm}\, e^{(-\Gamma_{m0} L)}}{\Gamma_{mo}}$$

11. $$Y_A = \sum_{n=1}^{\infty} \left[\frac{Z_{22n} - Z_{12n}}{(Z_{11n} Z_{22n} - Z_{12n}^2)} \right]$$

12. $$Y_B = \sum_{n=1}^{\infty} \left[\frac{Z_{12n}}{(Z_{11n} Z_{22n} - Z_{12n}^2)} \right]$$

13. $$Y_C = \sum_{n=1}^{\infty} \left[\frac{Z_{11n} - Z_{12n}}{(Z_{11n} Z_{22n} - Z_{12n}^2)} \right]$$

14. $$jX_s' = jX_{s1} + jX_{s2}$$

15. $$jX_{si} = -j\, Z_{c10} (\frac{a}{\lambda_g})(\frac{\pi d_i^2}{a}) \sin^2 (\frac{\pi s_i}{a})$$

tance is taken into account. Impedance or admittance elements which represent the effect of various (m, n) modes are isolated in the circuit models. The network labeled (b) is applicable to the coplanar arrangement (see Fig. 2(d)) where both posts are located in the same waveguide cross-sectional plane. The circuit shown as (c) is useful when one post is closer to the output. Let's define the illustrated network (c) as Type 1, since the varactor diode is nearest to the short-circuit plane. Likewise, we'll call a Type 2 circuit one in which the Gunn device is nearest to the short circuit; this can be analyzed by simply interchanging Gunn and varactor diode representations in Fig. 3(c).

The key equations that define the various equivalent circuit elements are listed in Table 1. Each is expressed in identifiable waveguide and post geometry parameters and the frequency of operation.

Although the theory behind the equivalent networks will not be propounded, some notes on the equivalent networks are in order. Branch 1-1′ represents the matched waveguide port, and takes the effect of post thickness capacitance into consideration. Branch 2-2′ represents the effects of a variable short circuit in waveguide arm two, and also considers contributions from post thickness capacitance. Transformer ratios k_{1p1} and k_{2p1} refer posts 1 and 2, respectively, to the center of the waveguide for the dominant (H_{10}) mode.

Admittance elements in the equivalent networks, Y (u, v, w), account for the coupling of the dominant H_{10} mode between the two posts (for a staggered arrangement). Impedance elements, Z (p, q, r) account for all modal components from m = 2 to ∞, for (n = 0 modal variation in the x-direction only). Admittance elements

(continued on p. 76)

Y (A, B, C) account for the double infinite summation for all modal variation except n = 0, in both x and y directions (that is, for m = 1 to ∞, and n = 1 to ∞). Upper limits for the summation of m and n modal values are spelled out in reference 5; identical correction factors are used for Z (p, q, r) elements.

The two gap ports are terminated in the device and package equivalent circuits for the Gunn and varactor diodes. Table 2 details 23 basic parameters, electrical and physical, which completely define the devices used in the VCO. The Gunn device is represented as a parallel equivalent circuit with negative conductance, $-G_D$, and device capacitance, C_D, in addition to a π-network which represents the package. Conductance and the capacitance of the device model are assumed to be independent of frequency, simply because there is as yet no satisfactory representation of variation with parameters such as frequency and bias voltage. The package representation in the form of a π-network is quite adequate, and the parameters for the typical S4 package in S-band are well known.

The varactor diode is represented by a capacitance, C_V, which is a function of bias voltage, and a series resistance, R_V, which is independent of bias. The S4 varactor diode package takes the form of a series-shunt network with package inductance and case capacitance, respectively.

Although these representations of the active devices are adequate for most applications, a computer program can be easily modified to suit alternative device and/or package representations one might encounter.

Look for stability

The equivalent circuits of Fig. 3, including representations for the Gunn and varactor diodes, are best analyzed by computer. The object: To evaluate the admittance appearing across the Gunn diode chip (looking into terminals X-X′). This load admittance, $G_L + jB_L$, can then be compared with the Gunn diode chip admittance, $G_D + jB_D$, to obtain stable oscillating points. Needless to say, G_L and B_L are complicated functions of frequency for a given configuration.

Two conditions must be satisfied to sustain circuit-controlled, steady-state oscillations using a negative conductance device:

$$G_D(\omega) + G_L(\omega) = 0 \quad (1)$$

$$B_D(\omega) + B_L(\omega) = 0 \quad (2)$$

where $G_D(\omega)$ and $B_D(\omega)$ are, respectively, the real and imaginary parts of the device admittance, and $G_L(\omega)$ and $B_L(\omega)$ are, respectively, the real and imaginary parts of the load admittance. For Gunn VCOs, the zero susceptance condition (Eq. 2) is a necessary condition for oscillation: It *must* be satisfied for oscillation to take place. Equation 1 is generally an indicator of output power.[3]

But even if a circuit satisfies the above two conditions, it may not sustain oscillations at that frequency, if it is an unstable operating point. Thus, a stability criteria must be imposed:

$$\frac{\delta B}{\delta \omega} > 0 \quad (3)$$

where $B(\omega)$ is the total susceptance, $B_D(\omega) + B_L(\omega)$, of the circuit in question.

In addition, one might consider two postulates ventured by Eisenhart and Khan for determining the stable operating points of a VCO using a Gunn device:[3]

1. The output power of the negative conductance device increases with load conductance, G_L, for $G_L < |G_D|$, with maximum output power as $G_L \rightarrow G_D$, where $|G_D|$ is the maximum value of conductance the device can deliver.

2. Under multiresonant circuit conditions, the oscillation will occur at the frequency for which G_L is maximum, though not greater than G_D.

The stable operating points of an oscillator determined by the above two postulates compare favorably with those predicted by the stability criteria.[6] In addition, tuning characteristics can be determined at a glance from the two rules.

Apply the equivalent networks

The challenge, then, boils down to writing a computer program which searches for an oscillation point and also determines whether it is a stable point of operation. This procedure is characterized by ten basic steps:

1. Recognize that all varactor-tuned, Gunn oscillators built in waveguide with constant-diameter posts can be represented by the equivalent networks of Fig. 3.

2. Select the correct equivalent network (one of three).

3. Determine the values of the 23 circuit parameters listed in Table 2.

(continued on p. 78)

Table 2: The 23 basic parameters

1. a = waveguide A dimension
2. b = waveguide B dimension
3. s_1 = Gunn post offset from sidewall
4. d_1 = Gunn diode post diameter
5. h_1 = Gunn height above broadwall
6. g_1 = Gunn post gap size
7. s_2 = varactor post offset from sidewall
8. d_2 = varactor post diameter
9. h_2 = varactor height above broadwall
10. g_2 = varactor post gap size
11. L_Z = separation between post planes
12. G_D = Gunn negative conductance
13. C_D = Gunn chip capacitance
14. L_D = Gunn package inductance
15. C_P = Gunn package capacitance
16. C_I = Gunn stray capacitance
17. R_V = varactor diode series resistance
18. C_V = varactor junction capacitance
19. L_{DV} = varactor package inductance
20. C_{PV} = varactor package capacitance
21. T = type of circuit (1 or 2)
22. f = frequency of operation
23. L = distance of S/C from nearest post

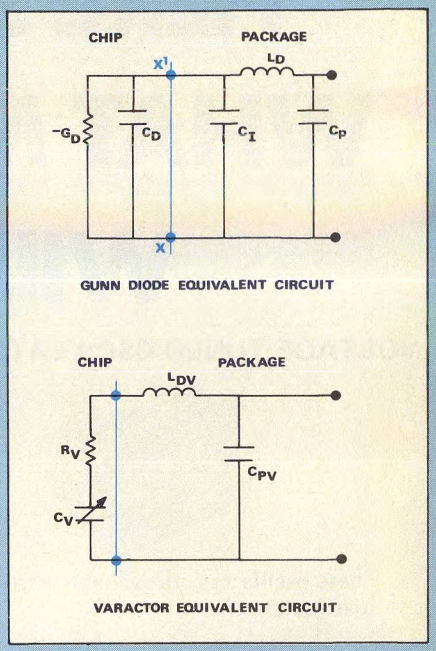

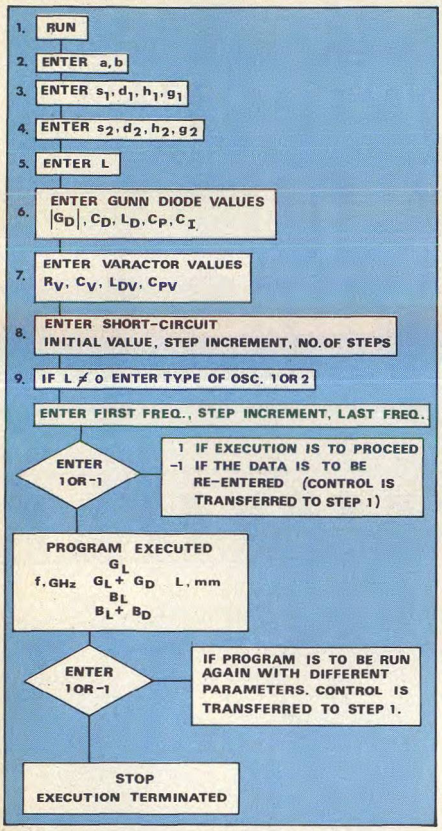

***4. Flow chart illustrates a program** written to calculate circuit conductance and susceptance.*

4. Determine the values of the circuit elements of Fig. 3 by using the values given to the 23 basic circuit parameters and feeding these into the 15 key equations listed in Table 1.

5. Transform the circuit elements, using transformations such as star-delta, to find the circuit admittance at terminals X-X′.

6. Segregate the real and imaginary parts of the circuit admittance.

7. Apply the oscillation criterion, and determine oscillation points.

8. Alternately, apply the stability criteria of Eisenhart and Khan to find the oscillation points.

9. Arrange for data to be presented in a usable format, for example a table of impedance versus short-circuit position and frequency, or oscillation frequency versus short-circuit position.

10. Finally, arrange a data return path, so that any one selected parameter or all parameters can be modified for successive computational trails.

Figure 4 outlines a flow chart for a computer program written along these

(continued on p. 80)

```
    GENERAL TWO POST CONFIGURATION

WAVEGUIDE SIZE   A=22.860   B=10.160  MMS.
POST PARAMETERS : POST NO.1   S1=11.430   D1= 4.800   H1= 5.080   G1= 1.600  MMS.
                  POST NO.2   S2= 4.330   D2= 3.800   H2= 5.080   G2= 1.600  MMS.
SEPARATION BETWEEN POST PLANES   L= 11.00  MMS.

GUNN PARAMETERS   |GD|= 0.030 MHOS CD= 0.250 PF. LD= 0.435 NH  CP= 0.150 PF CI= 0.100 PF
VARACTOR DIODE PARAMETERS   RV= 1.000 OHMS   CV= 0.750 PF   LDV= 0.435 NH   CPV= 0.100 PF

COUPLING FACTOR FOR POST 1:  KP11=.94228   POST 2:  KP21=.54015


FREQ.   GHZ.                        SHORT CIRCUIT POSITION  MMS.
          5.00      6.50      7.00      7.50      8.00      8.50      9.00      9.50

11.00   0.034015  0.045975  0.072461  0.148841  0.201570  0.037320  0.006217  0.001320
        0.004015  0.015975  0.042461  0.118841  0.171570  0.007320 -0.023783 -0.028680
        0.075494  0.086020  0.101142  0.104614 -0.080948 -0.038932 -0.039622 -0.014896
        0.092772  0.103298  0.118420  0.121893 -0.063670 -0.071653 -0.022344  0.002382

        S.C. POSITION FOR OSCILLATION= 7.83 MMS
        LOAD SUSCEPTANCE BL= -0.017279 SIEMENS
        LOAD CONDUCTANCE GL=  0.183478 SIEMENS
        CONDUCTANCE SUM:INDICATOR OF O.P. POWER=  0.153478 SIEMENS

        S.C. POSITION FOR OSCILLATION= 9.45 MMS
        LOAD SUSCEPTANCE BL= -0.017279 SIEMENS
        LOAD CONDUCTANCE GL=  0.001791 SIEMENS
        CONDUCTANCE SUM:INDICATOR OF O.P. POWER= -0.028209 SIEMENS

        0.046646  0.073568  0.150431  0.200424  0.037666  0.006270  0.001267  0.000899
        0.016646  0.043568  0.120431  0.170424  0.007666 -0.023730 -0.028733 -0.029101
        0.086324  0.101294  0.103556 -0.081382 -0.089270 -0.040057 -0.015197 -0.001221
        0.103760  0.118730  0.120991 -0.063947 -0.071834 -0.022621  0.002239  0.016215

        S.C. POSITION FOR OSCILLATION= 7.33 MMS
        LOAD SUSCEPTANCE BL= -0.017436 SIEMENS
        LOAD CONDUCTANCE GL=  0.183138 SIEMENS
        CONDUCTANCE SUM:INDICATOR OF O.P. POWER=  0.153138 SIEMENS

        S.C. POSITION FOR OSCILLATION= 8.95 MMS
        LOAD SUSCEPTANCE BL= -0.017436 SIEMENS
        LOAD CONDUCTANCE GL=  0.001718 SIEMENS
        CONDUCTANCE SUM:INDICATOR OF O.P. POWER= -0.028282 SIEMENS

11.20   0.071793  0.143979  0.209367  0.041992  0.006871  0.001287  0.000815  0.001467
        0.041793  0.113979  0.179367  0.011992 -0.023129 -0.028713 -0.029185 -0.028533
        0.100286  0.104846 -0.068656 -0.092985 -0.042076 -0.016197 -0.001747  0.007399
        0.117878  0.122439 -0.351063 -0.075392 -0.024483  0.001396  0.015846  0.024992

        S.C. POSITION FOR OSCILLATION= 6.85 MMS
        LOAD SUSCEPTANCE BL= -0.017593 SIEMENS
        LOAD CONDUCTANCE GL=  0.190123 SIEMENS
        CONDUCTANCE SUM:INDICATOR OF O.P. POWER=  0.160123 SIEMENS

        S.C. POSITION FOR OSCILLATION= 8.47 MMS
        LOAD SUSCEPTANCE BL= -0.017593 SIEMENS
        LOAD CONDUCTANCE GL=  0.001588 SIEMENS
        CONDUCTANCE SUM:INDICATOR OF O.P. POWER= -0.028412 SIEMENS

        0.130889  0.222559  0.051998  0.008265  0.001417  0.000725  0.001352  0.002263
        0.100889  0.192559  0.021998 -0.021735 -0.028583 -0.029275 -0.028648 -0.027737
        0.106951 -0.038889 -0.100213 -0.046037 -0.018065 -0.002701  0.006901  0.013509
        0.124701 -0.021139 -0.082463 -0.028287 -0.000315  0.015049  0.024651  0.031259

        S.C. POSITION FOR OSCILLATION= 6.43 MMS
        LOAD SUSCEPTANCE BL= -0.017750 SIEMENS
        LOAD CONDUCTANCE GL=  0.209272 SIEMENS
        CONDUCTANCE SUM:INDICATOR OF O.P. POWER=  0.179272 SIEMENS
        S.C. POSITION FOR OSCILLATION= 8.01 MMS
        LOAD SUSCEPTANCE BL= -0.017750 SIEMENS
        LOAD CONDUCTANCE GL=  0.001403 SIEMENS
        CONDUCTANCE SUM:INDICATOR OF O.P. POWER= -0.028597 SIEMENS

11.40   0.225690  0.071763  0.011013  0.001743  0.000638  0.001208  0.002138  0.003103
        0.195690  0.041763 -0.018987 -0.028257 -0.029362 -0.028792 -0.027862 -0.026897
        0.008741 -0.110203 -0.052576 -0.021078 -0.004216  0.006105  0.013104  0.018218
        0.026649 -0.092302 -0.034669 -0.003171  0.013691  0.024012  0.031011  0.036125

        S.C. POSITION FOR OSCILLATION= 6.11 MMS
        LOAD SUSCEPTANCE BL= -0.017907 SIEMENS
        LOAD CONDUCTANCE GL=  0.191206 SIEMENS
        CONDUCTANCE SUM:INDICATOR OF O.P. POWER=  0.161206 SIEMENS

        S.C. POSITION FOR OSCILLATION= 7.59 MMS
        LOAD SUSCEPTANCE BL= -0.017907 SIEMENS
        LOAD CONDUCTANCE GL=  0.001535 SIEMENS
        CONDUCTANCE SUM:INDICATOR OF O.P. POWER= -0.028465 SIEMENS

        0.109021  0.016395  0.002450  0.000580  0.001031  0.001977  0.002984  0.003943
        0.079021 -0.013605 -0.027550 -0.029420 -0.028969 -0.028023 -0.027016 -0.026057
       -0.117576 -0.062736 -0.025686 -0.006494  0.004907  0.012476  0.017922  0.022087
       -0.099511 -0.044672 -0.007622  0.011570  0.022971  0.030540  0.035987  0.040151

        S.C. POSITION FOR OSCILLATION= 7.20 MMS
        LOAD SUSCEPTANCE BL= -0.018064 SIEMENS
        LOAD CONDUCTANCE GL=  0.001707 SIEMENS
        CONDUCTANCE SUM:INDICATOR OF O.P. POWER= -0.028293 SIEMENS

11.60   0.027491  0.003946  0.000615  0.000826  0.001770  0.002826  0.003840  0.004781
       -0.002509 -0.026054 -0.029385 -0.029174 -0.028230 -0.027174 -0.026160 -0.025219
       -0.077996 -0.032640 -0.009851  0.003153  0.011540  0.017450  0.021900  0.025426
       -0.059775 -0.014419  0.008370  0.021375  0.029761  0.035672  0.040122  0.043648

        S.C. POSITION FOR OSCILLATION= 6.82 MMS
        LOAD SUSCEPTANCE BL= -0.018221 SIEMENS
        LOAD CONDUCTANCE GL=  0.001839 SIEMENS
        CONDUCTANCE SUM:INDICATOR OF O.P. POWER= -0.028161 SIEMENS
```

***5. Printout reproduces data fed into program,** and provides short-circuit position, load susceptance, load conductance, and an indicator of output power at discrete frequency steps.*

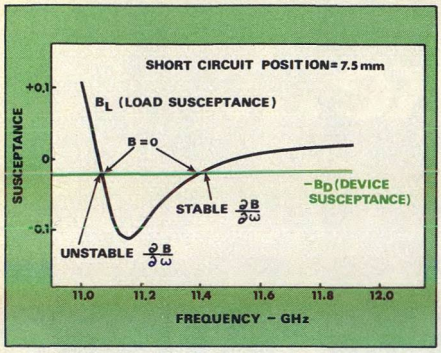

6. Stable and unstable regions *are determined by plotting load and device susceptance and evaluating their relative magnitudes*

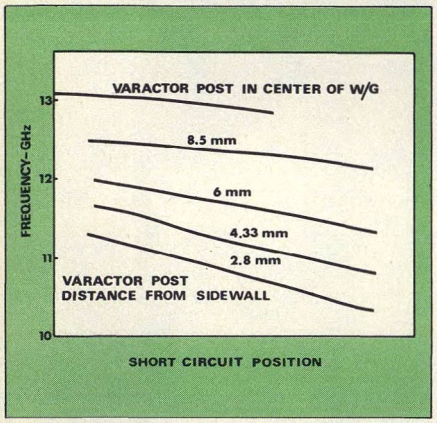

7. Frequency drops, but mechanical tuning range increases *somewhat as varactor post is offset from the centerline of the waveguide.*

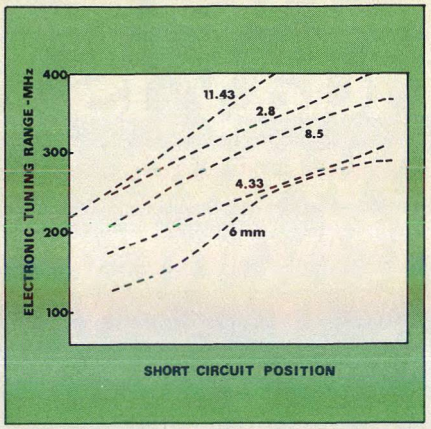

8. Electronic tuning range *depends on distance between varactor post and waveguide sidewall.*

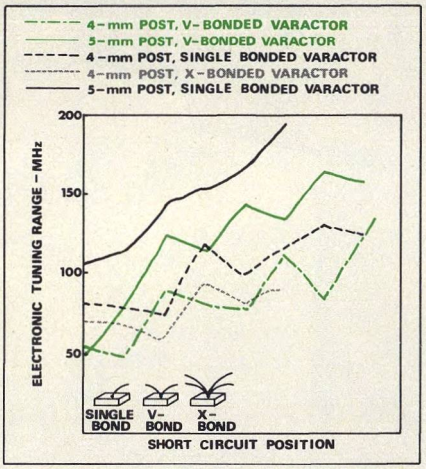

9. Tuning post diameter and bonding wire scheme *also influences electronic tuning range.*

lines. When the program is run, control instructions are first printed out, then a request is made for input data describing the 23 basic oscillator parameters of the circuit to be analyzed. Figure 5 illustrates a typical printout. Note that it begins by listing, for reference with the results, the basic parameters. This data is followed by the predicted microwave performance for each frequency, arranged in four lines according to G_L (circuit conductance), $G_L + G_D$ (total conductance, circuit plus active device), B_L (circuit susceptance) and $B_L + B_D$ (total susceptance, circuit plus active device). The variation of these parameters with short-circuit position is also computed.

The points of oscillation are obtained by linear interpolation between data points with the application of the oscillation condition and the two stability postulates of Eisenhart and Khan. Figure 6 illustrates the typical variation of B_L and $-B_D$ with frequency; the stable oscillation points can be isolated by determining the value of the slope ($\delta B/\delta\omega$) at the oscillation point.

Data gained from this type of analysis program can be used in a number of interesting ways. For example, Figs. 7, 8 and 9 illustrate the effects of changing short-circuit position, varactor-diode post diameter, varactor post offset from waveguide center, and varactor bonding arrangement. Other circuits have been optimized with respect to varactor loss factor, varactor height above the broadwall of the waveguide (h^2), distance between Gunn and varactor post planes, and Gunn-diode bonding arrangement.

The typical accuracy achieved to date in studies of X-band oscillators is ±1 per cent for prediction of center frequency, although some predictions have been within ±0.1 per cent. Sensitivity measurements—gauging the effect of changing one circuit parameter to observe a change in frequency—can be much more accurate, typically 0.02 per cent of center frequency. This corresponds to an electronic tuning range prediction accurate to ±2 per cent.

It should be noted, however, that accurate package and device description in the CAD work is of paramount importance since it transfers the circuit impedance to the active terminals. Any inaccuracy in defining these parameters directly affects the oscillation frequency, and hence, the accuracy of the CAD prediction. Be sure to use the most accurate device and package description available to you!

Afterthoughts on applications

Although CAD is normally associated with the initial design phase of a component, it is extremely useful at other stages. In troubleshooting, for instance, computer simulations can often reproduce undesirable modes of operation or frequency jumps in the operation of an oscillator. These may then be controlled through either a change of circuit parameters or device impedance characteristics.

One of the most useful applications of the CAD technique is the extension of circuit performance. Computer-aided analysis can quickly indicate how a familiar production VCO can be simply modified to produce an entirely new range of circuits. One production circuit at Mullard has three commercially viable off-springs which have been either described or optimized by the CAD process described here.

Finally, analysis with a computer allows one to select the optimum package and chip parameters for both Gunn and varactor diodes. Varactor loss resistance, chip capacitance, capacitance ratio and Gunn chip impedance parameters, as well as package inductance and capacitance can be quickly fed into the program to determine their influence on the circuit.••

References

1. N. Marcuvitz, "Waveguide Handbook", *MIT Rad. Lab. Series*, Vol. 10, McGraw-Hill, New York, (1951).
2. R. L. Eisenhart and P. J. Khan, "Theoretical and Experimental Analysis of a Waveguide Mounting Structure," *IEEE Transactions Microwave Theory and Techniques*, Vol. MTT-19, pp. 707-719, (August, 1971).
3. R. L. Eisenhart and P. J. Khan, "Some Tuning Characteristics and Oscillation Conditions of a Waveguide Mounted Transferred-Electron Diode Oscillator," *IEEE Transactions on Electron Devices*, Vol. ED-10, pp. 1050-1055, (September, 1972).
4. J. S. Joshi and J. A. F. Cornick, "Analysis of Waveguide Post Configurations: Part 1 - Gap Immitance Matrices," *IEEE Transactions on Microwave Theory and Techniques*, Vol. MTT-25, No, 3, pp. 169-173, (March, 1977).
5. J. S. Joshi and J. A. F. Cornick, "Analysis of Waveguide Post Configurations: Part II - Dual Gap Cases," *IEEE Transactions on Microwave Theory and Techniques*, Vol. MTT-25, No. 3, pp. 173-181, (March, 1977).
6. J. S. Joshi and J. A. F. Cornick, "Analysis of a Waveguide Mounting Configuration For Electronically Tuned Transferred-Electron Device Oscillators and Its Circuit Application," *IEEE Transactions on Theory and Techniques*, Vol. MTT-24, No. 9, pp. 573-584, (September, 1976).

Part II

VCO Subsystems: What To Test, How To Test It

Settling time and post-tuning drift measurements are big challenges to the VCO designer. The conclusion of this two-part series offers six methods, automated and manual, for mastering these tough tests.

THE transient performance of a voltage-controlled oscillator to an impulse stimulus is one of the most critical of all VCO measurements, and one of the most difficult to accurately determine. Since the time domain of these measurements extends from tens of seconds down to nanoseconds, the instrumentation and techniques used must be carefully chosen.

The most important of the transient measurements are those which describe tuning speed performance. Here, the dependent variable is the VCO frequency measured in time against the independent stimulus variable, the tuning voltage.

Transient measurements are normally divided into two areas. The first deals with the very fast transient performance of the VCO to a step function of tuning voltage in which the electrical time constants of the VCO circuit dominate the results. These *settling time* measurements occur in the timeframe of nanoseconds to microseconds, and tell how quickly and to what accuracy a VCO can be tuned from one frequency to another.

The second area deals with measurements in which several relatively long time constants—such as thermally related phenomena—come into play. These *post-tuning drift* measurements occur in the timeframe of tens of microseconds to tens of seconds, and basically tell how well a VCO will remain tuned to the newly commanded frequency.

A true transient measurement would be based on a "one-shot" impulse —in this case, the tuning-voltage change—being applied to the circuit under test, and the desired output results being recorded during an appropriate following timeframe. Unfortunately, for very short-term data outputs a one-shot measurement does not yield sufficient information for the degree of accuracy required. For example, if a frequency counter requires 10 μs of total sampling time to read frequency to a desired accuracy, it cannot be used to measure a frequency that occurs, say, 100 ns after the tuning impulse. Obviously, some compromises have to be made between true one-shot transient measurements and pseudo one-shot techniques in which a number of repetitive samples can be acquired and averaged to yield sufficiently accurate data.

Charles A. Bissegger, Manager, Special Programs, and **P. Michael O'Hara,** Associate Engineer, Omni Spectra, Inc., Microwave Subsystems Division, 2626 South Hardy Drive, Tempe, AZ 85282.

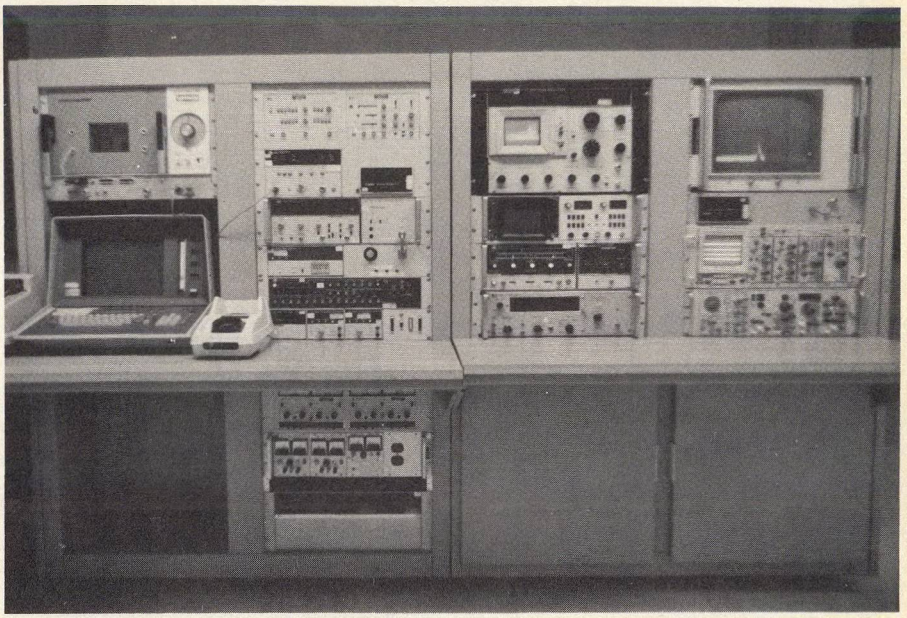

***1. Compete VCO testing station** includes calculator-controlled (automated) test instruments in the two left-hand bays, and transient test equipment in the two right-hand bays. Hard copier and X-Y plotter are not shown.*

Automated tests for PTD

While transient measurements generally output their data most conveniently on instruments such as high-speed oscilloscopes and spectrum analyzers, excellent use can be made of the computerized instrumentation (Fig. 1), used for the steady-state measurements described in Part I of this article (see "VCO Subsystems: What To Test, How To Test It, *MicroWaves*, pp. 60-64, May, 1977). Figure 2 lists some of the techniques that can be used for settling time and PTD measurements, along with the suitable timeframes for each. Note that two are "one-shot" and three use a repetitive stimulus.

The ideal transient performance test of a VCO would run something like this:

1. Computer commands VCO tuning to a resting frequency, f_r, and waits a predetermined time interval for the oscillator to stabilize.
2. Computer commands VCO tuning to a new test frequency, f_t, and instructs sampling counter and sampling voltmeter to take readings at times t_1,

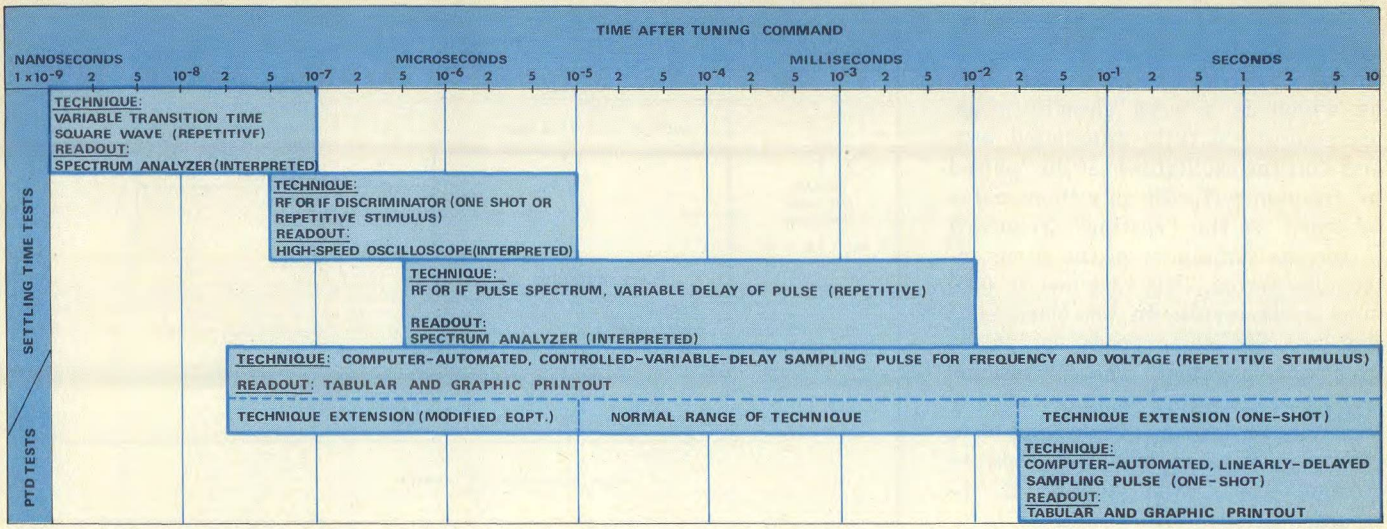

***2. Computer-controlled tests** are mainly used for the measurement of post-tuning drift, although equipment modifications can stretch the methods toward the 100 ns mark. Manual methods measure settling times as soon as 1 ns after tuning.*

t_2, etc., to end of test period, t_f.

3. Computer processes frequency and voltage readings versus time and outputs data in tabular and/or graphical form.

The test setup diagrammed in Fig. 3 will do exactly that required by the ideal sequence described, with two obvious limitations. First, a finite amount of time is required by the test equipment and the computer to interact with each other under the control of the general purpose interface bus (GP-IB). Typically, this is 10 to 20 ms per sample and depends on the equipment used. Second, a finite sampling time is required to obtain the necessary frequency resolution. While both the frequency and voltage sampling gates can be made as small as 30 ns in duration, a typical sampling type counter requires a total sample time of 10 μs for $\pm$50-kHz resolution, or 100 μs for $\pm$5 kHz resolution. Obviously, using even a 10-μs sample, the first time interval sampled on a one-shot basis would be a full 5 μs after the oscillator had been tuned. (This is the average time of the first sample period: from t_0 to t_0 + 10 μs).

The test then resolves itself into a repetitive type, with a number of samples taken, each on a successive tuning pulse at the same point in time, until a *total* sample time of 10 μs is accumulated. If the test were to use, say, a 50-ns sample time (per sample), then a total of 200 samples would be required. Remembering that the required handshaking time of the computer and the other instruments is about 15 ms, then a single point of data, resolved to a frequency accuracy of $\pm$50 kHz, would require 200 samples x 15 ms per sample, or 3 seconds.

Measure in 50 ns-10 μs range

Using the foregoing sampling times, an automated, repetitive test can be performed for either settling time or post-tuning drift. The measurement is based on a repetitive stimulus and variable delay sampling gate. The recommended time domain for the approach ranges from 50 ns to 10 μs.

If, for the moment, we confine ourselves to the settling time of t_0 to t_0 + 10 μs, we can set up a test which will measure the frequency variation of the VCO versus time during the first 10 μs after transition, with a 50-ns sample window, to an accuracy of $\pm$50 kHz. The test equipment is set up as shown in Fig. 3, except that the delay generator is a modified piece of standard equipment. If time increments of 50, 100, 200 and 500 ns, and 1, 2, 5 and 10 μs are sampled and recorded, and if the interpulse period is 20 ms (to allow adequate handshake time during the data acquisition), then 200 samples per time increment x 20 ms per sample x 8 time increments = 32 seconds per complete test. Figure 4 outlines a typical timing sequence.

(continued on p. 84)

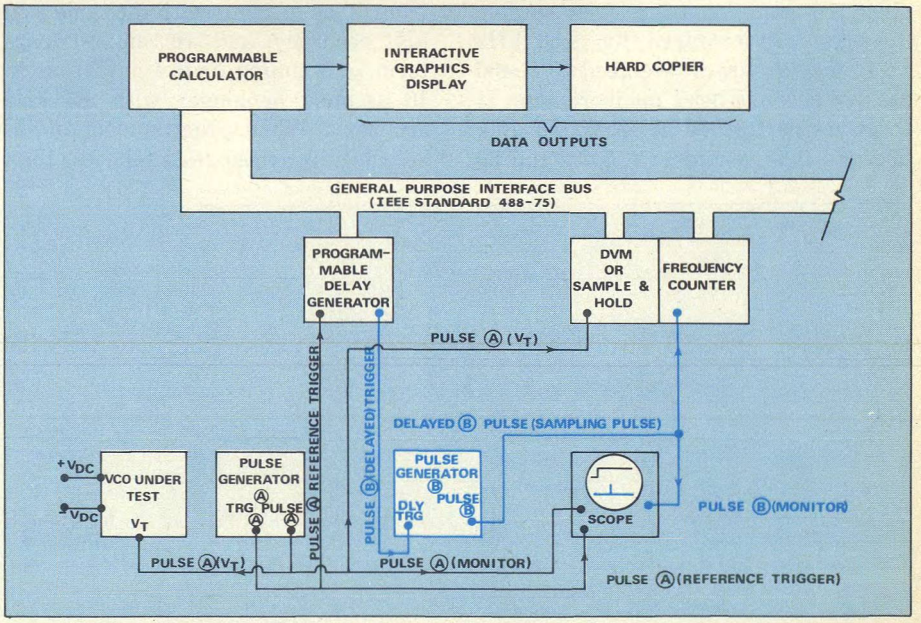

***3. Automated test setup** relies on two pulse generators to provide tuning and gating signals. Here, the gating pulse circuit is traced in color.*

Two points of note for this test are that the first time increment was the 50 ns span from t_o +25 ns to t_o to 75 ns which is a *very* close-in measurement for a fully automated test, and that the oscillator is at the "pulsed to" frequency (f_t) for only 10 μs and is returned to the "resting" frequency (f_r)for the remainder of the 20-ms interpulse period. This very low (0.0005) duty cycle results in test conditions that are, for all purposes, equivalent to a one-shot test. The 32 seconds required for the total test preclude any significant variations from long-term effects such as ambient temperature change, and power supply or instrumentation drift.

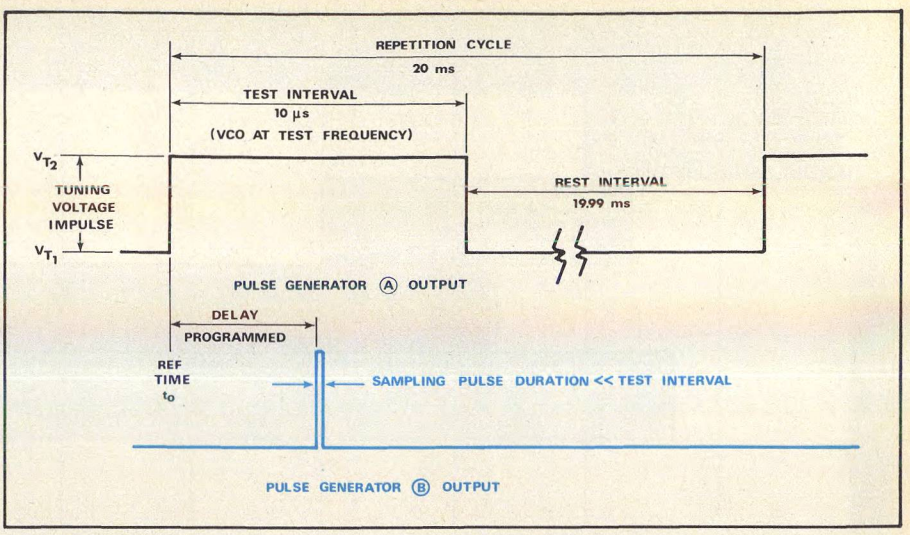

***4. Test and rest intervals** are established by pulse generator A in Fig. 2, while a delayed sampling window is set up by pulse generator B.*

Extend tests to 20 ms

A second automated test, covering the time period from 10 μs to 20 ms, falls in the category of a post-tuning drift measurement. The test equipment setup is identical to that of Fig. 3, but timing sequences are modified. The primary difference is that, since the first time increment is at 10 μs, the sampling gate can be opened up, perhaps to 1 μs, thereby reducing the number of repetitive pulses required for the total sample time of 10 μs (for ±50-kHz accuracy) to only 10 pulses. This is desirable because the interpulse period must be extended to retain some reasonably low duty cycle if the "pseudo one-shot" reasoning is maintained.

A 20-ms pulse and a 400-ms interpulse period corresponds to a 0.05 duty cycle—which is adequate. Also, since 10 samples of a 1-μs sample duration are required for ±50 kHz frequency accuracy, we need 10 × 400 ms = 4 seconds per time increment. If tests are performed at 10, 20, 50, 100, 200 and 500 μs and 1, 2, 5, 10 and 20 ms, then the 11 test times should require 11 x 44 seconds, or 44 seconds for the full test.

Determine drift to 10 seconds

The last automated test will be a real "one-shot" test as we have now reached the point where samples are being taken every 20 ms. This is sufficient time for the instruments to handshake between samples. If a 100-μs sampling gate is used, frequency resolution can be improved to ±5 kHz. Taking samples at 20, 50, 100, 200 and 500 ms, and at 1, 2, 5 and 10 seconds, only 10 seconds of test duration are needed to acquire and process the data.

Summarizing this sequence of three automated tests, we can test set-on time from 50 ns to 10 μs with ±50-kHz accuracy; we can test post-tuning drift from 10 μs to 20 ms with the same ±50 kHz accuracy; and we can test long-term post-tuning drift from 20 ms to 10 seconds or longer with ±5 kHz accuracy. When programmed to run sequentially, these tests take less than five minutes and provide data with 26 data points on a logarithmic time scale from 50 ns to 10 seconds. A typical run is plotted in Fig. 5.

An alternative to the 20 ms to 10 s test just described, which will yield a data point every 16 milliseconds or so (limited by handshake time of instruments), is accomplished by bypassing the delay generator and allowing the command calculator to sample frequency on a linear time scale. During the 10 seconds of the V_t pulse duration, some 640 samples are obtained.

Before proceeding to manual methods, consider for a moment the flexibility of automated measurements. Changes may be readily made to the program to meet specific test requirements. For example, higher accuracy may be obtained in exchange for longer sampling gates or longer test time.

Looking at the first 50 ns

For some transient VCO tests, there is no practical way to automate the

(continued on p. 88)

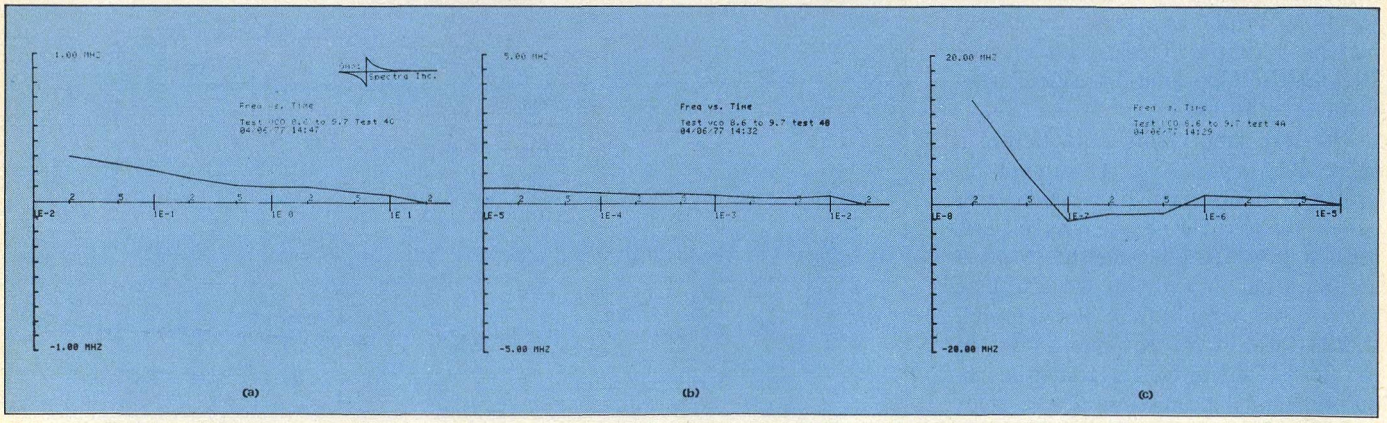

***5. Composite of three automated test** data presents the time domain from 10 ns to 20 seconds. Note changes in frequency scale between the plots.*

testing. Here, the best tools are your spectrum analyzer, your high-speed oscilloscope and your common sense.

Measuring the frequency of a VCO within the first 50 ns after a tuning impulse has been applied is a formidable task. Complicating the problem is the difficulty of producing a very fast risetime pulse (less than 10 ns risetime) of 10 V or greater, with a minimum of transient conditions such as overshoot or ringing, and a reasonably flat pulse top (±2 to 5 mV) for the duration of the test interval. But there are several techniques to work with the less-than-perfect signals and equipment available, yet come up with realistic data.

The first manual test to consider is a pulsed RF or IF spectrum method using variable pulse delay. This approach is convenient for quickly assessing an oscillator's post-tuning drift performance in a commonly used time domain—1 μs to 10 ms. It is recommended, for example, during the breadboarding phase of VCO development when a gross evaluation needs to be made. It is not recommended, however, for final test or proof of performance.

The only equipment needed for this method are two pulse generators (one of which has a variably delayed output), an RF or IF amplitude-gating device, such as a PIN switch or a double-balanced mixer, and a spectrum analyzer.

The equipment is set up as shown in Fig. 6. Pulse generator Ⓐ supplies the V_T stimulus and a trigger to pulse generator Ⓑ. This generator supplies a gating pulse approximately 1 μs wide at some manually set delay to fall within the duration of pulse Ⓐ. The 1-μs Ⓑ pulse gates the PIN RF switch or the double-balanced mixer (used as an amplitude modulator) to permit only that pulsed output to be passed on to the spectrum analyzer, which then displays the pulse spectrum signal. Using the center of the spectrum (or, preferably, one of the nulls) as a relative frequency reference, the frequency shift of the VCO can be determined at any point along the time duration of the Ⓐ pulse, by moving the gating Ⓑ pulse to that point and observing the spectrum's frequency shift.

The authors prefer to gate the IF by inserting a double-balanced mixer in the spectrum analyzer's IF system (usually at the first IF) as this eliminates some expensive RF modulators. Using the IF gating technique, the flat leakage through the mixer in the gated "off" condition is about −35 dBm. This method produces a CW signal on the analyzer display which is a handy reference indication of the VCO's final settled frequency (Fig. 7).

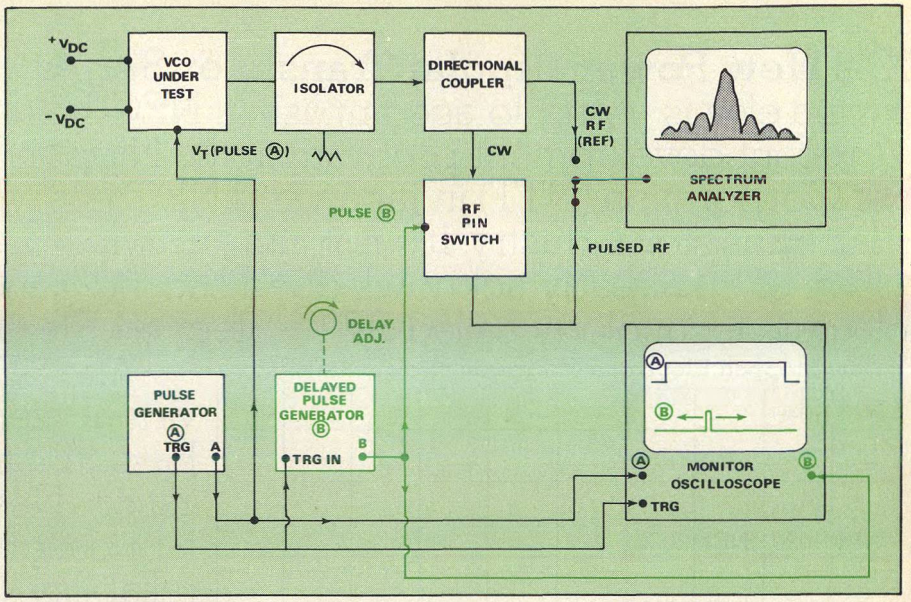

***6. Pulsed RF or IF spectrum method** measures settling time from 1 μs to 10 ms. It is recommended for breadboard evaluation.*

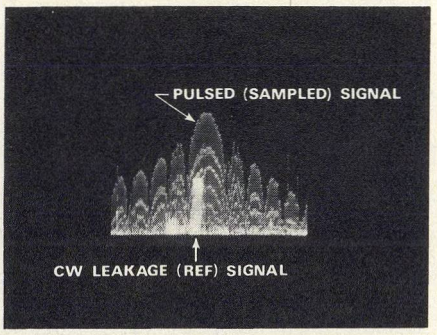

***7. IF gating method** allows a small level of CW leakage that can be used as a reference.*

The technique is limited by the minimum width of the gate which generates the spectrum, and the repetition rate for the Ⓐ pulse sequence. Using a recommended 1-μs pulse (which gives a satisfactory pulse spectrum for viewing), the minimum time delay from the start of the Ⓐ pulse would be 500 ns. At the other extreme, that of the recommended time domain of the Ⓐ pulse of 10 ms, the spectrum of the pulse signal becomes too dim to be viewed conveniently, even with a variable persistance storage CRT on the analyzer.

Again, this test, like all the others described here, is only as good as the fidelity of the pulse generator used to supply V_T.

Convert frequency to voltage

One obvious device to measure a frequency variation that occurs in a range of 50 ns to 100 ms would be a frequency-to-voltage converter, or a discriminator. Although either an RF or an IF discriminator would be usable, an IF-type preceded by a hard limiter is recommended. An IF discriminator has some definite advantages which include:

- A well-controlled, voltage-to-frequency transfer function.
- The capability of excellent hard-limiting to remove undesired AM.
- A high output level from the discriminator diodes.

A test setup incorporating IF discrimination is shown in Fig. 8. Note the use of a frequency generator and counter to calibrate the discriminator characteristic at the "pulsed-to" frequency range. Care must be taken to produce an output signal mixed to the proper level to yield optimum limiting in the limiter/discriminator.

The limiter/discriminator, a key component, can be home-built or purchased from several sources. The most important characteristics of the discriminator are bandwidth and video amplifier response. Since settling measurements may look at a frequency excursion of tens of megahertz, a minimum recommended bandwidth would be 60 MHz. This would, in turn, require an IF of at least 160 MHz. If a useful

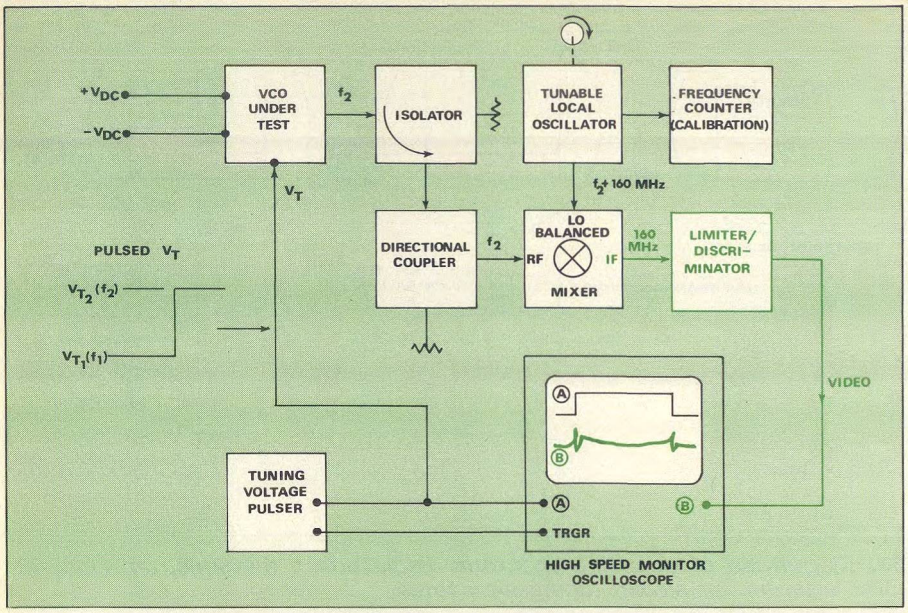

***8. This setup uses an IF limiter/discriminator** to measure settling time in the 50 ns to 100 μs range. Method converts VCO frequency to IF voltage,*

output from the discriminator is sought only 10 ns after the tuning pulse, the discriminator's video response must be capable of handling less than 10-ns risetimes. This implies minimum video response of DC to 35 MHz. Be careful in selecting the limiter/discriminator, as not all units have video bandwidths compatible with the discriminator range.

Once set up, the driving voltage pulse and the discriminator output response are simultaneously viewed on the dual-trace, high-speed oscilloscope. Figure 9 shows an oscilloscope recording of a 500-μs pulse repeated on a 0.1 duty cycle. Note that the final output from the discriminator at the end of the 500-μs pulse period is aligned with the quiescent zero. Signal output of the discriminator is used as the settling-time frequency reference. Also note in the expanded view of Fig. 10 that the transient responses of the mixer, limiter/discriminator, video amplifier and other components make accurate measurements impossible below 30 ns. If desired, a triggered one-shot display may be presented on the scope face and recorded by an oscilloscope camera. (The authors usually set up the display on a repetitive pulse basis first, and then one-shot it).

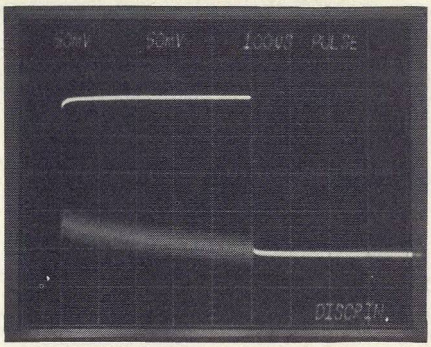

***9. Post-tuning drift over a 0.5 ms range** is shown in this oscilloscope display of the IF discriminator output. VCO modulation sensitivity is 50 MHz/V while discriminator sensitivity is 160 mV/MHz.*

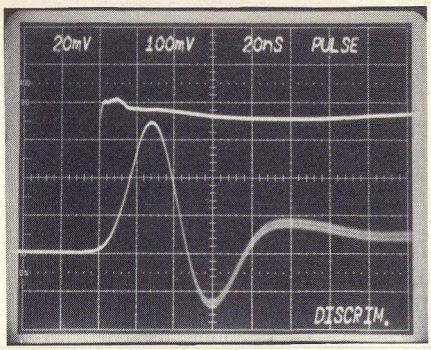

***10. Discriminator output is captured** 100 ns after tuning impulse. Note that the discriminator takes about 20 ns to respond (rising side of lower trace), then follows the oscillator's transient response (falling side of first peak thereafter).*

The ultimate challenge

The challenge of transient VCO measurements finally boils down to how you can realistically measure the oscillator's performance from the application of a tuning signal, t_o, to 10 ns thereafter. Suggested solutions range all the way out to some very exotic digitizing techniques which require elaborate, expensive computer equipment and processing, and still offer only vague accuracy in the 1-ns range.

The authors have struggled through a number of techniques in this difficult time domain and feel that the method now presented holds the most promise. Its most important advantage is that it requires only three pieces of equipment—and these are commonly used laboratory instruments—a spectrum analyzer, a high-speed oscilloscope and a variable risetime/falltime pulse or square-wave generator. The technique uses the spectrum analyzer to convert amplitude display into a slewing speed indication, using the variable transition time of the square-wave generator to control and calibrate the slew rates.

The typical spectrum analyzer uses two or more conversions to a final IF bandpass before detection and display on the CRT. This final bandpass can be imagined as being slowly (relative to the fast-moving VCO) scanned in frequency across the CRT face by the analyzer's YIG-tuned first local oscillator. If the VCO signal is rapidly slewed through this sampling window, only a small portion of the generated IF energy is detected and displayed. In fact, as long as the detected energy does not remain in the IF window long enough for the detector to recover the peak signal level, the relative amplitude of the displayed IF output is a direct indication of the speed at which the VCO signal was slewed through that IF window. If our slew rate is slowed to only one-tenth its previous rate, then the VCO signal is in the analyzer's IF window for 10 times as long and produces a signal that is 10-dB larger on the CRT display.

Figure 11 depicts a few typical slewing signals and the resultant displays. In Fig. 11 (a), the slewing signal is assumed to be able to change from $V_{T1(f_{low})}$ to $V_{T2(f_{high})}$ in zero time and the VCO is assumed to be able to follow it. The display, therefore, shows only a signal at f_L and f_H. In Fig. 11(b), a finite transition time (perhaps 10 ns) is used to slew the VCO over the 1000 MHz range from f_L to f_H, and the slewing rate of 100 MHz/ns results in the amplitude comb shown. In Fig. 11(c), an abrupt change in tuning voltage slope at the midway point of the transition results in a reduction of slew rate and an increase of amplitude for the displayed signal. (Note that the transitional interval of the V_T signal is much smaller than the repetition

(continued on p. 90)

rate to minimize pulse spectra in the displayed analyzer signal).

Using appropriate changes in the transition times of the tuning signal, the analyzer display can be calibrated over several decades from transition times ranging from 10 ns to perhaps 10 μs. (The authors use slope change increments of $\sqrt{10}$, resulting in 5-dB changes on the CRT display).

Maximum slew rate and settling time can now be determined using the calibrated display. If the VCO is capable of slew rates faster than 100 MHz/ns, the transition time of the square-wave generator must be reduced to less than 10 ns. The maximum slew rate is obtained when further reduction of the transition time fails to reduce the amplitude of the comb. Modern fast-tuning VCOs do not slew faster than 200 MHz/ns below 5 GHz, nor are pulse or square-wave generators available with good, sharp rise and fall times under 5 ns. This places a limit on the slewing speed test.

A well-designed (*video* as well as RF) VCO, driven by a pulse of square-wave generator with sharp transition-time responses, will generate a signal like that in Fig. 12. If the center of the V_T driving pulse is used as a timing reference (call this zero), the display near f_{high} can be interpreted as follows:

- **Point A** is the point where the oscillator begins to slow down below 100 MHz/ns. It reached point A, which is 450 MHz from the center of the display, in 450/100=4.5 ns.
- **Point B** is where the slew rate has slowed to 31.6 MHz. An average rate of 50 MHz/ns is assigned to the slew interval between f_a and f_b. The VCO covered this interval in 25/50 = 0.5 ns.
- **Points C, D and E** and frequencies f_c, f_d and f_e are reached in delta times of 0.5, 1.4 and 1.5 ns, respectively.
- Thus, the VCO arrived within 5 MHz of f_H in 8.4 ns.

The variable transition-time technique is more useful as an analytical tool used during the engineering phase than as a final test method. With a little practice, the spectrum analyzer display can yield quite a bit of valuable performance data on the VCO during those first crucial tens of nanoseconds after tuning. The display can be used to optimize the VCO video and RF constants to yield, for example, minimal overshoot performance. Like many of the other techniques, however, it is only as good as the fidelity of the driving V_T pulse—you cannot read out

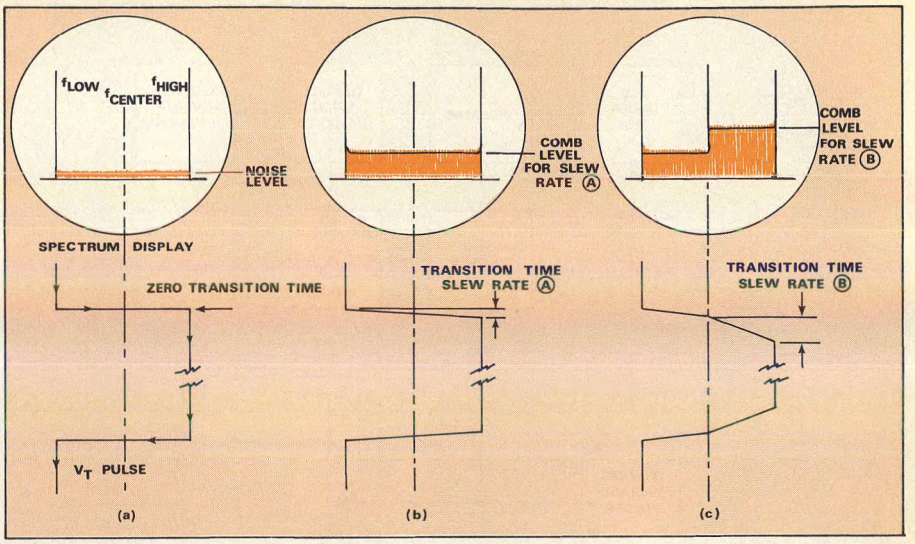

***11. Magnitude of combline spectrum** displayed on the spectrum analyzer CRT is larger for slower tuning slew rates.*

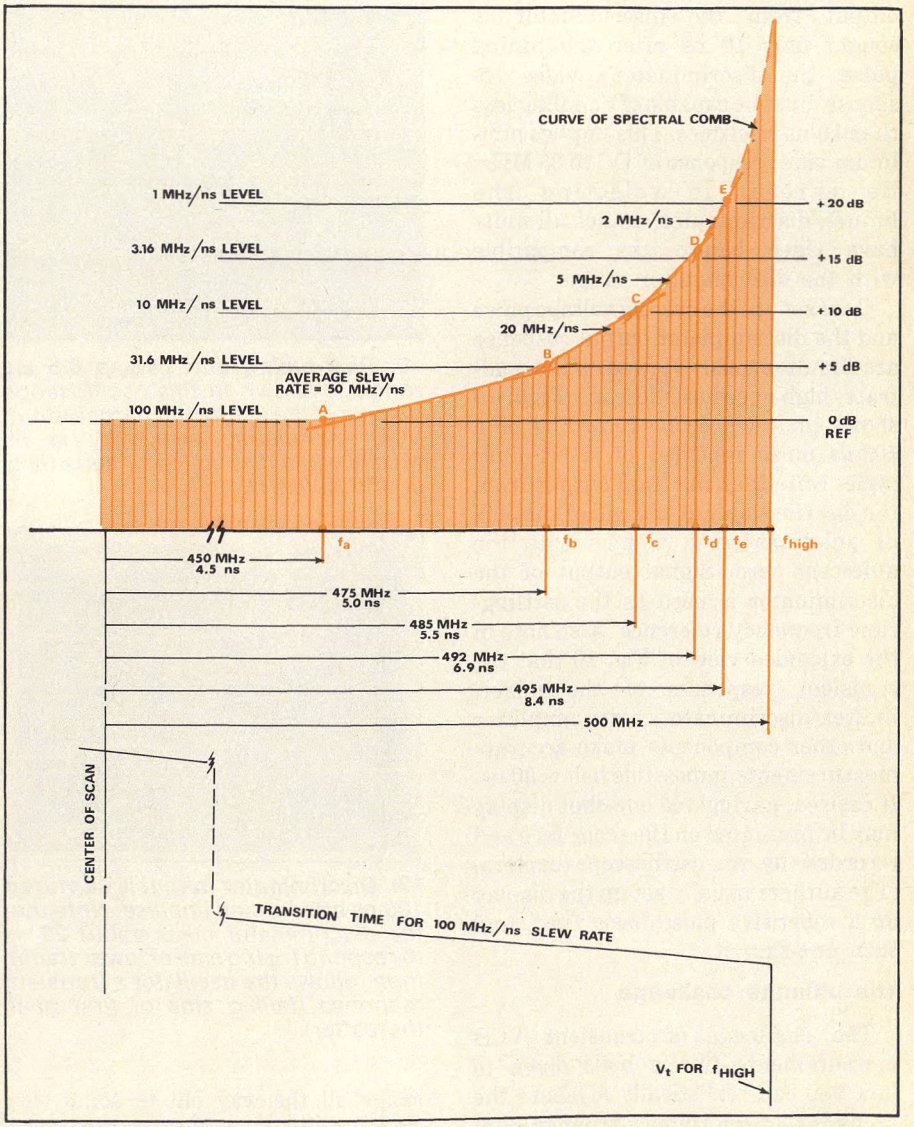

***12. A well-designed VCO** will generate this type of signal when driven by a pulse or square-wave generator with sharp transition time responses. See text for an explanation of points A through E.*

GaAs FET oscillators break into K band

Users of YIG-tuned, Gunn-effect oscillators who are seeking a more efficient method of generating power in K band will welcome model AV-71201, a YIG-tuned, GaAs FET source that covers the 12 to 18 GHz range.

The hermetically sealed, 14-ounce component delivers +7 dBm, flat to ±3 dB, with rather modest input power requirements: +15 V @ 125 mA and −6 V @ 60 mA. There are no extraordinary startup or threshold current requirements as with Gunn-effect oscillators.

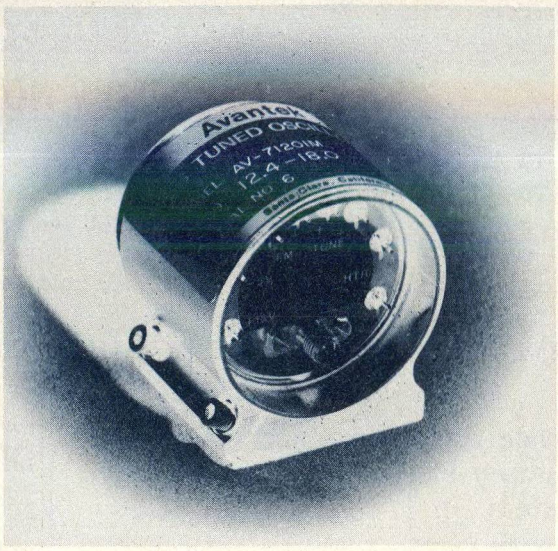

The new GaAs FET oscillator tops off a new product line that includes C and X-band models. Recommended applications include local oscillator functions in receivers, sweepers and spectrum analyzers. Harmonic multipliers are **not** needed to cover the 12 to 18 GHz range. Second and third harmonic output specifications for the fundamental transistor source are −15 dBc and −20 dBc, respectively. Spurious outputs are suppressed by more than −60 dBc.

Frequency drift is 50 MHz maximum over the rated case temperature range of 0 to +60° C. Achieving controlled oscillation at the lower end of the temperature range is said to be no problem, in contrast to some Gunn-effect designs. Other frequency stability specifications include a pulling figure of 5 MHz (at 12-dB return loss) and pushing figures of 1 MHz/V for the +15 V supply and 3 MHz/V for the −6 V supply.

The internal YIG tuning circuitry provides a typical sensitivity of 20 MHz/mA with a nominal 3-dB bandwidth of 5 kHz. Typical tuning linearity is ±0.1 per cent over the rated frequency range, while hysteresis is held to a typical value of 12 MHz. Input impedance of the tuning port is approximated by 5 ohms in series with 47 nH. Magnetic susceptibility at 60 Hz is typically 200 kHz/Gauss. The integral heater for the YIG tuning circuit draws a maximum of 2 W at 25° C (3 W at 0° C) and operates from a supply voltage of 20 to 28 V.

An auxiliary port allows frequency modulation. Sensitivity is 310 kHz/mA with a typical 3-dB bandwidth of 400 kHz. Maximum deviation at a 400 kHz modulation rate is 50 MHz. The FM port presents an impedance of 1 ohm in series with 1.25 μH. P & A: $1200 — $1500 depending on specifications. **Avantek, Inc., 3175 Bowers Avenue, Santa Clara, CA 95051 (408) 249-0700.** CIRCLE NO. 110

Performance Summary

Frequency range	12-18 GHz
Power output (min)	+7 dBm
Output variation (max)	±3 dB
Operating temperature	0-60° C
Drift with temperature (max)	5 MHz
Second harmonic (min)	−15 dBc
Third harmonic (typ)	−20 dBc
Spurious outputs (min)	−60 dBc
Tuning sensitivity (typ)	20 MHz/mA
Tuning sensitivity (typ)	±0.1%
FM sensitivity (typ)	310 kHz/mA
DC operating bias (max)	+15 V @ 125 mA −6V @ 60 mA
Frequency pushing (typ)	
for +15V bias	1 MHz/V
for −6 V bias	3 MHz/V
Weight (typ)	14 oz.

OSCILLATORS

BWO replaced by solid-state source

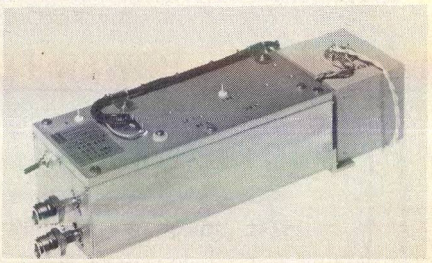

Improved performance and reliability are highlighted by a recently released 2 to 4 GHz YIG-tuned oscillator manufactured to replace the backward-wave oscillator in HP 8551 spectrum analyzers. Model FAM-21A features sweep and phase-locking interface circuits. Also, a dual-channel amplifier provides a minimum of 40-mW RF output from each channel. Residual FM is less than 30 kHz. Instant-on performance enhances the operation of the HP 8551. This new oscillator simplifies installation by conveniently attaching to the BWO mounting plate. The linearizing network requires no alignment, saving the user valuable technical time. High-voltage circuitry has been eliminated. Reflecting improved reliability, the warranty period has been pushed up to three years. P&A: $1,975; stock to 30 days. **Electronics Surveillance Components, Inc., 991 Commercial Street, Palo Alto, CA 94306 (415) 494-7803.** CIRCLE NO. 111

Constant-current source powers Impatt oscillators

A constant-current power supply is available to operate X-band GaAs Impatt oscillators, and Si devices in the 40 to 300 GHz range. Offered with either 115 or 240 VAC inputs, the power supply can be ordered with outputs up to 250 mA between 10 and 70 V. Units can also be supplied with an optional capability for frequency modulation using an external signal generator. **Plessey Optoelectronics and Microwave, Wood Burcote Way, Towcester, Northamptonshire, England Towcester (0327) 50312.**

CIRCLE NO. 112

AUGUST
1977

MICROWAVES

laser technology

SPECIAL REPORTS ON

Communications

Commercial Satcom Takes Off
Military Strategists Plan Future Systems
New Designs Considered For Mobile Radio
Japanese Designers Stress High-Capacity Links

PLUS:
Senate Orders Probe Of RF Hazards
Six-Ports Simplify Network Analysis
Define Spectrum Analyzer Dynamic Range

SPECIAL SECTION: Your guide to the
EUROPEAN
MICROWAVE
CONFERENC
See cov
facin

MICROWAVES

August 1977
Vol. 16, No. 8

news

editorial

technical

Special reports on

COMMUNICATIONS

departments

Product Features

About the cover: The Washington-to-Moscow "hot line" relies on parallel circuits in the Intelsat and Molniya II systems. This earth station is one of two located at Fort Detrick, MD, and was constructed by the Harris Corp., which kindly supplied the cover photograph.

coming next month: Electronic Warfare

A series of special reports will examine trends in a variety of important EW design areas ranging from acousto-optics to high-power jamming. News reports will include a survey of how microwave equipment is aiding cancer therapists, an examination of the first kilowatt-level transistorized L-band amplifier, and the latest news from the European Microwave Conference.

Publisher
Howard Bierman

Editor
Stacy V. Bearse

Associate Editor
Robert Wollins

Western Editor
Steven Peliotis
1870-E Ednamary Way
Mountain View, CA 94040
(415) 969-9452

Washington Editor
Paul Harris
Snyder Associates
1050 Potomac St. NW
Washington, DC 20007
(202) 965-3700

Editorial Assistant
Gail Murphy

Production Editor
Sherry Lynne Karpen

Art Director
Robert Meehan

Art Illustrator
Janice Tapp

Production
Dollie S. Viebig, Mgr.
Anne Molfetas

Circulation
Barbara Freundlich, Dir.
Sherry Karpen,
Reader Service

Directory Coordinator
Janice Tapp

Editorial Office
50 Essex St.,
Rochelle Park, NJ 07662
Phone (201) 843-0550
TWX 710-990-5071

A Hayden Publication
James S. Mulholland, Jr.,
President

MICROWAVES is sent free to individuals actively engaged in microwave work. Prices for non-qualified subscribers:

	1 Yr.	2 Yr.	3 Yr.	Single Copy
U.S.	$25	$40	$ 60	$3.00
Foreign	$40	$70	$100	$4.00

Additional Product Data Directory reference issue, $15.00 each (U.S), $27.00, (Foreign), POSTMASTER, please send Form 3579 to Fulfillment Manager, MicroWaves, P.O. Box 13801, Philadelphia, PA. 19101.

Back Issues of MicroWaves are available on microfilm, microfiche, 16mm or 35mm roll film. They can be ordered from Xerox University Microfilms, 300 North Zeeb Road, Ann Arbor, MI 48106. For immediate information, call (313) 761-4700.

Hayden Publishing Co., Inc., James S. Mulholland, President, printed at Brown Printing Co., Inc., Waseca, MN.

Japanese designers stress high-capacity links

Designers of Japan's fast-growing terrestrial communications network are taking a number of different approaches to transmit more information on fixed frequency allocations. Careful system design and construction along with innovative component developments are increasing the channel capacity of analog systems by more than a factor of two. Digital modulation, although poor in terms of spectral efficiency, is allowing designers to push to K-band frequencies where wide bandwidths can be exploited without the stringent noise and interference criteria required by FM/FDM systems.

Japan is considerably ahead of the US in the manufacture and implementation of digital systems, especially at K-band frequencies. Early this year, for example, the cities of Tokyo and Yokohama, and Osaka and Kobe were linked by 400-Mbit/s digital systems that operate in the vicinity of 20 GHz and carry eight active radio channels, each accommodating 5,760 voice circuits.

Designers of this system faced a major challenge common to all digital radio: spectral inefficiency. Although digital modulation is considerably less susceptible to noise and interference than analog techniques, it requires more bandwidth per channel. In fact, the voice channel capacity of current high-density PCM digital radios operating in the 6 and 11-GHz common-carrier bands is 25 per cent less than the US analog capacity and 50 per cent less than CCIR analog capacity, according to Harold Sobol, at Collins Commercial Telecommunications Div., Dallas, TX. Sobol, speaking at the International Microwave Symposium (San Diego, June 21-23), pointed out that proposed high-density single-sideband analog radio could have up to four times the channel capacity of present digital radios (see, "Bell System to begin SSB field trials," p. 12).

A closely interleaved frequency arrangement was devised by system planners from Nippon Telephone and Telegraph Public Company (NTT) to increase the channel capacity of the 20-GHz digital systems. As Fig. 1 points out, nine channels (eight active, one protection) are squeezed in the 3.5-GHz bandwidth from 17.7 to 21.2 GHz. Adjacent channels are spaced by only 320 MHz (1.6 f_p), which improves frequency usage, but also raises the potential for cross-polarization interference.

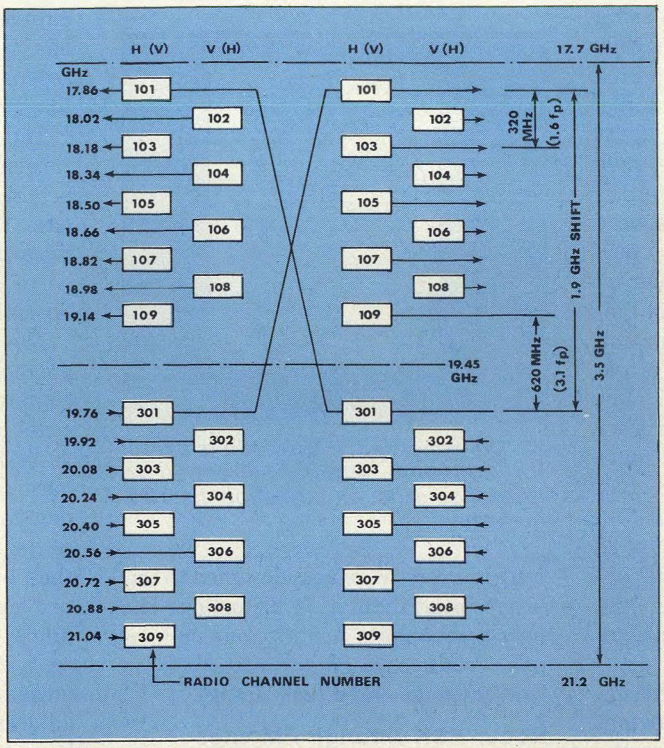

1. A closely interleaved frequency arrangement improves the spectral efficiency of digital modulation, but raises the spector of cross-polarization interference.

"There is the possibility of improved frequency utilization using closely interleaved frequencies," Yoshio Nakamura told an audience at the International Conference on Communications (Chicago, June 12-15). "For example, it might become possible to increase the transmission capacity by a factor of more than 1.5 by employing 16-level QAM modulation techniques, which can be realized as an extension of the current 4PSK techniques, and by reducing the cross-polarization interference by a slight reduction in clock frequency."

Nakamura, a member of the technical staff at the Yokosuka Electrical Communication Laboratory of NTT, notes that when such tight frequency spacing is attempted, cross-polarized co-channel interference becomes a prime concern, especially during heavy rainfall. His calculations show that cross-polarization discrimination (XPD) of better than 32 dB is necessary to insure an outage time rate of less than 0.1 per cent/2500 km in rain storms of 1.5 mm/min. Most repeaters in the 120 station digital network exhibit XPD values of 35 to 45 dB.

It should be mentioned that although operation at 20 GHz provides a wide bandwidth to accommodate many channels, transmission at the high frequency is subject to considerable propagation loss. In fact, losses increase so significantly with rainfall that the 160-mW repeater sites can be separated by no more than 3 km. Thus, the relatively short, 29-km link between Tokyo and Yokohama requires ten intermediate stations, in addition to the two terminal sites.

Increasing analog capacity

Digital systems at near-millimeter wavelengths are glamorous technological stars in the Japanese high-capacity network, but the real workhorses are still analog systems in frequency bands at 4, 5 and 6 GHz.

System architects from NTT, for example, have recently demonstrated the practicality of increasing the transmission capacity of FM/FDM radio systems from 1800 channels to 2700 channels and from 2700 channels to 3600 channels without changing the frequency arrangement. NTT has recently placed into commercial service

(continued on p. 44)

Stacy V. Bearse, Editor
Steven Peliotis, Western Editor

a 6-GHz, 2700 channel system (with 29.65-MHz carrier separation) between the cities of Hamada and Fukuoka. A field test has been underway for the past nine months on a 5-GHz, 3600-channel system (with 40-MHz carrier separation) between Funabashi and Hiihari.

"When increasing the transmission capacity in an FM/FDM microwave system, it is important to keep thermal, intermodulation and interference noise within the noise budget," Jiro Ohi of NTT explained to conferees at the ICC. "When increasing the transmission capacity from 1800 channels to 2700 channels or from 2700 channels to 3600 channels, for example, the interference noise from adjacent channels increases as much as 2800 times (34.5 dB) or 600 items (28 dB)."

Ohi said that the NTT systems were upgraded by improving two performance parameters that have a great influence on adjacent channel interference: interference reduction transfer factor (IRF) and cross-polarization discrimination (XPD). Improved XPD proved to be the tougher specification to meet, since the high-capacity systems require more than 38.5-dB discrimination compared to a conventional system requirement of 28 dB. Interestingly, the higher XPD objectives were largely met by developing a new, more accurate method of antenna pointing.

In conventional systems, Ohi explains, XPD objectives are usually met by simply adjusting antennas at the direction where the main polarized receiving power is at a maximum. NTT designers, however, adjust the direction of the horn-reflector combination by closely monitoring and nulling the received TM_{01} mode. Figure 2 illustrates the sharp directivity that can be achieved with this technique.

Field tests on 2700 and 3600-channel systems confirmed that XPD could be maintained at about 40 and 46 dB, respectively, by better antenna positioning. Ohi drew several important conclusions regarding XPD fading from these trials. He feels that a 1.5-dB margin is required on each hop to counteract multi-path fading, but notes that the effect of XPD on short-term noise can be neglected. Interestingly, he reports that the increase in adjacent-channel interference due to rainfall can be neglected, as long as linear polarization is used. Circular polarization his data point out, leads to serious fading.

Several other design modifications were made to increase the radios' capacity. Pre-emphasis was increased to 10 dB in contrast to the CCIR recommendation of 8 dB. Ohi suggests that this helps maintain a flat distribution of noise in the baseband, considering the frequency dependence of adjacent-channel interference. Thermal noise was reduced by 5.5 and 6.5 dB in the conversions by boosting transmit power by 1.5 dB and reducing receiver noise figure by 3 and 4 dB. New RF

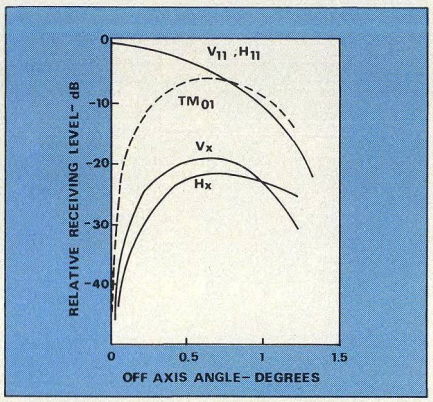

***2. The received TM_{01} mode** is useful for adjusting antenna direction to maximize cross-polarization discrimination.*

multiplexers were also designed to improve intermodulation distortion. The new components include four or five-pole Tchebychev filters instead of the conventional three-pole design.

Route PSK through FM sites

Japan is crisscrossed by an existing network of 4, 5 and 6 GHz analog radio routes, with non-regenerative repeaters at most sites. This poses a problem for planners of new digital systems who, in the worse case, would merely like to co-exist with the analog world without interference problems, and in the ideal case, would like to share facilities with existing FM/FDM links. Well, an experimental 100 Mbit/s system constructed by NTT demonstrates that with some mild precautions, the ideal case can be realized.

Masayoshi Murotani of NTT discussed the experiment at the recent ICC, and concluded that non-regenerative repeating over six hops is feasible using repeaters designed for FM/FDM systems, with RF multiplexers replaced to handle PSK data streams. Frequency sharing of PSK and FM/FDM systems at junction stations is feasible with some reasonable restrictions, he observed, while a comparatively large frequency separation would be necessary between PSK and FM/FDM radio channels operating on the same route.

One of the "reasonable restrictions" identified by Murotani is the need to reduce the output of the final TWT to about 6 dB below saturation. "A PSK signal varies in amplitude during the conversion to different phases," he explains. "This amplitude modulation component causes AM-to-AM and AM-to-PM conversion effects when the signal passes through a nonlinear circuit like a TWT." Since the system is not regenerative, distortion caused by nonlinearities would be cumulative.

The second proviso to PSK operation through a non-regenerative FM repeater deals with the roll-off of the low-pass filters in the QPSK modulator circuit. This, Murotani advises, must be in the order of 0.5 for successful operation.

The QPSK experiment was conducted over an existing, six-hop, 2700-channel analog system between the cities of Osaka and Fukuchiyama. The 20-W TWTs in the 5-GHz system were backed down to an output of 5 W, and new modulator circuits were installed at the repeater sites. Murotani reports that bit-error rate of the 100-Mbit/s test signal remained below 10^{-4} (probability of exceeding this is 0.01 per cent/2500 km). Carrier-to-thermal noise ratio was 62 dB, while carrier-to-adjacent channel interference was at least 42 dB (both figures under normal conditions). Frequency separation of 40 MHz provided acceptable adjacent-channel interference levels if analog and digital signals were cross-polarized. Frequency separation must be increased to at least 80 dB, Murotani concludes, if co-polarized signals are carried on the same route.

Semiconductors set the pace

It turns out that much of the work aimed at increasing channel capacity deals with limiting interference. And to improve this performance aspect, Japanese engineers are hard at work developing solid-state amplifiers that not only meet tough standards for linearity and AM-to-PM conversion, but that also promise long life and efficient operation.

The push to replace TWTs with high-power solid-state microwave sources is expecially strong at Mitsubishi Electric Corporation, Hyogo, Japan. Here, at

(Continued on p. 46)

Mitsubishi's Central Research Laboratory, investigators have examined the applicability of GaAs Impatt diodes as TWT replacements, and report quite impressive results. Studies initially centered on the GaAs Impatt diode with a platinum Schottky barrier, but it was discovered that reliability suffered due to rapid interdiffusion of platinum with GaAs. Rapid temperature rise during operation are blamed for this phenomenon.

"Better stability makes a p-n junction-type Impatt much more attractive than a Schottky-barrier diode," claims Dr. Kazuo Nishitani. At the recent San Diego conference, Nishitani reported 10-watt p-n diodes, built with a hi-lo structure, that exhibit an MTTF of greater than 10^6 hours.

The Impatts are fabricated from epitaxial p^+-n-n^--n^+ on n^{++} GaAs wafers. The p^+ region is doped with Ge; the n region, which acts as an avalanche zone, is doped with Sn. Mitsubishi's diode design differs from conventional diodes in that the avalanche region increases its carrier concentration and narrows its width to achieve high efficiency. Maximum efficiency is thus obtained at current densities as low as 300 A/cm², which contributes to the high MTTF rating. "The MTTF of 10^6 hours is one order of magnitude longer than the Pt Schottky-barrier-type GaAs Impatt diode, and 50 times longer than the TWTs," Nishitani reports.

Diodes are mounted in a J-band waveguide cavity with a "hat" for frequency determination. The highest efficiency reported by the Japanese researcher, obtained with a single, 300-μm square chip, is 26.6 per cent at 7.3 GHz. The highest-output power reported, 11 watts at 5.7 GHz, was obtained with four chips bonded in a single package. Nishitani states that 10-W output powers with efficiencies of greater than 20 per cent are reproducibly obtained at junction temperatures of less than 200°C.

At this early stage of development, 5-to-6-watt amplifiers are being fabricated in a semi-production environment with more than 10-dB gain and 17 per cent efficiency. The amplifiers exhibit 80-dB of thermal noise with a bandwidth of 150 MHz—enough for an 1,800 channel radio.

GaAs FETs gain acceptance

Researchers from Fujitsu Laboratories, Kawasaki, Japan, have announced a 7-GHz FM transmitter that relies on power GaAs FETs for final output stages, as well as for a novel modulator/oscillator circuit. Designed for use in FM radio-relay equipment, the transmitter provides an output power of 1 W with 11.5 per cent efficiency. The bandwidth of 400 MHz and unloaded signal-to-noise ratio of better than 76 dB meet the requirements for 960 telephone-channel service.

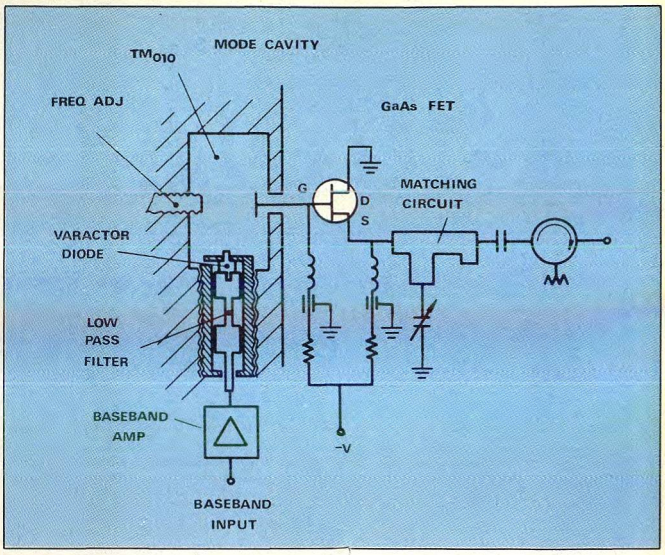

3. A grounded-drain GaAs FET (Fujitsu FLC-15) is at the heart of this 7-GHz FM modulator.

Fujitsu's transmitter is designed to fit in a remodulating-type FM radio-relay system operating in the 6.57 to 6.87 GHz band. The FM signal from the

Bell System to begin SSB field trials

Single-sideband (SSB) radio, an old idea perhaps best known to amateur radio operators, is about to undergo a rigorous field trial for use in high-capacity, long-haul routes in the Bell System. If the approach proves satisfactory, plans are to overbuild selected 4-GHz FM radio routes with 6-GHz, SSB replacements.

The new system, formally introduced by R. E. Markle of Bell Laboratories, North Andover, MA, at the International Conference on Communications (Chicago, June 12-15), uses the standard TH frequency plan; receive channels are in one-half of the band, while transmit channels are in the other half. "Eight channels of 29.65 MHz bandwidth will be available in each direction of transmission," Markle notes. "In concept, a maximum of 7,400 4-kHz voice circuits could be squeezed into each channel."

Practical plans call for 6,000 voice circuits per channel, however, since a portion of the channel bandwidth must be used for filtering, control pilots, and as a guard against excessive co-channel interference.

Many component developments contributed to the SSB design (Bell has been seriously studying the potential of SSB since 1960), but the design of an ultra-linear 4-GHz power amplifier is singled out by Markle as the key element. Early studies centered on feed-toward techniques to limit third-order nonlinearities, but these were eventually abandoned in favor of a method called predistortion. The predistorter circuit, combined with a driver amplifier in the IF stage immediately preceding the transmit modulator, reduces the third-order distortion of the output TWT by 30 dB in laboratory tests (Markle estimates this will drop to a 25-dB improvement in the field). To achieve even better linearity, the transmitter modulator is operated with higher local oscillator drive than in FM radios.

Other important design areas identified by the Bell researcher include an amplitude equalizer that keeps worst circuit dynamic misalignment within ±2 dB for at least 99.9 per cent of the time, and a GaAs FET preamplifier that provides a noise figure of less than 3-dB with 9-dB gain, and has sufficient linearity to allow FM and AM channels to share a common path on the same polarization.

The new radio, dubbed AR 6A, will be tested this year over a single hop in Massachusetts. A more extensive evaluation is planned for next year over a six-hop route in Missouri. Units should be ready for installation in other routes by mid-1980.•• SVB

modulator is amplified by a two-stage power amplifier to the 1-W level. A small amount of the amplified signal is extracted through one of the arms of a dual directional coupler and fed to a frequency discriminator operating at 7 GHz. The discriminator feedback to the modulator's AFC circuit establishes a frequency stability of $\pm 5 \times 10^{-5}$. A transmit power monitor is incorporated in the other side of the dual directional coupler.

The FM modulator circuit (Fig. 3) illustrates yet another innovative application for the versatile GaAs FET. Here, the FET is operated in a grounded-drain circuit with an external resonator connected between gate and ground. This resonator not only acts as a feedback network but, according to H. Komizo of Fujitsu, also reduces the oscillator's FM noise; signal-to-noise ratio of the component is 76 dB at 70 kHz from the carrier.

Modulation linearity is enhanced by using a double-tuned circuit consisting of a main resonator and sub-resonator which includes the varactor diode. The sub-resonator assembly is built in a threaded metal pipe. Coupling to the main resonator is primarily magnetic, and can be adjusted by rotating the pipe. The baseband signal is fed to the varactor through a low-pass filter.

The compact, MIC transmitter turns in respectable performance. Differential gain and phase are less than 1 per cent and 1 ns, respectively, at ±10 MHz from the carrier. Modulation sensitivity is 4.5 MHz/V and operating bias voltage is only −8 VDC—quite low for a 1-W transmitter.••

Processors to play key roles in future military satellites

An intelligence officer in Eastern Europe sets up a portable, UHF earth terminal in a dark, deserted pasture, and transmits vital information back to the US using FSK modulation. The message is received in Washington with 8PSK modulation by a large dish operating in X-band, deciphered, and orders are immediately transmitted in the same manner to a submarine patrolling the Pacific. The sub receives the message from Washington in K-band with QPSK modulation, using a small, periscope-mounted dish.

This scenario, apparently riddled with technical inconsistencies, illustrates a major goal of military planners now laying the foundation for the next generation of defense communications satellites: complete interoperability between earth terminals of different services, frequencies and modulation schemes. Unlike today's essentially transparent, repeater-type satellites, the military communications satellite of the 1990s will probably include complex processing systems to link a wide variety of users, operating in a broad spectrum of frequency ranges, and with a mixed bag of digital modulation schemes.

Satellites get smarter

The idea of a "processor in the sky" was described by Robert Drummond of the Defense Communications Agency, Washington, DC, in a survey of "Future Trends in Milsatcom Systems" at the International Conference on Communications (Chicago, June 12-15). "With hundreds of earth terminals being procured and maximum interoperability being a system goal," he summarized, "intuition says that the greatest cost savings can accrue if earth terminals are simplified and the system complexity features are placed in a few satellites in orbit."

The missing link

Interoperability was a recurring word in the presentation given by Drummond, who is the assistant for system integration and control at the Military Satellite Communications Systems Office of the DCA. "The World War II separation of tactical and strategic communications no longer truly exists," he explained. "Command and control must encompass nearly all levels of authority down to a ship, an aircraft, or a land force."

DCA's dream is to enable all users of the military satellite communications system to correspond with one another without the need for similar ground equipment. This requires signal processing on-board the satellite—an idea considered for the latest generation of DOD satellites, DSCS III (now under construction at GE Space Center in Valley Forge, PA), but abandoned at the outset because, according to Drummond, proven technology was not available.

The satellite processor outlined by the military planner would basically serve as a signal interface and routing device. Accesses to the satellite at UHF, L, X and K bands would be tied together, simplifying the interface challenges introduced by earth terminals having different modulation and multiple-access techniques. Specific functions under the processor's control could include telemetry, command and control, message processing, demodulation, baseband buffering and store-and-forward modes.

What kind of hardware developments will be necessary to meet the ambitious plans of the DCA? Aside from the digital advances necessary for the processor itself, Drummond sees many RF challenges. "Improved transmit efficiency is needed at K band," he observes. "The 20 to 30 per cent values presently achieved at K band should be made comparable to the 55 to 60 per cent achieved at X band. Low-noise receivers will be required at 20 GHz and above, high-power (kW) transmit tubes are needed at 30 GHz and above, and satellite-borne processors for small mobile terminals such as P3 size aircraft terminals, three-to-four foot shipboard terminals and man-pack terminals."

Antennas will change

But the concept of a processor in the sky promises to influence antenna design more than anything else. Drummond envisions large-aperture, multiple-beam antennas (MBAs) operating at UHF, X and K bands, with the capability to time-hop their beams using the on-board processor. "You could tie an MBA to a TDMA (time-division multiple access) system," he speculates. "Now, if you could tie that to a hopping system, you could turn spot beams on when you wanted to and get the satellite in synchronization with the ground TDMA system to have a very high capacity system with anti-jam (capabilities)."

These antennas, in conjunction with the on-board processor, should also be capable of detecting and automatically nulling multiple jammers, says the military system architect. But to develop such a system, beam-switching networks must first be designed that switch rapidly without degrading G/T

(Continued on p. 48)

Stacy V. Bearse, Editor

or EIRP performance to any great extent.

Drummond views phased arrays as a reasonable alternative to the MBA approach, in spite of their added complexity and weight. Graceful degradation and ease of integration with an onboard processor are the two main merits identified by the DCA designer.

Testing must improve

Lady luck has not smiled on past defense communications satellites. In fact, the Defense Satellite Communications System (DSCS) has been plagued by an incredibly high rate of spacecraft failures, in marked contrast to commercial communications satellite ventures such as Intelsat. Of eight spacecraft launched since 1968 under the second phase of the DSCS program, only one remains operational with seven birds victims of mechanical, electrical and launch failures.

"Automated testing of complex systems and circuitry with thousands of possible tests needed to minimize the chance of chain reaction failures or of sneak currents or voltages being induced from what are assumed to be unrelated effects could save a mission or program," DCA's Drummond observes. "Automated test equipment and test facilities, under software control, can significantly aid in the design, development and manufacturing phases of a satellite system, yet few companies have developed adequate test facilities due to a lack of appreciation of what advantages such test facilities offer in the decision to award a competitive contract."

But Drummond does not cast total blame on industry. "The purchaser," he admits, "must also recognize the importance of such capabilities in total system procurement, and be willing to allocate sufficient resources to guarantee the best possible end product."••

Earth station weighs just 25 pounds

Tomorrow's soldier will keep touch with ships, aircraft and ground stations many thousands of miles away using portable satellite communications earth stations that are about the same size as the field radios used by yesterday's GI for short-range communications.

The forerunner of this class of communications gear is the AN/PSC-1, a 25-pound satcom transceiver recently demonstrated by Cincinnati Electronics Corp., Cincinnati, OH. Despite its light weight and small size (see photo), the new earth terminal boasts such features as a 35-W output, BPSK or QPSK modulation at data rates to 16 kbit/s, 16-channel operation, and voice, secure voice, data, selective-call, and conference-call modes.

The radio can access either line-of-sight or satellite systems. For satellite operation, a helical antenna provides a gain of 6 dB. The antenna folds up into a 300-cubic-inch package, and can be assembled and be ready for operation within two minutes. A whip antenna is used for line-of-sight operation.

While the transmitter and receiver sections of the set are based on conventional UHF designs, the control section of the transceiver is unusual. A CMOS microprocessor together with an internal frequency synthesizer control operating frequency, mode, and receiver off-set frequency.

Voice transmission calls for a standard handset, while data transmission is entered by a 32-switch ASCII keyboard. Sixteen alphanumeric LED characters read received messages in ticker-tape fashion.

The portable terminal was designed for the US Army Satellite Communications Agency, Ft. Monmouth, NJ.•• SVB

Earth stations to triple by 1985, as systems move up to 30 GHz

Investments in satellite and message communications will increase at a rate of 15 per cent per year through 1985, predicted spokesmen from Arthur D. Little, Inc., at a recent seminar on Future Directions In International Telecommunications. In addition, studies by the Cambridge, MA firm indicate the number of earth stations will triple by 1985 due to the heavy demand for domestic networks based on satellite service. Key technological changes in new designs are the growing importance of digital modulation and satellite systems operating up to 30 GHz.

Howard Bierman, Publisher

11-30 GHz satellites readied

To relieve spectrum congestion in the crowded 4 and 6-GHz bands, satellite transmission systems designed to operate in the 11 to 14 GHz and 20 to 30 GHz bands are now under construction, explained Arthur H. Solomon, senior staff member of Arthur D. Little's Telecommunications Sciences Section. The 4 and 6-GHz bands are presently shared by both satellite and terrestrial systems, posing significant interference problems when a large number of earth stations are planned. This, in turn, severely limits the number and location of earth stations. However, higher frequency bands have been assigned exclusively for satellite transmission service by international agreement. Since there is no need to impose flux density restrictions on the higher bands to minimize interference with terrestrial systems, higher-power satellite downlinks are feasible, thus allowing the use of smaller earth station antennas and/or less sensitive

'Logical' Design Relaxes Tough Crystal Standards

Tight stability standards in the new 900-MHz band call for expensive crystals with month-long aging. An alternative is to design mobiles with memory that rely on base stations for frequency corrections.

THE Federal Communications Commission has given a green light to the development of mobile radio systems at 900 MHz, with a new allocation that provides more usable bandwidth than all previous allocations combined[1]. While this new band holds promise for innovative, new types of communication services (see "New systems stress spectrum conservation"), technical requirements at 900 MHz, especially those related to frequency stability, are rigorous compared to standards for other land-mobile bands at 50, 150 and 450 MHz.

Frequency control requirements for mobile communications at 900 MHz stretch today's state of the art in crystal technology, particularly in the area of aging. A conventional radio design, tailored to meet FCC regulations of ±2.5 parts per million (ppm) frequency stability, would require the best available grade of crystal, custom-cut to a tolerance of 3. Although such components are available, they are relatively expensive, require extra characterization, and must pass through a preconditioning cycle that typically lasts one month.

The alternative is to take a new approach to mobile radio design, one that relies on the frequency stability of the base station as a reference. This can be done conveniently by adding digital logic and memory elements to what is now strictly an RF/IF design. The mobile unit can actually refresh its memory of frequency stability whenever it hears a base station. As a result, the radio designer would be free to specify a standard crystal, with looser specifications. This could translate into significantly lower cost and faster delivery, perhaps from inventory.

Stuart J. Lipoff, Engineer, Electronic System Section, Arthur D. Little, Inc., Acorn Park, Cambridge, MA 02140.

Stability specs are tougher

The technical characteristics[3] of the various radio services, both existing and proposed, are summarized in Table 1. Note that the FCC has not constrained cellular systems as greatly as other approaches to encourage technical innovation. The technical characteristics of the cellular services shown in Table 1 represent the proposals of AT&T and Motorola, and are intended to show typical requirements.

All systems, except cellular, share the same FM deviation of 5 kHz and occupied bandwidth of 16 kHz. Channel spacings, while slightly different, are comparable. For the UHF band of 450 to 512 MHz and the new 900-MHz band, 25-kHz channel spacing is specified. Since the occupied bandwidth and channel spacing of all the systems are comparable, the required frequency stability specification becomes more stringent at the higher frequencies. Taking high-power mobiles as typical examples, highband VHF and UHF (150 and 512 MHz) limits are ±5 ppm, while radios in the 900-MHz band require ±2.5 ppm.

The true importance of this apparently small difference can be appreciated by investigating current state-of-the-art UHF equipment. A 5-ppm tolerance maps into an absolute frequency error of about 250 Hz. This 250-Hz error must be maintained over calibration tolerance, power supply voltage variation, time and temperature. A field study of current production UHF portable gear from several manufacturers reveals that few units even meet the calibration tolerance requirements, let alone the combined power supply and temperature requirements. Thus, a requirement of 2.5-ppm stability where the state of the art barely meets 5-ppm is a severe requirement.

Table 1 also reports an interesting 45-MHz constant spacing between duplex transmitter and receiver frequencies; this constant spacing can be used to advantage, as described later. The last entry in Table 1 spells out a one-year requirement for rechecking the transmitter frequency. This requirement has been recently dropped by the FCC, but for all practical purposes is still necessary. The one-year measurements interval sets the design target for maximum frequency variation with time (aging).

The need to transmit control data to mobiles at high-speed coupled with the extreme frequency agility requirements of the mobile and the interference reduction of enhanced capture, place a different set of technical requirements upon cellular systems. The FCC has left open some of the technical requirements to the manufacturers so that competitive techniques can be employed to foster development of new concepts. Motorola has proposed a system with deviation and occupied bandwidth equal to the conventional system. However, adjacent channel spacing is only 8.3 kHz. Since the occupied bandwidth of 16 kHz is greater, interference could be expected to result. To reduce interference from the shared frequencies of cell-to-cell leakage, a system geographic limit is set. Channels spaced within 25 kHz of each other can be in adjacent cells, but the tertiary offset 8.3-kHz channels are geographically removed from each other. In the Motorola approach, the equipment technical standards are the same as conventional and trunked systems.

The original system as proposed by AT&T, however, employs a larger FM deviation of 12 kHz to enhance the capture effect and minimize adjacent

cell interference of co-channel operations. Occupied bandwidth for the AT&T system will approach 30 kHz, which is almost double that of conventional systems.

While the wider channel bandwidth may permit the transmitter stability requirements to be opened up, the FCC has not made a provision for looser specifications for cellular systems. Thus, we must consider that the frequency stability requirements of cellular systems are equal to conventional and trunked systems.

Receiver stability is critical

The FCC sets no standards on receiver frequency stability. Nonetheless this is still an important parameter to control, since ultimate system range and performance demands the receiver be close enough to the transmitter frequency not to compromise sensitivity or not to cause distortion.

Figure 1 suggests a possible receiver implementation for mobile radios at 900 MHz. A dual-conversion, superheterodyne scheme has been chosen for good RF image rejection. The 45-MHz, first IF crystal filter provides a passband barely wider than the channel occupied bandwidth, thus protecting the second mixer from adjacent channel interference and improving intermodulation performance. There is some question if this degree of performance improvement will be necessary in a low-power, short-range cellular system, but the crystal filter can be expected to be necessary in conventional and trunked systems.

Even though additional selectivity may be used downstream from the crystal filter, the frequency stability of the first local oscillator must be high enough to avoid sensitivity degradation or distortion due to moving the first IF away from the crystal filter nose. The use of a phase-locked loop detector has been suggested as a means to reduce crystal stability performance, but this technique will not work in receivers that have a narrow crystal filter as described above. The circuit in Fig. 1 includes an automatic frequency control (AFC) loop around the crystal oscillator. This eliminates any degradation since the first IF is recentered in the passband of the crystal filter.

The role of the second local oscillator is much less critical, since the frequency is scaled down. A 25-ppm variation in the second local oscillator corresponds to a mere 1-ppm variation in the first local oscillator.

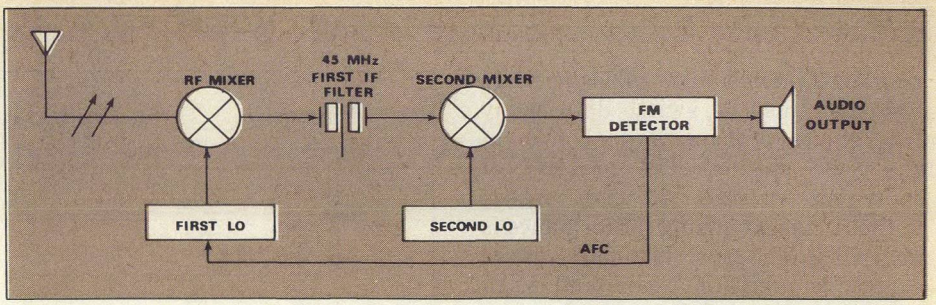

1. Although FCC regulations do not govern receiver stability, *good design practice is to apply the same specification given for the transmitter section. Key element is the first LO; second LO performance is much less critical.*

Superheterodyne receiver implementations in the existing land-mobile UHF band have shown that receiver modulation acceptance is such that a rule-of-thumb requirement of receiver stability equal to transmitter stability results in minimal degradation of system performance. If the AFC loop is used, however, this rule of thumb can be opened up.

Switched crystal or synthesizer?

Unless AFC concepts are employed, one can assume that the frequency control requirements of both the receiver and transmitter parallel each other. Figure 2 presents two methods of frequency control, a switched-crystal approach commonly used in existing mobile radio services, and a synthesizer[4] approach that has not been extensively employed for land-mobile applications.

The switched crystal approach requires that at least one crystal be custom-made for each transmitter channel associated with a channel switch postition. Each transmit crystal must be ordered from the crystal manufacturer after the radio order is booked; the exact frequency is usually the channel frequency divided by N. Similarly, the receiver frequency calls for a special crystal according to a formula that relates the channel frequency to the operate frequency of the crystal. In a duplex system, it is possible to employ the transmitter crystal as the first local oscillator injection and eliminate the receiver crystal, providing that a 45-MHz first IF is also used. In a simplex system it would also be possible to use a standard 45 MHz÷M offset crystal to heterodyne the receiver crystal onto the transmitter frequency. But this technique requires two crystals with drift and stability requirements that are twice as good as a single unit, and would not be practical.

The switched-crystal approach should find some application in single-frequency conventional systems, but would be a poor choice for cellular and

Table 1: Technical requirements of FM land-mobile transmitters

	low-band 30 to 50 MHz	high-band 150 to 174 MHz	UHF 450 to 474 MHz	UHF 470 to 512 MHz	806 to 947 MHz conventional and trunked	806 to 947 MHz Motorola proposed cellular	AT prop cell
FM deviation (kHz)	5	5	5	5	5	5	1
Occupied bandwidth (kHz) (1)	16	16	16	16	16	16	3
Channel spacing (kHz)	20	30	25	25	25	8.3	4
Unrestricted spacing (kHz)	20	30	25	25	25	25	4
Base station freq. stability (ppm) −30° to 60°C (2)	20	5	2.5	2.5	1.5	1.5	1
Mobile <3W freq. stability (ppm) −30 to 60°C	50	50	5	5	2.5	2.5	2
Mobile >3W freq. stability (ppm) −30 to 60°C	20	5	5	5	2.5	2.5	2
Repeater spacing (MHz)	none	not uniform	5	3	45	45	4
Measurement interval (3)	one year						

1) FCC authorizes 20 kHz but, at 3 kHz maximum audio frequency, 16 kHz is the calculated 99% power value.
(2) EIA temperature limits of −30 to +60°C are shown. FCC limits are −30 to +50°C.
(3) Frequency measurement interval requirement of 1 year has just been dropped by the FCC but, for all practical matters, is still necessary.

trunked systems since radios in these systems must be switched to many frequencies, probably under control of the base station. The problem of switching crystals at high speeds without compromising performance is not trivial. The crystals themselves are expensive precision items, and when several are needed for multiple-channel radios they add considerably to unit cost. Finally, to achieve the time stability (aging) performance necessary, the crystal manufacturer must have several weeks lead time to properly condition the crystal. Since the crystal can not be ordered until the radio order is booked, equipment delivery turnaround will suffer.

The synthesizer approach, on the other hand, permits a single crystal to control both transmitter and receiver frequencies. This crystal does not need to be custom made. It is a standard part that can be inventoried like any other part. The block diagram in Fig. 2(b) suggests a possible synthesizer implementation for 25-kHz channel spacing. The output of the crystal oscillator is divided down until the reference frequency is equal to the channel separation (25 kHz) divided by the transmitter multiplication factor (M). A phase-locked loop slaves a VCO to the proper channel determined by a programmable divide-by-N counter. Changing N by one step moves the transmitter up or down one channel (25 kHz).

The divide-by-N counter provides a simple digital interface for signals from the base station in a trunked or cellular system. A single synthesizer can be used for receiver and transmitter control by using the 45-MHz first IF technique described earlier in duplex systems, or by switching the divide-by-N counter after transmit to the receiver frequency.

Factors affecting the exact design of a synthesizer will not be resolved in this paper but include loop lock time, modulation methods for FM, broadband transmitter multiplier stages, clock speed of the divide-by counters and enhanced FM sideband noise due to multiplication. Other approaches that involve trade-offs are: VCO prescaling, VCO heterodyning, and VCO 'K' modulus prescaling.

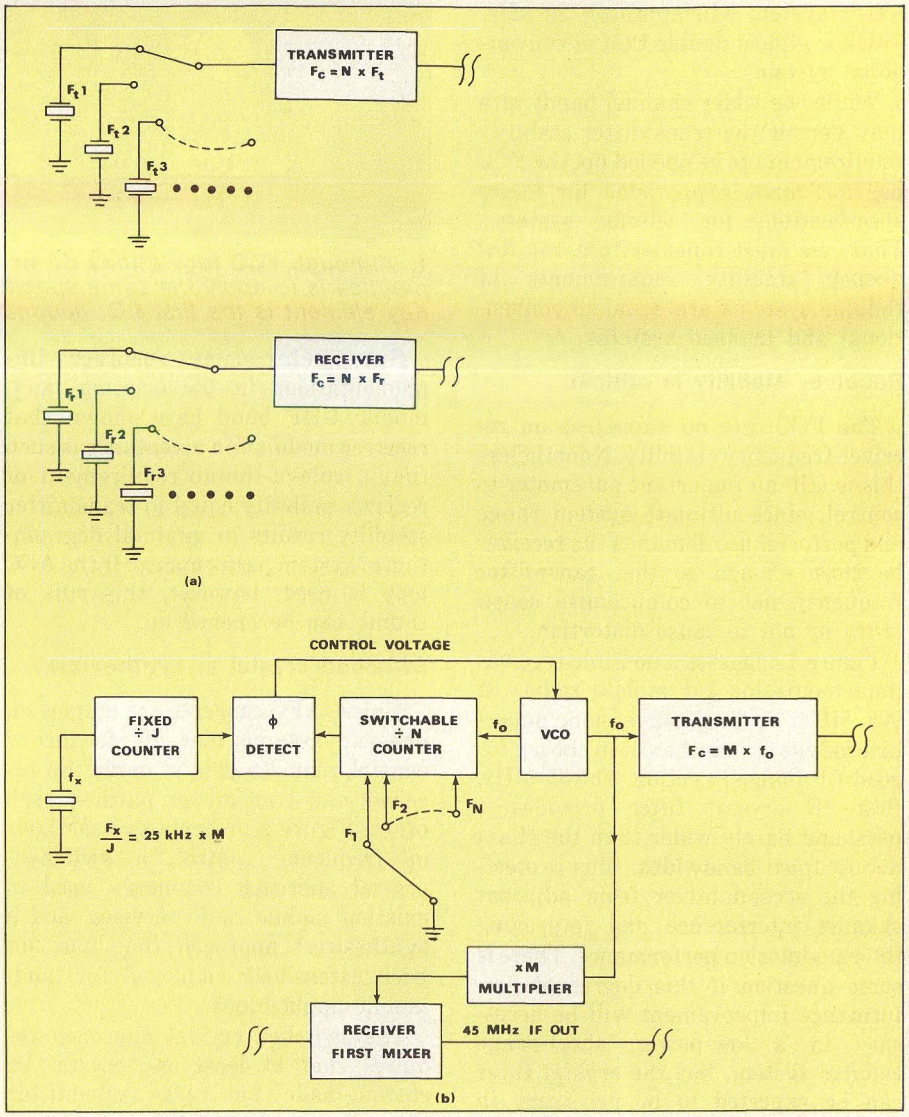

***2. Switched crystals (a)** can be used for conventional systems, but due to required conditioning delays, inventory is a problem. Synthesizers (b) offer the greatest flexibility, but have not been fully exploited for FM land-mobile radios.*

Good crystals take time

The foregone conclusion has been made that a quartz crystal will in some way be necessary to control the 900-MHz mobile transmitter. Surface acoustic wave devices have been proposed, but do not currently come close to the required temperature performance. The quartz crystal has proved its worth in the lower frequency radio services, and may be expected to be the only choice available at 900 MHz for some time.

Several important crystal parameters are outlined in Table 2. Three holders are considered to compare cost and long-term stability (aging). The aging specifications shown are state of the art for volume manufacture devices (drive levels affect aging and must be kept low for optimum performance). The fundamental frequency range of 2 to 5 MHz was selected since AT-cut crystals exhibit best aging[5] performance here. With a requirement of 2.5-ppm maximum transmitter drift due to aging, voltage variation and temperature, it is clear that the only candidate is the expensive HC-27/U[6,7] crystal in a glass holder. Note that to achieve a 0.5-ppm aging rate, 3 to 5 weeks of preconditioning are necessary.

Table 2 indicates a temperature coefficient of ±5 ppm from −10 to +60°C. However, the technical requirements of Table 1 show the necessity for ±2.5 ppm from −30 to + 60°C. (The FCC temperature range is −30 to +50°C, but the EIA specifies the more restrictive range of −30 to +60°C).

The manufacturing tolerances on a crystal are such that a ±5 ppm specification over the restricted temperature range down to −10°C is all that is possible. Figure 3 shows the variation

in series resonant frequency of a fundamental-mode, AT-cut crystal for several different angles of cut to a reference axis[8]. Note the angle of 35° 17′ is just barely capable of ±5 ppm over the full temperature range to −30°C. A manufacturing tolerance of 3′ of arc gives rise to the ±5 ppm spec in Table 2.

If we assume for the moment that we know the exact angle of cut of the crystal, we can devise a temperature compensating network that corrects for the cubic natural crystal variation. Networks, such as the one in Fig. 4, have been widely used and analyzed. Two thermistors provide a temperature-dependent voltage to a varactor diode in series with the crystal, which pulls the crystal back to frequency. It is possible to achieve performance to within ±0.5 ppm which is adequate to meet the ±2.5 ppm specification.

Returning to Fig. 3, we can see that 3′tolerance results in about ±15 ppm variation at −30°C. This means that the exact angle of cut of the crystal must be known in order to temperature compensate it to ±2.5 ppm. Since the manufacturing control is only 3′, each crystal must be measured, and a compensating network designed to match. Table 1 provides approximate price information for a crystal manufacturer to take the required "two point" temperature measurement. This measurement consists of two data points at two temperatures, usually the +25 and −10°C turning points. When this data is supplied with the crystal, a linear temperature compensating capacitor can be introduced into the crystal circuit to rotate the curve of Fig. 3 about 25°C. With the curve rotated, a single compensating circuit like Fig. 4 can be used.

The final crystal parameter of note in Table 2 is Δf_{32pF}. This parameter gives a measure of the ease with which the varactor diode (Fig. 4) can pull the crystal back on frequency. This parameter must either be controlled or measured to insure compensating circuit performance.

The crystal parameters listed in Table 2 do represent state-of-the-art performance for volume manufacture. In small quantity, however, it is quite possible to achieve better performance by additional preconditioning time and fine-tuning with temperature measurements. While cost and lead time prevent using these techniques for volume mobile and portable production, they are quite feasible for low-volume base stations. Base stations can also employ reference to secondary standards such as WWV for control. We will assume that frequency control problems for base stations are easily solved, and can be assumed not to represent a problem.

Refer mobile to base stability

Since we can assume the base station to be on frequency, we can use it as a reference to control the mobile. The crystal specifications may be relaxed and cost savings may result. Figure 5 introduces the approach for a simplex radio.

The receiver operates with an AFC loop controlling the receive crystal while a base station signal is being received. The receiver AFC voltage is loaded through an analog-to-digital converter into a non-volatile, sample-and-hold memory. When the base station shuts down, the correct receiver AFC voltage is maintained open-loop to the receiver crystal through the temperature-compensation network. As long as the receiver hears the base station every few weeks the memory is updated. Aging requirements of the receiver crystal are greatly reduced by the AFC loop, with substantial cost reduction realized by the ability to use HC-6/U crystal holders (see Table 2).

In the transmit mode, the stored AFC voltage in the receiver memory permits the receiver to act as a short-term stable reference for the transmitter, correcting the transmitter frequency in a closed AFC loop. Thus, the transmitter crystal requirements are

Table 2: Typical crystal specifications and pricing

parameter	HC-6/U solder seal	HC-36/U coldweld seal	HC-27/U glass
cut	AT		
mode	fundamental		
calibration	series		
frequency	2 to 5 MHz		
series resistance	25Ω		
TC (−10 to+60°C)	5 ppm		
finish	10 ppm		
drive level	1 mw	0.5 mw	0.01 mw
preconditioning	<1 day to 1 week		3 to 5 weeks
aging/year @25°C	5 ppm	3 ppm	0.5 ppm
C_0	<7pf		
spurious modes	>75Ω		
Δf_{32pf} (1)	330 ppm ± 33 ppm		
cost	$12.50	$15.75	$17.00
premium for two point temp. measurement	.50¢		

(1) Note: Alternative Spec of $\frac{C_1}{C_0} = 2\Delta f\ 32pf\ \left(1 + \frac{32pf}{Co}\right)$

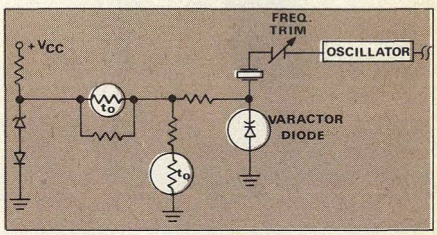

***4. Thermistor/varactor circuits** can compensate for the crystal's poor temperature performance, but to meet FCC stability requirements individual crystals must be measured carefully.*

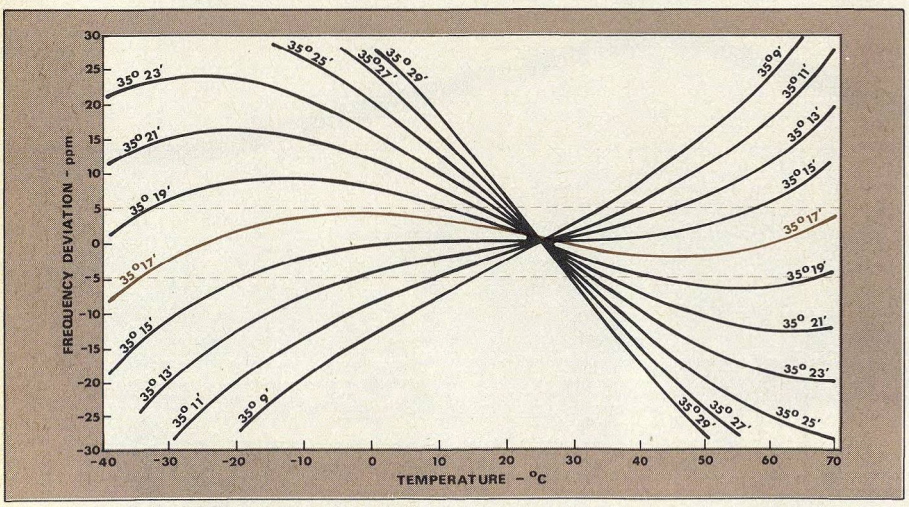

***3. Tight manufacturing tolerances** are necessary to keep frequency deviation small with changes in temperature. Note that the 35°17′ crystal cut is the only angle that meets ±5 ppm from −30 to +60°C. Standard manufacturing tolerance is 3′, which moves the spec grossly out of limits.*

also reduced in performance and cost.

The simplex technique described above maps directly over for duplex systems, as shown by Fig. 6. Here, one oscillator provides the transmitter and receiver frequency control: placing the oscillator in the receiver AFC loop corrects the transmitter frequency also. A sample-and-hold memory as described above can be used if the mobile is permitted to bring up carrier before the base station transmits.

The additional logic required to implement these frequency control schemes should not be a problem, since the other logic demands of call supervision would probably best employ a microprocessor which could handle frequency control memory and logic as a sideline.

Choose phase modulation

The circuits laid out in Figs. 5 and 6 provide for frequency control, but not for FM modulation. Approaches taken in equipment for the existing frequency allocations, 512 MHz and below, fall into two categories: phase modulation or direct FM.

Direct FM modulation employs a varactor diode like that used for AFC in Fig. 5. The audio modulation is applied to the varactor making the circuit function as a voltage-controlled crystal oscillator (VCXO). To apply this approach successfully it may be neces-

New systems stress spectrum conservation

The FCC's allocation of a new land-mobile communications band between 806 and 947 MHz immediately opens 70 MHz of bandwidth to developers of new systems, with another 45 MHz held in reserve for future growth. System concepts for landmobile radio fall into three categories[2]: conventional, trunked and cellular. Of special interest are the trunked and cellular approaches, which promise to use the spectrum more efficiently than existing land-mobile services.

Conventional systems at 900 MHz will parallel the operation of existing land-mobile services at VHF and lower UHF frequencies. They are characterized by a small number of independent base stations associated with a group of mobiles (Fig. a). When several base stations exist, as in police radio services, they are on different frequencies; mobile users determine the base station they wish to communicate with by manually selecting the proper frequency. The system may operate in a simplex mode with one common transmit and receive frequency, or employ a duplex mode with the base station repeating the mobile's signal at a different output frequency for other mobiles to hear.

Trunked systems represent a new concept in land-mobile radio service, in that they include several base stations interconnected to a central controller. Each base station is assigned a different frequency, and each mobile in the system is capable of receiving any of the base stations (Fig. b). System implementations may permit the mobile to manually control frequency, but it is more likely that base stations will transmit information that selects the mobile operating frequency automatically. A system operator might lease base station facilities to several users who have no need to interact with each other. A dispatch station is linked by wireline to the user's base station, and mobiles wander freely throughout the coverage area of the base. When a dispatch station initiates a call, it is routed to a free base station frequency and mobiles are alerted and switched to the frequency. One frequency is retained throughout the interchange. When a mobile initiates a call on a free channel, it must transmit an identification code to the base station. The system then routes the mobile to the proper dispatch station. It is hypothesized that this frequency trunking will improve spectrum utilization and permit more stations to share the same frequencies.

The most radically different concept for mobile communications made possible by the 900-MHz allocation is the cellular system. Several base stations on different frequencies are tied to a central controller as in the trunked system, but the cellular system also reuses the base station frequencies within the system without interference (Fig. c). The system coverage area is divided into cells with a specific group of frequencies assigned to each cell. The transmitter power and antenna pattern in each cell is limited so that these same frequencies can be reused in cells that are located several units away. As a mobile transverses the coverage area, the base-station controller tracks its position and reassigns the mobile a clear frequency while simultaneously directing the landline interface to the correct base station in the correct cell. Like the trunked system, the cellular system operator can be expected to lease the services to mobiles not associated with each other. The greatest utilization of this system is expected to be by mobile radiotelephone users, but dedicated dispatch stations may be accommodated by the system and will also be offered service.••

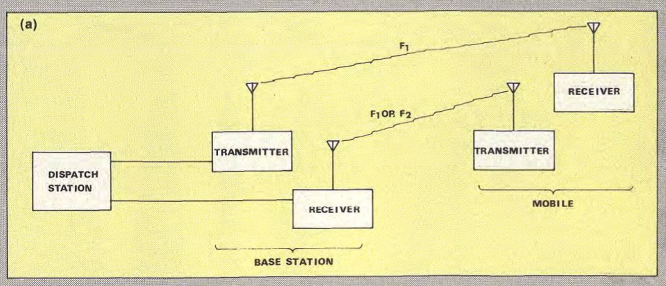

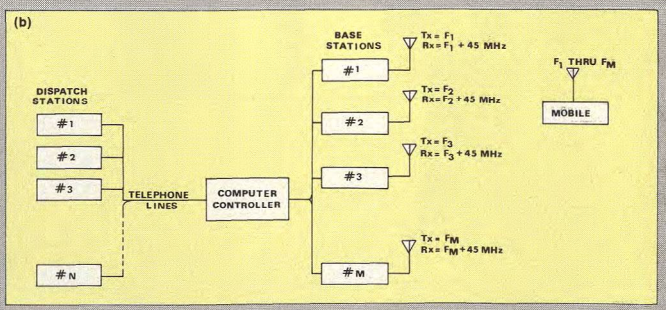

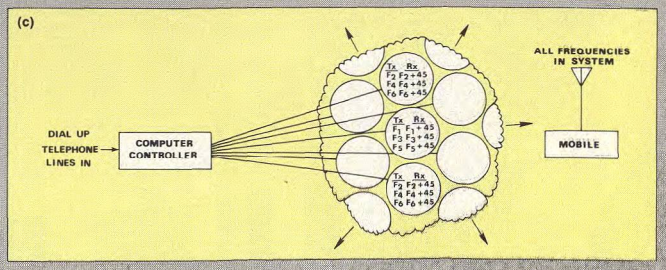

sary to limit the swing of the applied audio voltage for acceptable distortion. If more deviation is necessary, frequency multipliers must be used. While this direct FM approach is suitable for the simplex system in Fig. 5, the designer must introduce a low-pass filter into the AFC loop to filter out the modulation signal.

Direct FM is not suitable for the duplex system in Fig. 6, however, because the one oscillator provides a signal for both the receiver and the transmitter. Use of direct FM would provide an undesirable sidetone, since the receiver would demodulate the FM deviation on the oscillator. Phase modulation is the practical alternative for the duplex system.

Figure 7 illustrates how phase modulation could be incorporated into a

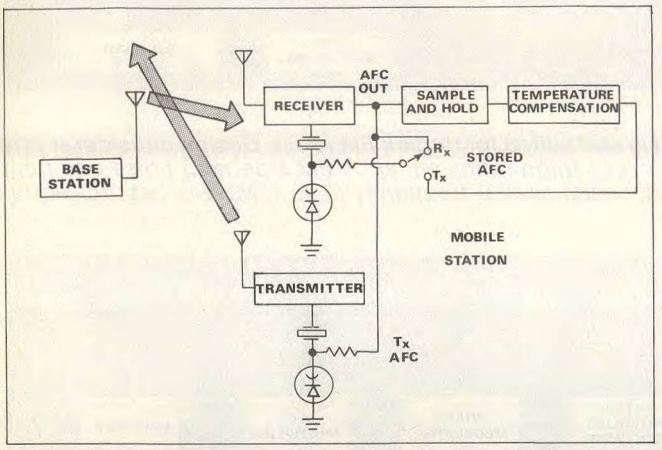

***5. Base-station stability is used as a reference** for mobile units in this simplex scheme. Transmit oscillator is compared with base-station signal, and a correction is recorded in non-volatile memory. Receiver offset is corrected while in receive mode.*

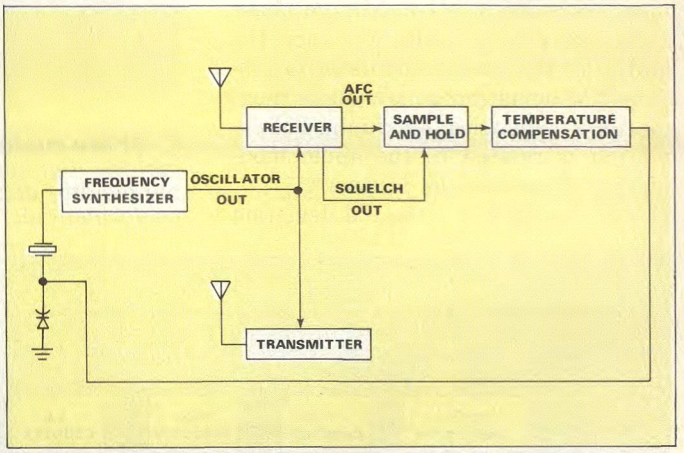

***6. Aging correction in a duplex radio** is achieved by modifying receiver offset in an AFC feedback loop. Transmitter is controlled by receiver time base, and follows receiver corrections. Compensation logic could be supplied by system controller microprocessor.*

duplex radio; the modulator is inserted after the synthesizer. The phase modulator provides a phase shift proportional to the applied audio modulation; if the audio modulation is integrated before being applied, frequency modulation will result. Since it is difficult to build a linear phase modulator with more than about $\lambda/4$ maximum phase shift, there is a limitation upon the ability of the phase modulator to produce FM deviation at low audio modulating frequencies. Maximum FM deviation is related to the audio modulating frequency as follows[10]:

$D = F \varnothing$ where D is the FM deviation

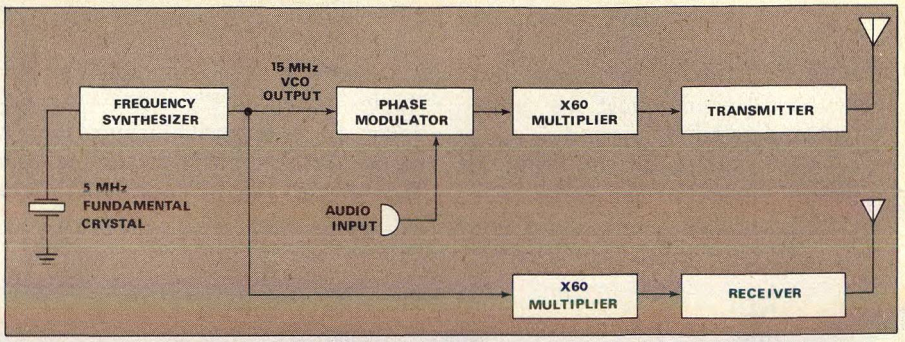

***7. Phase modulation** is well suited for duplex FM radio. Design considerations include multiplication ratio (high ratios enhance FM sideband noise and limit bandwidth) and fundamental crystal frequency (2 to 5 MHz is best for aging performance).*

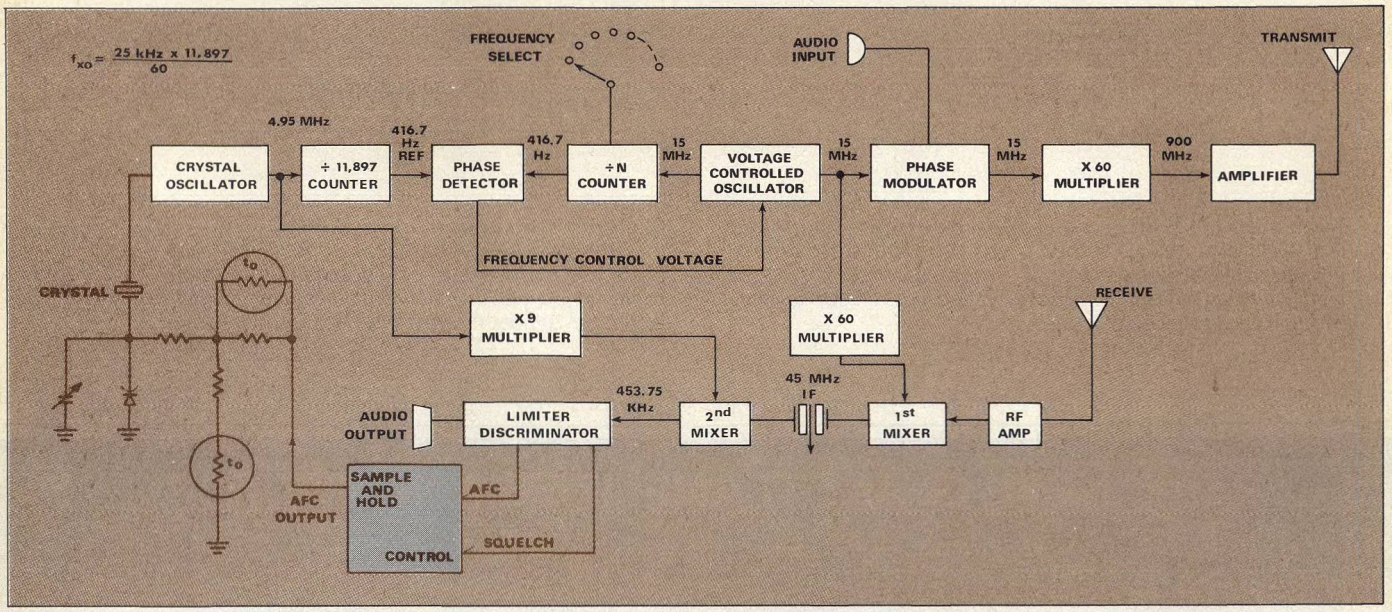

***8. This duplex mobile radio design** incorporates memory to use base-station stability as a reference. Stabilizing circuit is shown in color.*

in Hz, F is the audio modulating frequency, and Ø is the maximum phase shift capability for the phase modulator in radians.

It was mentioned earlier that cellular and trunked systems will require the base station to send supervisory data to the mobiles. Now, assume that the minimum frequency the transmitter will handle will be due to the supervisory data. Let us pick a modulating frequency limit of 100 Hz for a design example. At the 100-Hz modulation rate and $\lambda/4$ phase shift, the maximum FM deviation at the fundamental frequency is about 80 Hz. To realize 5 kHz at the operating frequency in the 900-MHz range, the phase modulator output must be multiplied by at least 60 times.

The circuit introduced in Fig. 8 incorporates all the concepts related to the duplex circuit into a design example. A multiplication ratio of 60 times is employed, which should not cause FM sideband noise problems. The crystal operates in the fundamental mode in the neighborhood of 5 MHz for optimum aging performance. An AFC loop with memory corrects the transmitter to the received base-station reference. A temperature-compensation network is provided for the crystal between the memory and the AFC element. A 45-MHz first IF is employed, permitting the transmitter control oscillator to be used as a first injection.

Injection for the second local oscillator has not been previously discussed, but is shown in Fig. 8 as nine-times the reference crystal oscillator. This scheme eliminates one more expensive crystal and results in a second IF frequency of 453.75 kHz which is in the neighborhood of the commonly used 455-kHz second IF for which many FM detector designs exist.••

References

(1) Federal Communications Commission, "Cellular, Trunk and Conventional Communications Systems," Docket 18262, Federal Register, Vol. 40, No. 62 (March 31, 1976).
(2) S. V. Bearse, "The Year of Giant Growth Arrives for Land Mobile Communications," MicroWaves, Vol. 13, No. 1 (January, 1974).
(3) Federal Communications Commission, "Rules and Regulations, Part 91," Washington, DC.
(4) R. Brubaker and G. Nash, "A New Generation of Integrated Avionic Synthesizers," Application Note AN-553, Motorola Semiconductor Products, Phoenix, AZ.
(5) E. Gerber and R. Sykes, "State of the Art - Quartz Crystal Units and Definitions," Proceedings of the IEEE, Vol. 54, No. 2 (February, 1966).
(6) D. Eisen, "New Developments in Glass Enclosed Crystal Units," 1964 Proceedings of the 18th Annual Symposium on Frequency Control, U. S. Army Electronics Command, Ft. Monmouth, NJ.
(7) R. Byrne and R. Reynolds, "Design and Performance of a New Series of Cold Welded Crystal Unit Enclosures," 1964 Proceedings of the 18th Annual Symposium on Frequency Control, U. S. Army Electronics Command, Ft. Monmouth, NJ.
(8) A. Chi, "Frequency Temperature Behavior of AT - cut Quartz Resonators," 1959 Proceedings of the 10th Annual Symposium of Frequency Control, U. S. Army Electronics Command, Ft. Monmouth, NJ.
(9) D. Newell, H. Hinnan, R. Bangert, "Advances In Crystal Oscillator and Resonator Compensation," 1965 Proceedings of the 19th Annual Symposium on Frequency Control, U. S. Army Electronics Command, Ft. Monmouth, NJ.
(10) S. Lipoff, "Design of Voltage Controlled Oscillators," 1976 Proceedings of the 30th Annual Symposium on Frequency Control, U. S. Army Electronics Command, Ft. Monmouth, NJ.

Define Dynamic Range For Better Spectrum Analysis

Dynamic range is deeper than the value quoted by most data sheets. Definitions vary with measurement tasks, and may consider resolution shape factor and bandwidth, noise, distortion and sensitivity specifications.

ONE of the more important specifications in spectrum analysis is that of dynamic range. Dynamic range basically expresses the range of amplitude levels that can be displayed together for measurement or analysis. It is expressed as a numeric of a ratio, usually in dB. The concept is outwardly quite simple; namely the amplitude measurement range of the spectrum analyzer. However, a more detailed examination reveals many potential misunderstandings.

The problem arises from the need to quantify the concept. Here, one must get involved with establishing the signal levels whose ratio is to be taken, and with the meaning of the word "together", since the signals have to be observed together. The result is a list of dynamic range specifications with qualifiers such as harmonic, linear, intermodulation, and on-screen. Each of these dynamic range specifications is different (see, "Dynamic range: More than one definition"). There are also questions concerning noise sidebands, incidental FM and resolution shape factor, which all affect signal separation, and hence, dynamic range measurement.

What is sensitivity?

All operational definitions of dynamic range involve the concept of a smallest signal, the divisor in the numeric ratio quantifying dynamic range. This smallest signal is usually termed sensitivity. The definition and measurement of sensitivity have their share of pitfalls since several definitions are currently in use. For this fundamental discussion we shall simply equate sensitivity to the internally generated noise referenced to the spectrum analyzer input. This definition permits the computation of sensitivity on the basis of instrument noise bandwidth and input noise figure.

Noise figure computations are based on various fundamental concepts which will not be discussed here[1]. For our purpose it is sufficient to note that all circuits generate noise due to thermal agitation of electrons. The noise power available to a matched load from an ideal, 1-MHz wide circuit at room temperature of 290°K (16.8°C) is −114 dBm. This is the least noise that such a circuit will generate. Actual circuits generate additional noise and/or attenuate the signal level with respect to the noise so that signal to noise ratio is further degraded.

Morris Engelson, Chief Engineer, Spectrum Analyzer Products, Tektronix, Inc., P.O. Box 500, Beaverton, OR 97077.

The amount of degradation suffered by a real circuit when compared to the ideal circuit is called the noise figure (F). Noise figure is specified as a power ratio number, or its dB equivalent. A 1-MHz wide circuit with a 20-dB noise figure will generate a noise level of −94 dBm (−114 dBm +20 dB), referred to the circuit input. Thus, the smallest observable signal for this circuit is equal to a sensitivity of −94 dBm.

Keep this concept of noise figure and sensitivity in mind, since it will reappear frequently as we explore the many dimensions of spectrum analyzer dynamic range.

"On-screen" range: Don't be misled

One popular method of specifying spectrum analyzer dynamic range is to provide an "on-screen" number; 70 dB is typical. The qualifier "on-screen" means that the specification deals with the display system of the instrument.

Consider the typical specification of 70 dB. Does this mean that dynamic range is never more than 70 dB, or that 70 dB can always be achieved? The answers to these questions

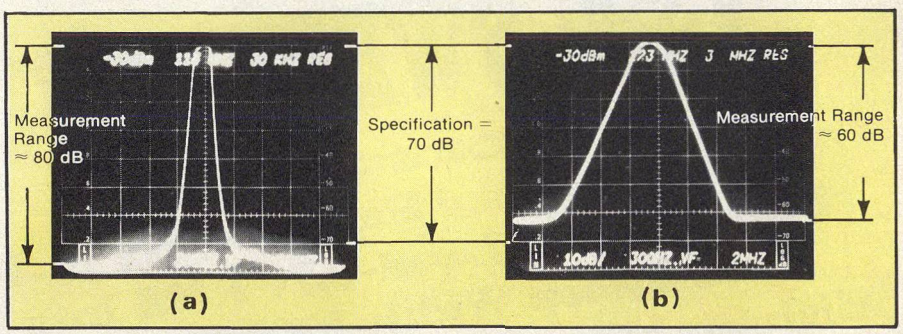

***1. On-screen dynamic range specifications** describe the response of the display system. More (a) or less (b) range may be available depending on factors such as calibration and noise.*

are illustrated by Fig. 1. Note that the CRT graticule is marked in 10-dB steps to a level of −70 dB with respect to full-screen reference. This leaves the bottom graticule of the screen unaccounted for. In fact, the bottom graticule on this particular spectrum analyzer (Tektronix 7L13) is about 15 dB, so that amplitude differences of over 80 dB can be observed when permitted by the instrument noise level, as shown in Fig. 1(a).

Note, however, that only 70 dB is calibrated. The display characteristics of the bottom graticule will vary from unit to unit, hence only 70 dB of on-screen measurement dynamic range is specified by the manufacturer.

Figure 1(b) shows the opposite situation. Here, the noise

Dynamic range: More than one definition

Think twice the next time you evaluate spectrum analyzer dynamic range. Are you referring to the display alone? Is intermodulation distortion significant? Have you considered the resolution shape factor of the instrument in question? Will incidental FM pose a problem? Are the two signals you wish to observe closely spaced?

The point is this: A dynamic range specification can mean many things to many people, depending on the individual measurement challenge. The dynamic range rating spelled out on the data sheet usually refers to the display alone. It's necessary to dig deeply into the relationships between the specifications shown on the right to get a true picture of dynamic range under all conditions. Six methods of specifying dynamic range follow. See the text for details of how to calculate and apply each.

Dynamic range is the ratio, or dB difference, between the largest permissible input signal and the sensitivity.

Harmonic or intermodulation (IM) dynamic range is based on the maximum input that guarantees a specified harmonic or IM level (typically 70 dB for −30-dBm input).

On-screen dynamic range specifies the display range, and is primarily determined by the logarithmic amplifier (typically 70 dB).

Maximum linear dynamic range uses the maximum signal input for linear operation in the dynamic range computation (typically 60 to 110 dB).

Optimum dynamic range is the maximum achievable dynamic range when the distortion products are at the sensitivity level (typically 80 to 100 dB).

"If you see it, it's real" dynamic range means that gain and attenuation settings are so arranged that harmonic and IM dynamic range is compatible with on-screen dynamic range (typically 70 dB for −30-dBm full-screen input).••

Resolution—Resolution bandwidth selections from 30 Hz to 3 MHz (7L13), and 300 Hz to 3 MHz (7L12) in decade steps are provided. Bandwidth accuracy, at the 6-dB down level, is within 20% of the resolution selected. Shape factor over the 60 dB to 6 dB level is 12:1 or better for 30-Hz resolution and 4:1 or better for 300-Hz to 3-MHz resolution settings. Signal level change over all bandwidths is less than 0.5 dB.

Sensitivity for a CW Signal (Signal + noise = twice noise)—in LIN vertical Mode. —128 dBm at 30 Hz, —120 dBm at 300 Hz (7L13 only), —115 dBm at 300 Hz, —108 dBm at 3 kHz, —100 dBm at 30 kHz, —90 dBm at .3 MHz, —80 dBm at 3 MHz. Sensitivity may decrease 2dB at 1.7 GHz and 4 dB at 1.8 GHz. Below 100 kHz, the sensitivity degrades no more than 0.3 dB/kHz in the 7L13.

Intermodulation Distortion—(100 kHz to 1800 MHz) The third order is down 70 dB or more from two —30 dBm signals within any frequency span. Second order is down 70 dB or more from two —40 dBm signals.

Spurious Signals from Internal Sources (Residual Response)—Equal to or less than —100 dBm, referred to the first mixer input when terminated in 50 Ω.

Incidental FM'ing (7L13)— 10 Hz (p-p) when phase locked. 20 kHz (p-p) for 5 seconds when not phase locked.

LOG 10 dB/div Mode—Provides a calibrated 70-dB dynamic range. Accuracy within ±0.1 dB/dB to a maximum of 1.5 dB over the 70-dB dynamic range.

LOG 2 dB/div Mode—Provides a calibrated 14-dB dynamic range. Accuracy within ±0.4 dB/2 dB to a maximum of 1.0 dB over the 14-dB range.

level is about 62 dB below full screen reference. The display still has 70 dB of accurate calibration, but signals more than about 60 dB below full screen are obscured by noise.

What, therefore, does the 70-dB on-screen specification mean? It merely means that the analyzer's display section, consisting of a logarithmic amplifier, detector and associated circuitry, provides 70 dB of calibrated measurement range for full-screen signals. It also implies that the instrument noise level is sufficiently low at most resolution settings to take advantage of the specified on-screen range. The specification, however, does not mean that 70 dB of measurement range is always possible, or that more than 70 dB is never possible.

Dynamic range can also be computed as the ratio (or dB difference) between the maximum linear display input level and the sensitivity. Maximum input level for linear display is given in two ways. One number gives a level assuring essentially no nonlinearity. Alternately, a figure can be specified at the 1-dB compression level, which results in considerable nonlinearity. The difference between specifications derived using these two methods ranges from 10 to 20 dB, depending on the instrument.

Using the Tektronix 7L13 as an example, we find that the maximum input for linear operation is −30 dBm with a −10-dBm, 1-dB gain compression point. Best sensitivity is −128 dBm at 30-Hz resolution, and worst sensitivity is −80dBm at 3-MHz resolution. The maximum linear dynamic range varies from 98 dB (−128 dBm - (−30 dBm)) for 30-Hz resolution, to 50 dB (−80 dBm − (−30 dBm)) at 3-MHz resolution. For some measurements it might be possible to get up to 20-dB more range by driving the input to the 1-dB gain compression point.

The maximum linear dynamic range should be compatible with the on-screen dynamic range. An on-screen range much less than the linear range means that the display system is the limiting factor. Conversely, a large on-screen range is useless when measurements are limited by linear input signal range. Other limitations, such as sideband noise, resolution filter shape factor and ultimate attenuation, are discussed in a later section.

Beware of distortion

Knowing the dynamic range on screen or the maximum linear dynamic range is no guarantee that a certain measurement can, in fact, be made. Harmonic measurements and intermodulation (IM) distortion cause particular difficulty: it takes very little nonlinearity to reach a typically specified−80-dB (0.01 per cent) distortion level.

An IM dynamic-range specification states a distortion level below a specified input. For instance, third-order IM distortion products for the Tektronix 7L5 are at least 75 dB below a −30-dBm input within any frequency span. This means that a 75-dB IM dynamic range is available, provided the noise level is at least 75 dB below the maximum input of −30 dBm. A glance at 7L5 specifications shows that worst sensitivity (at the widest resolution bandwidth) is −105 dBm. Therefore, the 75-dB IM dynamic range can be achieved at all resolution bandwidth settings.

(continued on p. 64)

All distortion products are affected by signal level. In addition, IM products are affected by frequency spacing of the input signals. Distortion products grow as the input level increases and the frequency spacing shrinks. While specifications uniformly will give an input level at which the distortion is specified, this is not always the case with IM signal spacing. Some data sheets state a signal spacing (e.g., 1 MHz) at which the specification applies.Presumably, performance degrades at closer spacings. Some instruments have the IM specification applicable "within any frequency span." This means that the specification is worst case; it applies everywhere. Finally, there are some instances where frequency spacing is not mentioned. The user should question this carefully if narrowly-spaced IM is of particular interest.

An understanding of how distortion products vary with input level is quite useful for determining best available performance, known as optimum dynamic range. Distortion products, whether harmonic or intermodulation, are caused by transfer function nonlinearily in the spectrum analyzer circuits. Thus, for a signal input level, V, the distortion products go as V^2, V^3—V^N, where N is the order of the distortion. Clearly, the distortion level proportional to V^N increases faster than the input level, V. This gives rise to the idea of an intercept point: the theoretical level where the distortion output equals the nondistorted output. The intercept point cannot be reached in practice since the device saturates before the level is reached. The intercept point in dBm, I, is related to input signal in dBm, S, to the distortion level relative to signal level in dB, Δ, and the distortion order number, N, as follows:

$$I\ (\text{dBm}) = \frac{\Delta\ (\text{dB})}{\text{N-1}} + S\ (\text{dBm})$$

Using this relationship, one can calculate the intercept point, and the best input level to achieve the optimum (largest) dynamic range for distortion measurements. For example, if third-order IM products for the 7L13 spectrum analyzer are 70 dB down from a −30-dBm input, the intercept point is:

$$I = \frac{70}{3\text{-}1} + (-30) = +5\ \text{dBm}$$

Suppose that the specification sheet for this instrument states a best sensitivity of −128 dBm. Ideally, the intermodulation products should be −128 dBm, thus permitting a lower input level which gives best dynamic range. Hence:

$$S\ (\text{dBm}) - \Delta(\text{dB}) = -128\ \text{dBm}$$

$$\frac{\Delta\ (\text{dB})}{2} + S\ (\text{dBm}) = +5\ \text{dBm, resulting in}$$

$$S = -39.3\ \text{dBm and } \Delta = 88.7\ \text{dB.}$$

Therefore, while the IM specification might be 70 dB, it is possible, under some conditions, to achieve an optimum intermodulation dynamic range of close to 90 dB.

The fact that distortion products generated by the spectrum analyzer change in level relative to the desired signal as a function of input level provides an easy check to see whether the spectrum analyzer is clean of IM distortion. Just change the input level by some amount, for instance

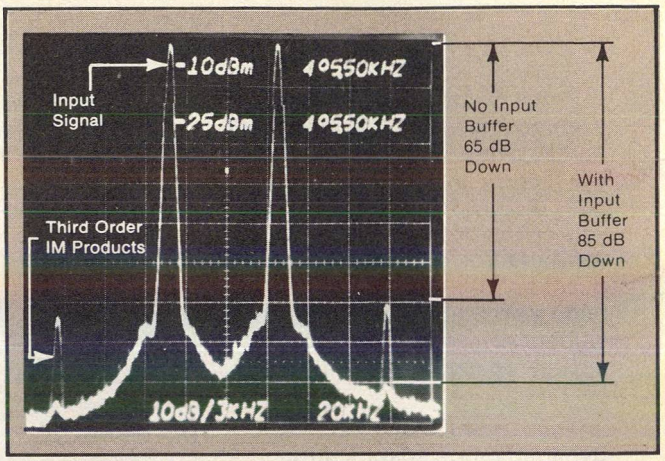

***2. An input attenuator circuit** that proportionally increases instrument gain to balance loss can reduce third-order IM products and thereby increase dynamic range.*

6 or 10 dB, and check that the distortion products go down by the same amount. If the distortion products fall at a faster rate than the input level, it is a sign that some of the distortion is generated by the spectrum analyzer and the measurement is not valid.

Some instruments incorporate a checking procedure called input buffer. Activating the input buffer inserts 8 dB of input attenuation while simultaneously increasing instrument gain by 8 dB. Hence, while the self-generated noise level raises by 8 dB, signal levels should remain unchanged. Intermodulation products generated by the instrument, though, are reduced.

An example of how an input buffer circuit can improve IM performance is provided by Fig. 2, a composite of two photographs showing signals purposely set 15-dB above full screen to generate distortion. The third-order IM products are 65 dB down. This, however, is not the true IM input level. Activating the input buffer circuit drops the IM to over 80-dB below the input signals.

If you see it, it's real

One of the annoyances in dealing with dynamic range specifications is that there are so many of them. One way of reducing the confusion is to use the "if you see it, it's real" method. To do this, the on-screen dynamic range has to be compatible with the maximum linear range, also gain and attenuation has to be arranged so that no on-screen signal will generate IM or harmonics on screen. This procedure makes for a single specification equal to the on-screen dynamic range. The disadvantage is, that by locking out certain control settings so that the user cannot overdrive the instrument, the measurement of nonharmonic signals is also somewhat restricted. Of course, the user can always let the larger signal go off screen, but this is not as convenient as reducing the gain.

Extending input limits

Dynamic range is basically the difference in dB between the largest permissible signal and the smallest observable signal (sensitivity). It would appear, therefore, that increasing the large signal limit or decreasing the noise level

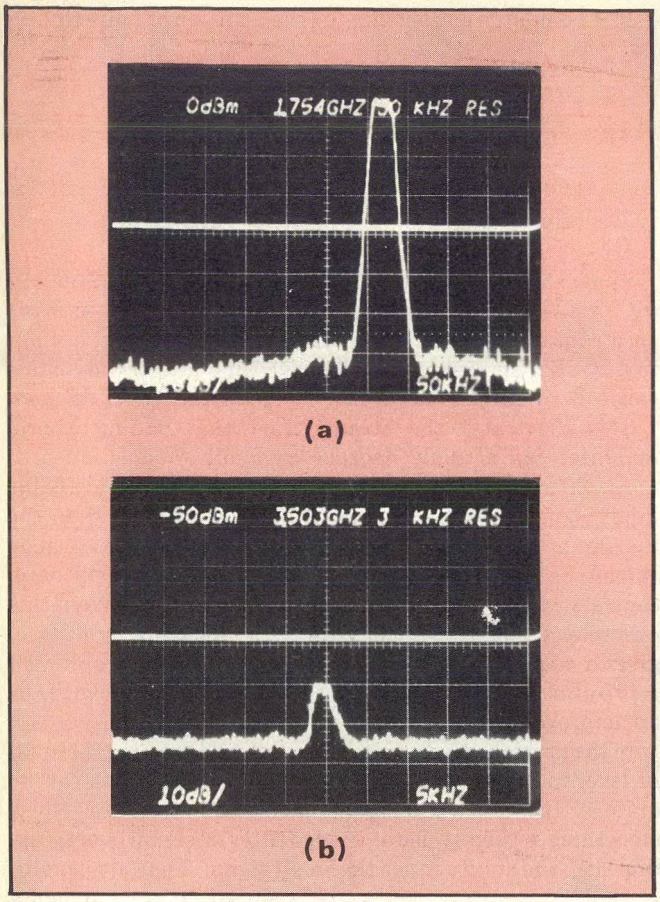

***3. Tracking preselectors** reject the fundamental while the spectrum analyzer tunes to the second harmonic; self-generated harmonics thus do not interfere with the measurement. Here, the fundamental is displayed at −5 dBm (a), while the second harmonic, at −100 dBm, is down by 95 dB (b).*

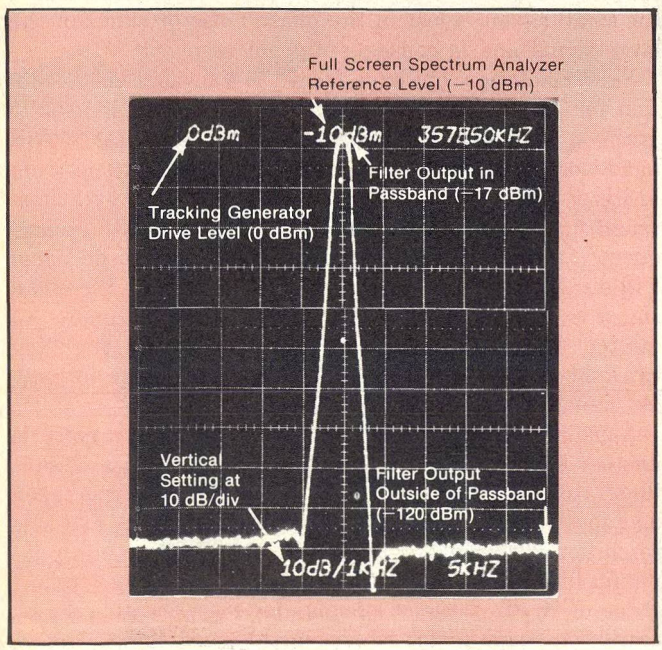

***4. High ultimate attenuation measurement** using a tracking generator shows over 100-dB of out-of-band rejection.*

(improving sensitivity) should increase dynamic range. This is usually true, but not always.

First, consider a few methods to increase the spectrum analyzer's upper input limit. An important distinction must be made when considering how distortion products due to excessively large input signals influence dynamic range. Clearly, if the generation of spurious responses and the observation of small input signals do not occur together, the former will not interfere with the latter. This obvious principle can be exploited to make measurements over a very wide dynamic range (greater than 100 dB) with the aid of a preselector or tracking generator.

A preselector is a tracking filter that sweeps in synchronism with the spectrum analyzer. This may be an external accessory or incorporated as part of the instrument. The preselector rejects the fundamental signal, while the spectrum analyzer tunes to the second harmonic. Thus, the self-generated harmonics are never observed.

Figure 3 illustrates this principle. Figure 3(a) shows a −5-dBm signal at 1.75 GHz, while Fig. 3(b) shows the second harmonic at 3.5 GHz. Note that the second harmonic is −100 dBm, or 95 dB below fundamental. Obviously, the fundamental is well above full screen when the second harmonic is measured. But the measurement is valid, since the preselector removes the fundamental when observing harmonics.

A similar situation applies to tracking generators. Here the input signal tracks the sweeping spectrum analyzer[2]. When the spectrum analyzer tunes to the signal harmonic, the signal is no longer at the fundamental frequency. Distortion products generated by the spectrum analyzer are never seen on screen.

The tracking generator/spectrum analyzer combination is particularly useful when determining the transmission characteristics of filters and other components. Figure 4 shows such a measurement. Output level from a tracking generator driving the filter under test is 0 dBm. The filter output level is −17 dBm in the passband and −120 dBm outside the passband. The display indicates over 100 dB of out-of-band rejection.

A particularly useful technique to improve dynamic range when measuring harmonics is to reduce the amplitude of the fundamental with a band-reject or high-pass filter (Fig. 5). Figure 5(a) shows the transfer characteristic of a high-pass filter; the response was obtained by sweeping the filter with a tracking generator/spectrum analyzer combination. Signal rejection may not match the swept response due to impedance mismatch. When in doubt, add a pad between filter and signal source to reduce mismatch reflections. Rejection of the fundamental compared to harmonics is 50 dB. Figure 5(b) shows a fundamental signal and its harmonics after passing through the filter of 5(a). The second harmonic is 38-dB down, the third harmonic is 18-dB down, and so forth. Add to this the filter rejection (50 dB), resulting in second and third harmonics of −88 dB and −68 dB, respectively. This technique, when exploited to the fullest extent, permits harmonic dynamic range measurements of over 120 dB.

The preamp paradox

Now, consider how dynamic range can be improved by working at the opposite extreme: sensitivity. Instrument sensitivity is synonymous with noise level[3], as discussed

(continued on p. 66)

earlier. Spectrum analyzer noise level is proportional to noise figure (F) and noise bandwidth (B). As resolution bandwidth is reduced, sensitivity falls and dynamic range improves. Thus, a highly stable spectrum analyzer that provides narrow resolution bandwidths not only provides high sensitivity, but high dynamic range as well. Therefore, if the signal to be measured is stable enough, it is wise to use narrow resolution bandwidth settings when dynamic range is of interest.

Another way to reduce instrument noise is to improve the noise figure by connecting a low-noise preamplifier in front of the spectrum analyzer. Paradoxically, while this will improve the sensitivity, dynamic range will be degraded. This point is illustrated by the following hypothetical example.

Suppose a spectrum analyzer has an input noise figure, F = 20 dB (ratio of 100). At a 1-MHz resolution bandwidth, the noise level is 20-dB greater than a perfect instrument of 0-dB noise figure. Since 0-dB noise figure corresponds to −114 dBm, the sensitivity is −94 dBm. Let us say that the maximum input level is −30 dBm. Hence, the dynamic range is 64 dB (−30 dBm − (−94 dBm)). Now, we connect in front of the spectrum analyzer a preamplifier having a 6-dB (4-times) noise figure and 20-dB (100-times) gain.

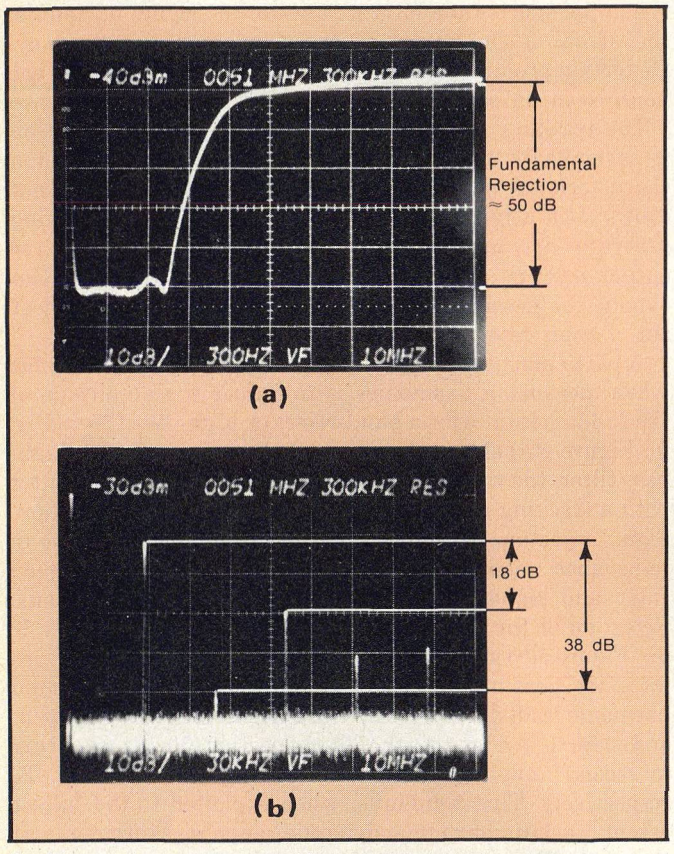

***5. Dynamic range can be extended** by reducing the amplitude of fundamental signals with a high-pass filter with a characteristic as shown in (a). A fundamental signal, passed through this type of filter, has second and third harmonics of −38 and −18 dBc, respectively (b). Harmonic dynamic range measurements of over 120-dB are possible with this technique.*

The standard relationship for the addition of noise figures is[1]:

$$F_{new} = F_1 + \frac{F_2 - 1}{G_1}$$

$$\text{Therefore, } F_{new} = 4 + \frac{100\text{-}1}{100} = 4.99 \text{ (7 dB).}$$

Thus, the new sensitivity is −107 dBm (−114 dBm + 7 dB), a 13-dB improvement. The maximum input into the spectrum analyzer is still −30 dBm, therefore, the input to a 20-dB gain preamplifier is −50 dBm. The new dynamic range is 57 dBm (−50 dBm − (−107 dBm)), a 7-dB loss. This illustrates the strange fact that adding a preamplifier can actually degrade dynamic range.

An obvious limitation on dynamic range is the available input signal level. If the input signal level is less than the maximum permitted input, then the full dynamic range cannot be achieved. A preamplifier can be of help here, contrary to the previous example. Using numbers from this example, a −94-dBm sensitivity with −50-dBm input level gives a 44-dB dynamic range. Using a 20-dB preamp to get −107-dBm sensitivity results in 57-dB dynamic range, or an improvement of 11 dB.

In the previous discussion it is assumed that a signal equal in level to instrument noise can be observed. This can be quite difficult, as the signal is masked by noise. Noise smoothing, either by use of a video filter or signal averaging, improves the ability to see the small signal. The only penalty is that sweep time has to be reduced to accommodate integration time.

Consider signal separation

So far we have considered that dynamic range is bounded by the largest input level and instrument noise. This is true for relatively wide frequency spacings. For small frequency spacings, however, it is possible that small signals will be obscured well before reaching the noise level. Essentially, the small signal is lost in the phase noise or skirts of the large signal and is consequently not resolved[4].

Skirt resolution, or shape factor, is a measure of resolution for small signals next to large ones. This is usually given as a ratio between spectrum analyzer 60-dB bandwidth and resolution bandwidth. Thus, a spectrum analyzer with a 30-Hz resolution bandwidth and 12:1 maximum shape factor has a 360-Hz, 60-dB bandwidth. Consequently, a small signal 180-Hz removed from a large signal will disappear into the large signal's skirt when the small signal is reduced by 60 dB compared to the large one. No matter what the sensitivity or large signal handling capability of the instrument, the dynamic range for 180-Hz signal separation is not more than 60 dB.

Noise sidebands due to local oscillator phase noise is another factor that affects close-in dynamic range. This is illustrated by the display shown in Fig. 6, which was taken on a spectrum analyzer with −108-dBm sensitivity at 3-kHz resolution (Tektronix 7L13). With −30-dBm maximum input for linear operation, we have a linear operating dynamic range of 78 dB. Close-in signals, however, are affected by resolution shape factor which, in this case, is 4:1. Hence, the 60-dB bandwidth is 12 kHz (4 × 3 kHz), and signals 60-dB down cannot be seen within 6 kHz of a large signal.

(continued on p. 68)

What of the transition between the filter skirt 60 dB down and the computed dynamic range of 78 dB? This is controlled primarily by the sideband noise characteristics. Some instruments do not specify sideband noise considering that this is part of an on-screen or "if you see it, it's real" type of specification. A typical specification might read: 70-dB down, 50-kHz away, with 3-kHz resolution. Therefore, the computed 78-dB dynamic range is not valid for signal spacing less than 50 kHz.

Another limitation on achieving good dynamic range is incidental FM. Spectrum analyzer incidental FM prevents the resolution of closely spaced signals. Obviously if you can't resolve (separate) a signal, you cannot measure its amplitude. Incidental FM of the signal similarly affects close-in signal measurements. Furthermore, accurate amplitude measurements require that the incidental FM of the signal be less than the resolution bandwidth. Hence, an unstable signal means a wider bandwidth setting which implies more instrument noise and hence, less dynamic range.

Finally, it should be noted that ultimate attenuation of the resolution filter constitutes a seldom specified limitation on dynamic range. Ultimate attenuation refers to stop-band rejection far enough away from the passband so that shape factor or other such effects are not involved. Basically, the signal simply leaks around the filter. A well-designed instrument will have a filter system with ultimate attenuation at least as good as the on-screen dynamic range. There is no certainty though, that ultimate attenuation will allow the maximum linear dynamic range. Figure 7 illustrates an ultimate attenuation dynamic range of 90 dB.

Keep in mind that ultimate attenuation does not limit tracking generator or preselected measurements, since large signals are not present when small signals are observed.

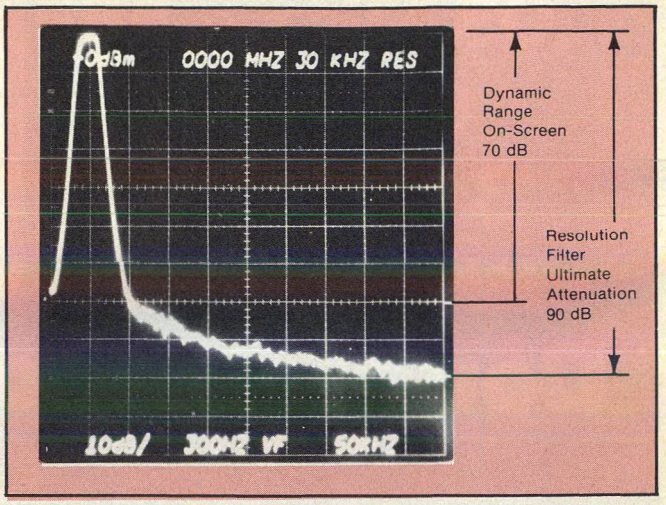

***7. The ultimate attenuation of the resolution filter** places a seldom-specified limitation on dynamic range.*

Pulses are different

Thus far, the discussion has dealt with CW signals. Best sensitivity and best dynamic range are obtained at narrowest usable resolution bandwidth setting. But pulses are different. Unlike the continuous-wave sinusoid, spectral power distribution for pulsed signals extends over wide frequency ranges. The spectrum analyzer establishes the spectral distribution by taking samples through the resolution bandwidth. The effect of resolution bandwidth setting on pulsed signal display is quite complex[5,6,7]. For our purposes, it is sufficient to note that the wider the resolution bandwidth, the greater the pulsed signal display level.

It can be shown that the display level for a pulsed RF signal compared to a CW signal of equal amplitude is $\alpha = \tau_0 B$, where τ_0 is pulse width and B is impulse bandwidth (assumed equal to resolution bandwidth in this discussion). Constraints limit α to less than 0.1. This means that under ideal conditions, pulse sensitivity is 20 log (0.1)= −20 dB compared to CW sensitivity, indicating a substantial loss is dynamic range. Instruments having wide resolution bandwidths, such as 3 MHz, will give best dynamic range for narrow pulse measurements.••

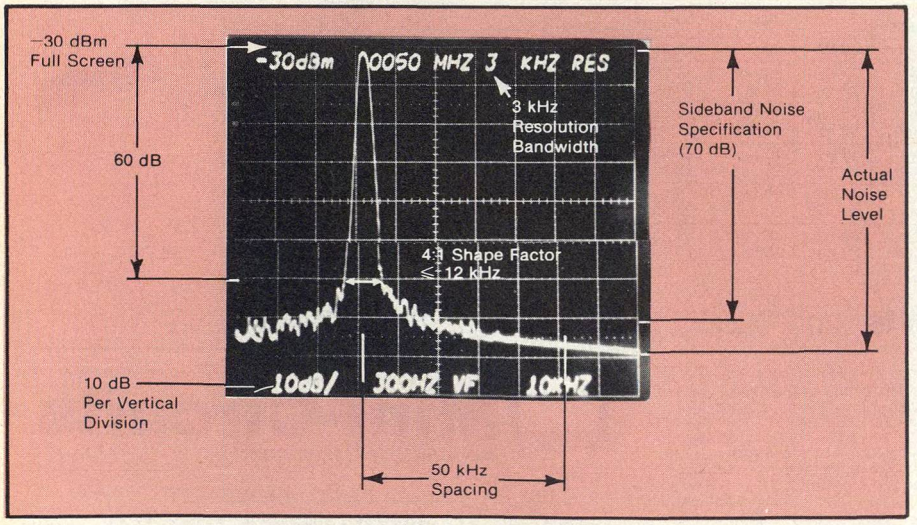

***6. Phase noise, resolution bandwidth and shape factor** are important specifications to consider when trying to measure small and large signals that are closely spaced.*

References

1. Mumford and Scheibe, "Noise Performance Factors in Communications Systems," Horizon House (1968).

2. Tektronix application note AX-3281: *The Tracking Generator/Spectrum Analyzer System.* Tektronix application note AX-3535: *Crystal Device Measurements Using The Spectrum Analyzer.*

3. Tektronix application note AX-3260: *Noise Measurements Using The Spectrum Analyzer: Random Noise.*

4. M. Engelson, "Understand Resolution For Better Spectrum Analysis," *MicroWaves,* pp. 32-36, Vol. 13, No. 12 (December, 1974).

5. M. Engelson, "Interpreting Pulsed RF Spectra," *MicroWaves,* pp. 52-55, Vol. 8, No. 3 (March, 1969).

6. Engelson and Telewski, "Spectrum Analyzer Theory and Applications," pp. 171-197, Artech House (1974).

7. Tektronix application note AX-3259: *Noise Measurements Using The Spectrum Analyzer: Impulse Noise.*